Zeolite facilitated adsorption of selected metals associated with mine drainage

L Dekker

orcid.org/0000-0002-1415-732X

Dissertation accepted in fulfilment of the requirements for the degree *Master of Engineering Chemical Engineering* at the North-West University

Supervisor:	Prof. S.K.O. Ntwampe
Co-supervisor:	Prof. F.B. Waanders, Mr. R. van Coller

Graduation:	May 2022
Student number:	27233448

Declaration

I, Leandri Dekker, hereby declare that the contents of this dissertation represent my own work. The dissertation is being submitted for a degree of Masters of Engineering in Chemical Engineering.

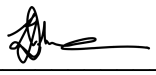

10/12/2021

Signature Date

Accepted extended abstract: *First Virtual Atlantic and Eastern Canadian Symposium on Water Quality Research, Nov. 2-3 2021.* **Supported by: Canadian Association on Water Quality (CAWQ) | Carleton University – Global Water Institute.** (International conference)

Kinetic modelling, isotherm determination and pH effects on the adsorption of selected heavy metals prevalent in mine drainage onto clinoptilolite

Leandri Dekker, Seteno Ntwampe, Frans Waanders, Ruveix van Coller

Center of Excellence in Carbon-Based Fuels, School of Chemical and Minerals Engineering, North-West University, Private Bag X1290, Potchefstroom 2520, South Africa

ABSTRACT – Adsorption column experiments were conducted to investigate the influence of pH on the adsorptive capacity of the zeolite, clinoptilolite, for the removal of some heavy metals prevalent in mine drainage (MD) i.e., cadmium, zinc, manganese and lead, besieging South Africa. Clinoptilolite is a natural, commonly available, and inexpensive zeolite found in SA, which can be used by impoverished communities for MD contaminated surface and groundwater treatment. The results indicated that the adsorption capacity of the clinoptilolite increased with a decrease in pH, albeit an indication that the adsorption is better when the solution is closer to a neutral pH with the Freundlich isotherm describing the adsorption capacity. It was indicated that the activated clinoptilolite used is suited both for acid and alkaline mine drainage. Furthermore, a Pseudo-second order kinetic model best described the adsorption of the investigated heavy metals.

Keywords: Acid mine drainage; Clinoptilolite; Adsorption; pH; Zeolite

1. INTRODUCTION

It is estimated that more than 300 million people in Africa do not have access to safe drinking water (Xu & Usher, 2006). South Africa (SA) is classified to be a water-stressed country (Donnenfeld, et al., 2018). The continuous population growth, urbanisation and pollution of available water sources may contribute to physical water scarcity in SA by the year 2025 (Otieno & Ochieng, 2004). For many years the mining sector has dominated SA's political, social and economic landscape (Minerals Council South Africa, 2021). However, the greatest impact of mining activities is its effects on water sources (Jhariya & Khan, 2016). The continuing increase in environmental contamination in SA is concerning (Agbenyeky, et al., 2016). Mining activities produce large quantities of solid waste and heavy metal-containing leachates which contaminate surface and groundwater sources (Munnik, 2020). Transport of heavy metals to various groundwater sources is not only dependent on the physiochemical properties of the metals but more so on the soil through which they travel (Dube, et al., 2001). Mainly due to its sorption properties, soil has the ability to immobilise heavy metal ions (Dube, et al., 2001). When a study of natural zeolites that occur in SA was done it was found that the main constituent of the zeolites present was clinoptilolite, with quartz being one of the most common impurities (Diale, et al., 2011). Due to its abundance, clinoptilolite is cheap. This study was focussed on the kinetic modelling, isotherm determination and pH effects on the adsorption of selected heavy metals prevalent in mine drainage (MD) onto table salt activated clinoptilolite (AC).

2. MATERIALS AND METHODS

I. Clinoptilolite, chemical reagents and mine drainage

Clinoptilolite used for the experiments (VLTR Creek Clinoptilolite 0.8 – 4 mm), was ordered from ChemLite Technologies (Johannesburg, SA). The $ZnCl_2$, $Cd(NO_3)_2$, $MnCl_2$ and $Pb(NO_3)_2$ were ordered from ACE Chemicals (Johannesburg, SA). All the materials were commercial grade while stock solutions were made with distilled water. Alkaline and acid mine drainage samples used were collected from mining environments in Middelburg and Witbank, SA.

II. Preparation of the clinoptilolite, metal concentrations and isotherm/kinetic model studies

AC (5 kg), i.e., activated by slurrification with 5 L of 100 g/L table salt solution and baked at 110°C for 24 hrs, was used.
For the effect of initial metal concentration on adsorption for isotherm models, individual metal solutions were prepared, namely 25, 50, 75, 100, 125 and 150 mg/L. The solutions were poured into 250 mL Erlenmeyer flasks and 0.5g of AC was added to each flask. All the samples were put into the shaking incubator at 25°C and 160 rpm for 90 minutes; thereafter, the slurries were centrifuged at 4000 rpm for 5 minutes to recover a clear solution.
Similarly, contact time effects for kinetic models were conducted using 100 mL of 100 mg/L of individual metal solutions, in 250 mL Erlenmeyer flasks with 0.5 g of AC using a sampling regime of 20, 40, 60, 80, 100 and 120 minutes using a shaking incubator at 25°C and 160 rpm. All samples during this step were also centrifuged at 4000 rpm for 5 minutes.
For pH effect analysis, i.e., at 3, 5 and 7, lead solutions were susceptible to precipitation, therefore were excluded with a mixture of metal solutions, i.e., all metals in a single solution, being at 400 mg/L. HCl was used to decrease the pH and NaOH to increase the pH of the solutions.
All experiments were done in triplicates.

III. Adsorption column studies

Adsorption columns (height: 23cm, diameter: 2.5cm, made of Perspex) loaded to a height of 5 cm of AC and 10 pore volumes of each pH variation of the mixed metal solution pumped at 5 mL/min, were used. Each pore volume of filtrate was collected sent for ICP analysis (EPA Method 6020B). The column experiments were repeated using real acid and alkaline mine drainage samples. All experiments were done in triplicate.

3. RESULTS AND DISCUSSION

The model parameters for each metal are listed in Table 1. The best isotherm for the adsorption of the selected heavy metals onto the AC was determined by considering the coefficient of determination (R^2 values), with Freundlich's isotherm describing the adsorption. This indicated that the adsorption process occurs through a heterogeneous binding to the surface and therefore implying that there are many layers involved in the adsorption. Furthermore, Pseudo-second-order was found to be the better fit, indicating that the surface adsorption involved, is chemisorption, i.e., the rate-limiting step; an indication that there was a stronger interaction between the surface of the AC and the heavy metal ions studied. Furthermore, at all pH's the adsorption of cadmium was least effective. This result correlates to the results obtained by (Erdem, et al., 2004) and is therefore likely due to the cadmium ion having the largest diameter resulting in less cadmium ions penetrating the small diameter channels of the adsorbent. It was also found that the initial metal concentrations were considerably lower than that of the sodium. The sodium in the filtrate decreases with an increase in pore volumes pumped to the column. This indicates that the metal ions are exchanged with the sodium ions on the surface of the clinoptilolite. This result therefore supports the ion-exchange properties of clinoptilolite stated by (Zanin, et al., 2017). Overall, the adsorption of each metal is directly proportional to the pH of the metal solution. The decrease in adsorption of the heavy metals in the more acidic solutions are due to the heavy metal ions having to compete with a larger concentration of proton ions to bind to the surface of the clinoptilolite. The surface of the clinoptilolite is therefore saturated quicker, decreasing the opportunities for the heavy metal ions to bind to the surface of the clinoptilolite resulting in more heavy metals present in the filtrate. In the neutral solution the concentration of the proton ions is less, resulting in the delay of surface saturation of the clinoptilolite. More heavy metal ions thus bind to the surface of the clinoptilolite causing

the heavy metal concentration in the filtrate to be lower. Adsorption of heavy metals from real alkaline and acid mine drainage samples were also successful at up to 80 % metal removal.

Table 1: Isotherm and kinetic model parameters

Isotherm/ Kinetic model	Adsorbent	Metal	q_m (mg/g)	k (L/mg)	R^2	n	k_F	q_e(exp) (mg/g)	q_e(calc) (mg/g)	k_1 (min^{-1})	k_2 ($\frac{g}{mg}/min$)
Langmuir	Clinoptilolite	Cadmium	9.07	0.02	0.94	-	-	-	-	-	-
		Manganese	4.68	0.01	0.65	-	-	-	-	-	-
		Zinc	12.3	0.02	0.91	-	-	-	-	-	-
		Lead	31.1	0.71	0.97	-	-	-	-	-	-
Freundlich	Clinoptilolite	Cadmium	-	-	0.96	1.96	0.60	-	-	-	-
		Manganese	-	-	0.70	1.99	0.28	-	-	-	-
		Zinc	-	-	0.97	1.82	0.64	-	-	-	-
		Lead	-	-	0.98	2.52	11.9	-	-	-	-
Pseudo-first order	Clinoptilolite	Cadmium	-	-	0.92	-	-	20	17.5	0.008	-
		Manganese	-	-	0.90	-	-	20	18.5	0.003	-
		Zinc	-	-	0.94	-	-	20	15.6	0.006	-
		Lead	-	-	0.88	-	-	20	7.92	0.085	-
Pseudo-second order	Clinoptilolite	Cadmium	-	-	0.94	-	-	20	12.9	-	812.2
		Manganese	-	-	0.98	-	-	20	5.63	-	280.28
		Zinc	-	-	0.97	-	-	20	9.96	-	252.8
		Lead	-	-	0.99	-	-	20	21.5	-	190.01

4. CONCLUSION

In this study, the adsorptive nature of table salt activated clinoptilolite and the influence of pH on its selected heavy metal adsorption capacity were investigated. The Freundlich isotherm model and the Pseudo-second order kinetic models better described the adsorption. It was also found that the adsorption capacity of the clinoptilolite increases as the pH decreases. Application of clinoptilolite in poor communities besieged by AMD can thus be adopted to remediate surface and ground water.

[1] Email: leandridekker@gmail.com
MEng: Chem Eng student
North-West University SA
Student number: 27233448

Acknowledgements

I would firstly like to thank my supervisors Prof. Karabo Ntwampe, Prof. Frans Waanders and Mr. Ruveix van Coller for their continual support and guidance throughout the course of the study. Secondly, I would like to thank Mrs. Renè Bekker for all her assistance with the experimental work. Finally, a word of gratitude to all my family and friends for their support.

Abstract

South Africa (SA) is a water scarce country, with 34 % of SA's total population living in rural areas with very limited access to safe surface and groundwater sources. The pollution of these water sources is caused by many natural and anthropic causes, with industrial effluents being of the greatest impact. Adsorption column experiments were conducted to investigate the influence of pH, water hardness and mineral characteristics on the adsorptive capacity of the zeolite, clinoptilolite, for the removal of heavy metals prevalent in mine drainage (MD) besieging in SA. Clinoptilolite is a natural, commonly available, and inexpensive zeolite found in SA, which can be used by impoverished communities for MD contaminated surface and groundwater treatment. The results indicated that the adsorption capacity of the clinoptilolite increases with a decrease in pH, albeit an indication that the adsorption is better when the solution is closer to a neutral pH with the Freundlich isotherm describing the adsorption capacity. It was indicated that the activated clinoptilolite used, is suited both for acid and alkaline mine drainage. A Pseudo-second order kinetic model best described the adsorption of the investigated heavy metals. Furthermore, it was indicated that due to its crystal structure, the impurity quartz, does not consist of a large adsorption capacity.

Keywords: Adsorption, Clinoptilolite, Heavy metals, Mine drainage, Zeolite

Table of Contents

Nomenclature

Zn^{2+}	Zinc ion
Pb^{2+}	Lead ion
Cd^{2+}	Cadmium ion
Cu^{2+}	Copper ion
Mn^{2+}	Manganese ion
Ni^{2+}	Nickel ion
FeS_2	Iron disulphide
m^3	Cubic meter
%	Percentage
mg/L	Milligram per Litre
cm^3/min	Cubic centimetre per minute
cm	centimetre
m/sec	Meter per second
mV	millivolt
$NaCl$	Sodium chloride
°C	Degrees Celsius
mm	millimetre
$ZnCl_2$	Zinc chloride
$Cd(NO_3)_2$	Cadmium nitrate
$MnCl_2$	Manganese(II) chloride
$Pb(NO_3)_2$	Lead(II) nitrate
kg	kilogram
rpm	Revolutions per minute
hrs	Hours
g	gram

mL/min	Millilitre per minute
µm	Micrometre
Θ	Theta
°	Degree
Al_2O_3	Aluminium Oxide
SiO_2	Silicon dioxide
Na_2O	Sodium oxide
MgO	Magnesium oxide
P_2O_5	Phosphorus oxide
K_2O	Potassium oxide
CaO	Calcium oxide
MnO	Manganese(II) oxide
Fe_2O_3	Ferric oxide
mg/g	Milligram per gram

Abbreviations

SA	South Africa
MD	Mine drainage
AMD	Acid mine drainage
WHO	World Health Organisation
AC	Activated clinoptilolite
PSD	Particle size distribution
GPD	Gross domestic product
DNA	Deoxyribonucleic acid
SEM-EDS	Scanning electron microscopy-energy dispersive spectroscopy

XRD	X-ray diffraction
XRF	X-ray fluorescence
FT-IR	Fourier-transform infrared spectroscopy
ICP-EOS	Inductively coupled plasma – optical emission spectrometry

List of tables

List of figures

Chapter 1: Introduction

1. Chapter 1: Introduction

1.1 Background and motivation

It is estimated that more than 300 million people in Africa do not have access to safe drinking water (Xu & Usher, 2006). South Africa (SA) is classified to be a water stressed country (Donnenfeld, et al., 2018). The continuous population growth, urbanisation and pollution of available water sources may contribute to physical water scarcity in SA by the year 2025 (Otieno & Ochieng, 2004). SA has an annual freshwater availability of less than 1000 m^3 per capita which is far less than the 1700 m^3 of renewable water resources per capita per year that The Falkenmark indicator proposes (Risjberman, 2005).

Numerous countries in Africa are dependent on groundwater as their main source of drinking water and domestic water supply (Xu & Usher, 2006). However, these groundwater supplies are threatened by human activities (Xu & Usher, 2006) with natural and anthropogenic factors causing contamination of the groundwater sources (Stefanakis, et al., 2015). Anthropogenic factors that affect the quality of the groundwater supplies include urban development, agriculture and mining activities (Stefanakis, et al., 2015).

Mining in SA started in the early 1850's (Mining in Africa, 2017) and for many years the mining sector has dominated SA's political, social and economic landscape (Minerals Council South Africa, 2021). In 2018, 456438 people were employed and R 351 billion was contributed to the South African gross domestic product (GDP) by the mining sector (Minerals Council South Africa, 2021). However, the greatest impact of mining activities is its effects on water sources (Jhariya & Khan, 2016) and the continuing increase in environmental contamination in SA is attracting major concerns (Agbenyeky, et al., 2016). Mining activities produce an enormous amount of solid waste and heavy metal containing leachates which can contaminate surface and groundwater sources (Munnik, 2020). Heavy metal pollution of these groundwater sources may also lead to soil contamination (Duruibe, et al., 2007) and can have bio toxic effects, may be life threatening to humans and can have serious effects on the environment (Duruibe, et al., 2007).

Mining activities bring forth another major pollutant, namely acid mine drainage (AMD). AMD is most typically formed when iron disulphide (FeS_2), or pyrite, reacts in the presence of oxygen and water to produce a product containing sulphuric acid (Gray, 1997). Records of AMD have been found where coal, silver, copper, lead and pyritic sulphur among others have been mined (Gray, 1997). AMD frequently consists of high concentrations of copper, manganese, lead, zinc, iron,

arsenic and sulphates (Luis, et al., 2009). AMD negatively impacts various water sources, causing ecological damage and serious health risks are associated with heavy metal toxicity (Sankhla, et al., 2016).

It is important to note that the transport of heavy metals to various groundwater sources is not only dependent on the physiochemical properties of the metals, but more so of the soil through which it travels (Dube, et al., 2001). Mainly due to its sorption properties, soil has the ability to immobilise heavy metal ions (Dube, et al., 2001). Zeolites are porous aluminosilicates and due to its structure, ion exchange is allowed (Zanin, et al., 2017). When a study of natural zeolites that occur in South Africa was done, it was found that the main constituent of the zeolites present was clinoptilolite, with quartz being one of the most common impurities (Diale, et al., 2011). Therefore, for adsorption studies, clinoptilolite is the best zeolite to be used as it is the most abundant zeolite in SA.

The effect of water hardness on the adsorption of heavy metals is not widely investigated (Panayotova & Velikov, 2003) where the water hardness is simply defined as the amount of dissolved minerals (largely magnesium and calcium) present in the water (USGS, 2021). The hardness of water is variable and completely dependent on the location of the water sources. Water hardness can vary from being “soft”, “moderately hard” and “very hard” when the concentration of the dissolved minerals is 0 – 60 mg/L, 61 – 120 mg/L and above 180 mg/L, respectively (Romano, et al., 2020).

In the present study the adsorptive nature of the natural zeolite, clinoptilolite, and the influence of pH and water hardness on the adsorption capacity of the adsorbent will be investigated.

1.2 Aim and Objectives

The aim of the study is to determine the impact of the sorptive nature of zeolite, as a mineral phase of soil above aquifers, on the mobility of heavy metals towards underground water. A column set-up will be assembled to test the effectiveness of the proposed method. The adsorptive behaviour of cadmium, zinc, manganese and lead onto the zeolite will also be studied. The effect of pH and water hardness on the ion-exchange capability of the zeolite surface will also be investigated.

The objectives of this study are to determine the adsorptive behaviour of cadmium, zinc, manganese and lead onto the surface of the clinoptilolite, to determine the effect of aqueous solution properties on the adsorption of these heavy metals and to determine the effect of pH and water hardness on the breakthrough point.

1.3 Scope of the project

Analyses including FT-IR, XRD, XRF, SEM-EDS and BET will be done to determine the characterisation of the clinoptilolite with regards to its structure and ability to enable the adsorption of heavy metals. Various column adsorption experiments will be conducted to investigate the adsorptive properties of the clinoptilolite, furthermore determining the influence of the aqueous solution properties on the adsorption capacity of the zeolite. In order to achieve the objectives set for the project, the report is divided into five chapters, where Chapter 1 gave the Introduction to the project:

Chapter 2 – Literature review: The literature review discusses water sources, their availability in arid and semi-arid regions, mining operations as a source of groundwater pollution, AMD migration and the pollution of soil and aquatic environments, water hardness and the effect of pH on adsorption, clinoptilolite as adsorbent and adsorption studies.

Chapter 3 – Methodology: will list the chemicals, equipment and instruments that was used to conduct all the experimental work. The method in which the various experiments were completed, will also be included.

Chapter 4 – Results and discussion: will firstly include the results obtained from the characterisation analyses. Secondly, the results obtained from the isotherm and kinetic studies will be discussed. Thirdly, the effect of the adsorbent particle size on the adsorption will be discussed followed by the effect of pH on the heavy metal adsorption. Fifthly, the results of the effect of water hardness on the adsorption will discussed and lastly, the effect of mineral characteristics will be presented.

Chapter 5 – Conclusion and recommendations: will summarise the final remarks of the results obtained and give recommendations for future studies.

Chapter 2: Literature Survey

2. Chapter 2: Literature Survey

Section 1: Water sources, availability and pollution in arid and semi-arid regions

I. Water as a scarce resource

Due to the physical descriptors like the increase in water demands and climate conditions, there are many regions globally where freshwater resources are inadequate to meet domestic, economic and environmental needs (Cosgrove & Loucks, 2015). It is estimated that 1.2 billion people globally do not have access to safe and affordable water for domestic use (Rijsberman, 2005). The lack of access to water that is safe for drinking and sanitation, causes many health issues (Rijsberman, 2005) and more challenges are posed by a rapid growth in population, globalisation and urbanisation (Cosgrove & Loucks, 2015). SA is considered as a water-scarce country (Mnisi, 2020) and Roodbol (2020) indicated that if the current rate of water usage in SA continues, the demand will most likely exceed the supply and availability of the economically usable freshwater resources. Therefore, various different water treatment techniques are studied to achieve more efficient and more cost-effective ways to remove contaminants from water (Fosso-Kankeu, et al., 2016).

II. Groundwater as a reliable water source in arid and semi-arid regions

It is projected that one third of the world population is dependent on groundwater as their primary source of drinking water (Gyamfi, et al., 2019) and it should also be mentioned that the groundwater is also used for various other domestic purposes. Especially in developing countries, groundwater is preferred as source for drinking water as it requires less treatment and it minimises the spread of water-borne diseases due to its better bacteriological quality (Appelo & Postma, 2010). Many activities contribute to the pollution of groundwater. The most common anthropogenic activities that influence groundwater quality either directly or indirectly, include indiscriminate waste disposal, farming and mining (Gyamfi, et al., 2019). For this study the focus will be placed on the pollution of groundwater due to mining activities.

Section 2: Mining operations as a source of groundwater pollution

I. Mining in South Africa

Mining activities in SA are of the largest contributors to the South African economy with an estimated worth of R20.3 trillion and accordingly, the mining sector accounts for one-third of the market capitalisation of the JSE (Kearney, 2012). However, the mining industry is also known for its role in causing important environmental pollution (Modoi, et al., 2014). Mining activities produce waste at numerous stages of the processing of the ore (Gyamfi, et al., 2019). Waste produced by mining activities is the largest amount of materials that is currently been handled globally (Blowes, et al., 2003). The waste generated by mining activities have the potential to penetrate the aquifers which leads to the direct pollution of the groundwater. Heavy metals that can be found in polluted mining water include lead, cadmium, copper, zinc and manganese. (Wang, et al., 2018). These heavy metals can cause serious health and ecological effects.

II. Impact of acid mine drainage on groundwater sources

In most cases, effluents produced from mining activities have a low pH. The low pH of these effluents results in acid mine drainage (AMD) (Gyamfi, et al., 2019). The acidic effluents contain sulphates which contaminate the groundwater (Gyamfi, et al., 2019). AMD contains many toxic metals including copper, arsenic, aluminium, iron and zinc that are dissolved in the solution (Natarajan, 2018) and is an unavoidable by-product of the mining industry (Kumari, et al., 2010). It is not only responsible for surface water contamination, but also for the degradation of the soil quality, aquatic ecosystems and the leaching of heavy metals into groundwater sources (Kumari, et al., 2010).

III. Differentiation of alkaline mine drainage

Another concern is alkaline mine drainage. According to Banks et al., (2002), alkaline mine drainage is the result of a small content of sulphide minerals, the presence of monosulphides rather than marcasite or pyrite, a restricted oxidation-rate due to a large pyrite grain-size, the neutralisation of acid by carbonate or basic silicate minerals, neutralisation of acid by natural occurring alkaline groundwaters, ineffective contact between circulating water and the

sulphide minerals, the lack of direct contact between oxygen and the sulphide minerals or due to the highly reducing nature of the influent water. Alkaline mine drainage also contains heavy metals, contributing to the heavy metal pollution of groundwater.

Section 3: AMD migration and the pollution of soil and aquatic environments

I. AMD migration through soil layers

As water is the main transport medium for contaminants, AMD migration control focusses mainly on controlling the water flow (Akcil & Koldas, 2006). The toxicity of heavy metals in the ecosystem does not only depend on their total concentrations, but also on their reactivity with other components and their mobility (Abollino & Barberis, 2002). The presence of carbonate and sulphur, the pH, adsorption and/or desorption are some of the most vital factors that affect the mobility of the heavy metals (Baran & Tarnawski, 2015). A common way to effectively study the mobility of an element in the soil, is by treatment with extractants and adsorbents with different chemical properties (Abollino & Barberis, 2002). A study on the mobility of metals through a soil layer was done by Lucia and McBride (1982) and they found that the mobility of metals depended more on the chemical properties of the soil, than the chemical properties of the metals.

Over the last 20 years, the behaviour of heavy metals in soil have been extensively studied and published (Wan Zuhairi, et al., 2008). A variety of procedures have been used to analyse the quality of soil with regards to heavy metal pollution (Gyamfi, et al., 2019), with one example being the geo-accumulation index (I_{geo}) In this method the soil contamination is assessed by comparing the concentrations of the heavy metals to their crustal levels (Gyamfi, et al., 2019).

Liu, et al., (2018) studied the migration of AMD pollutants in calcareous soil where different volumes of simulated AMD were added to soil columns containing 20 cm of surficial soil (refer to Figure 1). The filtrate as well as the soil were analysed and it was found that almost all of the iron ions (>99%) were retained by the soil and that >80% of the sulphate ions were retained. Copper was nearly totally retained by the soil, but copper did show the tendency to migrate downward with the gradual acidification of the upper soil.

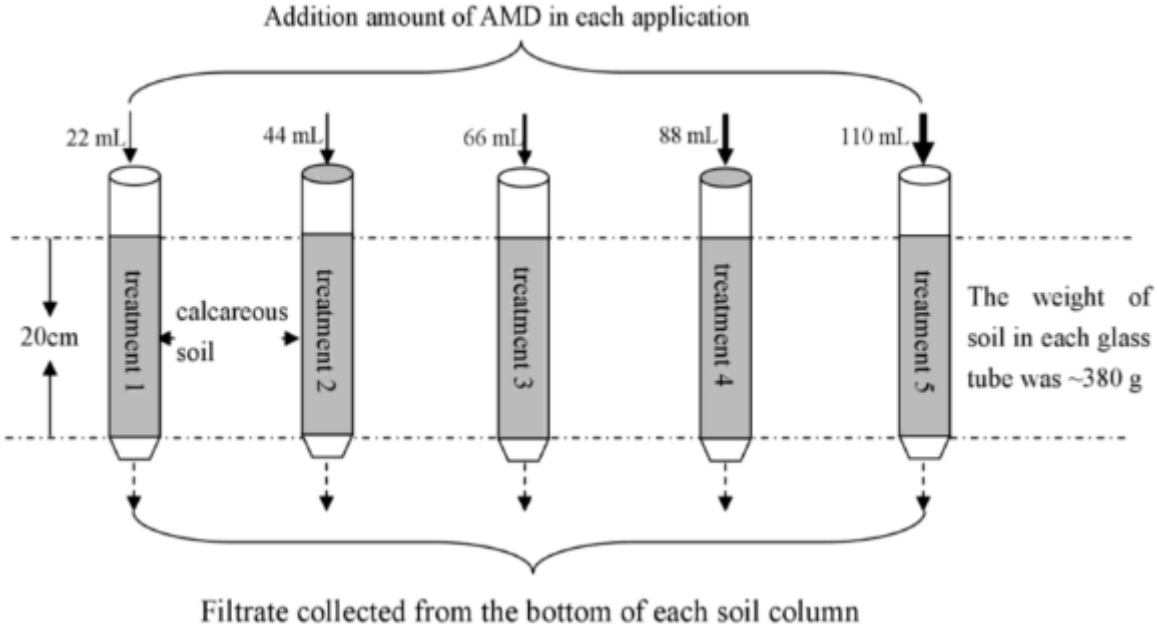

Figure 1: Schematic diagram of reaction columns (Liu, et al., 2018)

Soil has the capability to physically and chemically retard the movement of the leachate produced by mining activities (Wan Zuhairi, et al., 2008) due to the soil's capability to be compacted. The compacting ability allows very low hydraulic conductivity (less than $1 \times 10^{-9}\, m/sec$) to be achieved (Wan Zuhairi, et al., 2008). By doing this, the soil acts as a layer of protection to the groundwater against a leachate (Wan Zuhairi, et al., 2008).

In soil environments the adsorption and/or desorption as well as the chemical complexation with organic and inorganic ligands and redox reactions are important. It has become more common to use soil as a natural clay liner underneath landfill sites to prevent the seepage of leachate into groundwater sources (Wan Zuhairi, et al., 2008).

Huang, et al., (2009) studied the removal of ammonium ions from an aqueous solution using a natural zeolite found in China. In their study the pH of the solution, the particle size, contact time and the adsorbent dosage were varied and the results indicated that all the parameters had a noteworthy effect on the effective adsorption of the ammonium by the natural zeolite.

II. Adverse effects of heavy metal pollution in aquatic environments

The heavy metal contamination of aquatic environments is of crucial concern due to their potential toxicity and accumulation in the waterbodies (Kumar, et al., 2019). Metals are described as conservative contaminants that are not readily transformed in such a way that they can be

removed from the ecosystem (Butler, et al., 2017). Heavy metals in water can accumulate to a noxious level, which can lead to serious ecological impacts as well as problems for human health (Kumar, et al., 2019). Heavy metals are non-degradable (Kumar, et al., 2019) and due to the non-degradable characteristic of heavy metals, they bioaccumulate along the food chain. This can cause toxic effects far from the actual source of the pollution (Kumar, et al., 2019). The World Health Organisation (WHO) recommends a very low maximum acceptable heavy metal concentration in drinking water (Li, et al., 2019) as high doses of heavy metals are toxic to the human health, because the metals bond to sulphur groups which can interrupt cellular activity and it can also cause oxidative damage (Butler, et al., 2017). Heavy metals can cause DNA damage, cancer and it can also induce clastogenic and aneugenic effects which include mitosis and cytokinesis disturbances (Zanin, et al., 2017). Among biological systems high doses of heavy metals can damage plant cell structures and it can also inhibit enzymatic activity (Butler, et al., 2017).

III. Soil contamination

The level of contamination is linked to the soil solution as well as the surface chemistry of the soil matrix with reference to the metal and waste matrix in question (Goienaga & Madariaga, 2015).

Several methods have been used to analyse the soil quality around places with active mining activities (Gyamfi, et al., 2019). Awadh (2013) used the geo-accumulation (I_{geo}) index to assess the extent of the contamination of the soil in these mining areas by comparing the concentration of the heavy metals to their crustal levels. The concentration of the heavy metals in the soil were above the crustal levels which indicates that the soil in these areas has been contaminated.

Liao & Wei (2016) studied the effects of AMD in plant, soil and human health at the Dabaoshan mine in China. They found that although large scale mining activities were stopped in 2011, the soil was still heavily contaminated with heavy metals from the AMD that migrated through the soil layers. The soils were highly polluted with cadmium, copper and arsenic and the I_{geo} value was as high as 3.77, falling into the class 4 classification of the I_{geo} index which indicates that the soils are strongly polluted. The classification of I_{geo} index values are located in Table 1.

Table 1: Geo-accumulation classification (Banu, et al., 2013)

I_{geo} values	I_{geo} class	Description of soil quality
0	0	Uncontaminated

0-1	1	Uncontaminated to moderately contaminated
1-2	2	Moderately contaminated
2-3	3	Moderately to strongly contaminated
3-4	4	Strongly contaminated
4-5	5	Strongly to extremely contaminated
5-6	6	Extremely contaminated

Section 4: Water hardness and the effect of pH on adsorption

I. Water hardness

The natural sources of hardness in water are the dissolved polyvalent metallic ions that are present in runoff and seepage from soils as well as from sedimentary rocks (Cotruvo, et al., 2011). The two principal polluting ions present in sedimentary rocks are calcium and magnesium. Calcium concentrations in natural water sources, especially groundwater, can exceed 100 mg/L, whilst magnesium also contributes to water hardness, but the concentration of magnesium in natural groundwater usually varies from insignificant to about 50 mg/L and very seldom above 100 mg/L. Therefore calcium-based hardness usually dominates (Cotruvo, et al., 2011). Dharmappa, et al., (1995) studied the characterisation of mining wastewater and found that the considerable amount of dissolved minerals results in the increasing hardness of the water.

Excess intake of calcium in humans can cause the reduction in magnesium, zinc and phosphorus absorption within the intestine as the calcium interacts with these metals before they can be absorbed (Cotruvo, et al., 2011). The increased intake of magnesium can have a laxative effect. Another health effect regarding the exposure of hardwater include the potential to exacerbate eczema (Cotruvo, et al., 2011). The general classifications of water hardness are: 0 mg/L – 60 mg/L of calcium carbonate is classified as soft, 61 mg/L – 120 mg/L is classified as moderately hard, 121 mg/L – 180 mg/L is classified as hard and concentrations that exceed 180 mg/L is classified as very hard (USGS, 2021).

Zeledon-Toruno, et al., (2005) studied the effect of water hardness on the adsorption of Ni(II) Cu(II) from an aqueous solution onto leonardite (an oxidation product of lignite). The results

indicated that the presence of the calcium ions influenced the removal of both of the metals, although the adsorption of the nickel was reduced to a further extend by the calcium ions than that of copper.

Martins & Boaventura (2004) studied the biosorption of zinc(II) and cadmium(II) ions onto an aquatic moss, namely *Fontinalis antipyretica* under different varying conditions including temperature, pH and water hardness. The cadmium removal was not affected by the presence of the calcium ions and as the hardness of the water increased, the competition between the zinc ions and the calcium ions, strongly reduced the affinity of the bio sorbent for zinc.

Dryer, et al., (2018) investigated the effect of magnesium and calcium concentrations on the adsorption of caesium and strontium using clinoptilolite as adsorbent. The study found that the calcium and magnesium ions compete with the caesium and strontium ions for adsorption. Higher concentrations of the calcium and magnesium ions resulted in the reduced removal from caesium and strontium ions from an aqueous solution. Higher concentrations of the competing ions also resulted in faster adsorbent saturation.

From these studies it is clear that the presence of calcium and magnesium ions in hardwater has different effects on metal adsorption depending on the adsorbent used. The studies also indicated that the effect that the hardwater has on the adsorption of metals onto an adsorbent will likely differ for different heavy metals. The effect that hard water will have on the adsorption capacity and efficiency of the metal removal using clinoptilolite as adsorbent should therefore be tested, both in single as well as multi-metal solutions.

II. Effect of pH on adsorption

The influence of pH on the heavy metal removal using the process of ion exchange has been reviewed in other reports (Sprynskyy, et al., 2006). Zeolites in nature are generally weakly acidic and sodium-form exchangers are more selective for hydrogen ions (Erdem, et al., 2004). Kithome, et al., (1999) studied the effect of pH on the adsorption capacity of clinoptilolite with regards to the adsorption of ammonium ions. The study concluded that the amount of ammonium ions adsorbed increased as the pH increased. No comments were made as to why this was the case. However, the effect of pH and temperature on the adsorption capacity of clinoptilolite with regards to Cd(II) and Pb(II) was also studied by Berber-Mendoza, et al., (2006). They found that by increasing the pH of the metal solution from 2 to 6 (at constant temperature), the negative charge of the zeolite surface increased from -12 mV to -36 mV. The negative charge of the zeolite surface also slightly increased by increasing the pH from 6 to 7. It was found that the cadmium and lead ions in the solution were attracted to the more negatively charged zeolite surface. The study

concluded that the ion exchange capacity of the zeolite increased with an increase in pH as more cations were attracted to the surface of the zeolite at these conditions. Erdem, et al., (2004) also studied the influence of pH on the adsorption of heavy metals and concluded that the adsorption of the heavy metals decreases with a decrease in pH due to the increase in competition between the metal ions and the increased hydrogen ions at a lower pH. As the pH increases, the concentration of the hydrogen ions decreases and the metals can adsorb onto the surface of the clinoptilolite with less competitor ions (Erdem, et al., 2004). The adsorption of the heavy metals onto the clinoptilolite is therefore directly proportional to the pH of the solutions.

Section 5: Clinoptilolite as adsorbent and adsorption studies

I. Clinoptilolite as natural zeolite

Electrochemical treatment, chemical treatment and reverse osmosis can effectively be used to decrease the heavy metal concentration in water; however, the application of these methods is costly (Li, et al., 2019). Coagulation and flocculation are also common methods for the treatment of industrial effluents, but due to the low efficiency of these processes to remove heavy metals from the wastewater, other treatment techniques are required. Alternative techniques like membrane filtration have been studied for the treatment of wastewater contaminated with heavy metals; however, it was found that adsorption was one of the most effective and economical treatment options. Sorption and ion-exchange are preferred for removing heavy metals from wastewater due to easy handling (Sprynskyy, et al., 2006). The zeolite group is the main group of minerals that can be used for mitigation amid the silicates and it includes more than 40 species that occur naturally (Can, et al., 2010). Zeolites are highly porous crystalline aluminosilicates which have different cavity and channel structures that make them a popular choice for adsorbents (Li, et al., 2019). Zeolites have a negatively charged lattice structure and it consist of a three-dimensional framework and the cations that balance the negative charge of zeolites will be exchanged with other cations present in solution (Li, et al., 2019). These cations can then be exchanged with certain cations in solutions including cadmium, zinc, manganese and lead (Erdem, et al., 2004). The exchangeable cations on zeolites are relatively innocuous which makes zeolites suitable for removing heavy metal ions that are present in industrial effluent water (Erdem, et al., 2004). Several factors influence the ion-exchange process in zeolites and can include concentration, temperature, pH-level, nature of cations and anions and the crystal structure of the zeolites (Sprynskyy, et al., 2006). Clinoptilolite has previously been used as ion-exchanger in hydrometallurgical processes (Mamba, et al., 2009).

Clinoptilolite is the most common natural zeolite and is part of the heulandite family (Sprynskyy, et al., 2006). It has the following chemical formula $(Na, K, Ca)_4Al_6Si_{30}O_{72}\bullet 24H_2O$. The three-dimensional structure of clinoptilolite is given in Figure 2.

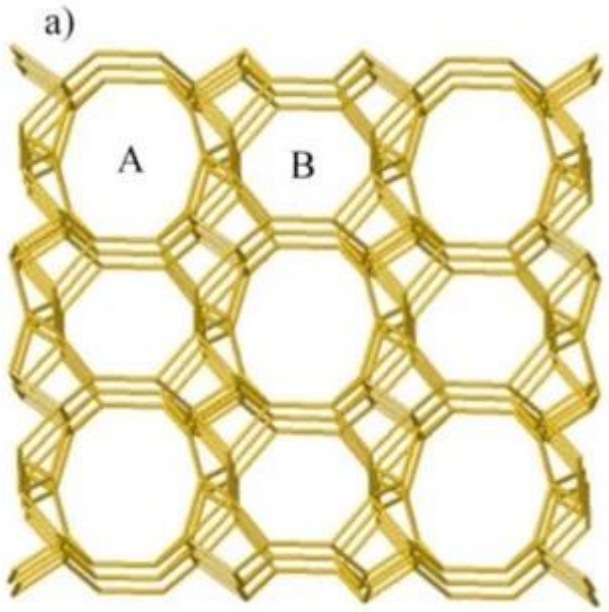

Figure 2: Three-dimensional structure of clinoptilolite (Castro De Souza, et al., 2018)

The effectiveness of the adsorption of heavy metals by clinoptilolite is contributed to its special porous cage structure, stable skeleton structure, its availability and low cost (Wang, et al., 2018). Quartz and clinoptilolite are very common mineral phases that are present in rock fractures or in the rock matrix (Prikryl, et al., 2001). Therefore, to get a more comprehensive idea of the sorptive properties of these mineral phases in a natural environment, experiments involving both clinoptilolite and quartz should be conducted. The aim of this study will be to determine how these mineral phases impact the mobility of heavy metals towards groundwater and to achieve this, a column study will be done. Haile & Fuerhacker (2018) investigated the adsorbent capacity of natural quartz sand, sandy soil and three mineral-based technical filter media to remove heavy metals from stormwater. The study indicated that the quartz sand had the lowest adsorption capacity. This result was attributed to the low surface area and few sorption sites present on the quartz.

Zanin, et al., (2017) performed adsorption experiments with clinoptilolite as adsorbent for copper(II), chromium(III) and iron(III) from wastewater. The kinetic assays performed for each of the metals indicated a removal of up to 95.4% iron, 96.0% copper and 85.1% chromium at 25°C and a pH of 4. The adsorption mechanism for copper and chromium followed a pseudo-first order

kinetic model and the adsorption mechanism for iron followed a pseudo-second order kinetic model (Zanin, et al., 2017). Li, et al., (2019) studied the adsorption and regeneration behaviour of modified synthetic clinoptilolite including the competitive adsorption behaviour of $Zn^{2+}, Pb^{2+}, Cd^{2+}\ and\ Cu^{2+}$. The study indicated that the adsorption capacity of $NaCl$ −modified synthetic clinoptilolite is much greater than the values reported in studies on both modified and unmodified natural clinoptilolite. The kinetic study indicated that the pseudo-second-order model describes the adsorption of the $NaCl$ −modified synthetic clinoptilolite better. An isotherm study revealed that the Langmuir isotherm model best suited the adsorption process of $NaCl$ −modified synthetic clinoptilolite. However, synthesis of clinoptilolite is not easy and studies in the process of synthesising clinoptilolite is also very limited. The reserve of natural clinoptilolite, on the other hand, is large (Li, et al., 2019).

Although there is a great interest in the ion-exchange properties of clinoptilolite, limited studies have been done on the effect of other ions on the heavy metal adsorption from mixed solutions (Sprynskyy, et al., 2006). The investigation of competitive adsorption suggests that some of the cation sites in the open-framework of clinoptilolite can be exchanged by only a selective group of alien cations (Li, et al., 2019). Characterisation of the clinoptilolite will include determining the morphology and elements composition (SEM-EDS), determining the mineralogical composition (XRD) and particle size distribution (Malvern mastersizer). FTIR analysis of the clinoptilolite will be done to determine the functional groups present. Presence of the OH-functional groups will indicate strong interactions between the adsorbed molecules and the zeolite (Akimkhan, 2012). The clinoptilolite will be activated using a sodium chloride solution as sodium was found to be the most effective exchangeable ion for the removal of heavy metals (Zamzow & Murphy, 2006).

II. Porosity and the effect of particle size

The porous structure of clinoptilolite was further investigated by Sprynskyy, et al., 2010. In this study it was found that the porous structure of the clinoptilolite is heterogeneous in nature with both primary porosity and secondary porosity being observed (Sprynskyy, et al., 2010). The primary porosity of the clinoptilolite is presented by the nanotube system of the clinoptilolite framework and is defined as microporosity (Sprynskyy, et al., 2010). Meso- and macropores forms the secondary porosity where the mesopores are due to the cleavability of the zeolite crystallite and the macropores are located between the blocks of zeolite crystallite and these pores may be different in form (Sprynskyy, et al., 2010).

Sprynskyy, et al., (2006) investigated the effect of the particle size of the clinoptilolite on the adsorption of $Pb^{2+}, Cu^{2+}, Cd^{2+}$ and Ni^{2+}. It was found that the adsorbed amount of all four metals

increased with a decrease in the particle size fraction of the clinoptilolite. This was explained by the accessibility of the adsorption centres improving as the sorbent fractions decreases (Sprynskyy, et al., 2006). Furthermore, it was found that the finer fractions of the clinoptilolite crystals have a higher cleavage which aids in the growth of the mesoporosity of the clinoptilolite which increases the accessibility to adsorption centres (Sprynskyy, et al., 2006).

III. Ion exchange

One of the most important properties of zeolites is its ability to assist in ion exchange (Sherry, 2003). Ion exchange entails a diffusion process that results in the exchange of ions between a liquid and a solid phase (Inglezakis, 2005). Ion exchange is the most attractive form of water treatment when the ion exchanger that is used is both effective and low-cost (Sprynskyy, et al., 2006). Therefore, it is a very popular method used for the treatment of municipal and industrial wastewater to remove several toxic substances (Inglezakis, 2005). To obtain the ion exchange capacity of a possible adsorbent (in this case clinoptilolite), a certain quantity of the zeolite is added to a quantity of solution at a constant temperature for a period of time. These two phases are then separated and one of the phases are analysed to determine the effect to which ions had been exchanged (Sherry, 2003). The porosity of the zeolite can enhance the adsorption of heavy metals by increasing the ion exchange rate of the zeolite (Ismail, et al., 2010).

IV. Column experiments

Column experiments offer a useful way to investigate the migration and attenuation of heavy metals through a soil layer (Wan Zuhairi, et al., 2008). Zeolite constitutes a large part of the mineralogical constitution close to an aquifer. Metals in aqueous solutions migrating to the groundwater sources have to pass through this layer of minerals, making the layer a perfect source for contaminant adsorption.

Can, et al., (2010) used column experiments to determine the adsorptive nature of zeolite tuff rich in clinoptilolite on copper, nickel and cobalt from metal (II) nitrate solutions at various concentrations. Experiments were conducted in a Pyrex ion exchange column with a height of 30 cm and an inner diameter of 1.5 cm. The feed was pumped with the use of a Cole-Parmer diaphragm pump. The flow rate varied from 1 to 50 cm^3/min. Samples were collected at specific time intervals and sent for ICP-EOS analyses. The study indicated that efficient metal ion removal is possible by using clinoptilolite rich tuff.

Baker, et al., (2009) did a study regarding the adsorption behaviour of natural Jordanian zeolites with regards to $Cd^{2+}, Cu^{2+}, Pb^{2+}$ and Zn^{2+} using glass column experiments. The concentration of metal ions ranged from 5 to 20 mg/L, the average particle size of the zeolite ranged from 90 to 350 µm and the ionic strength ranged from 0.01 to 0.05. The results of the study indicated that the zeolite tuff is an effective ion exchanger for the removal of heavy metals.

Medvidovic, et al., (2006) used column experiments to investigate the adsorption of lead ions from a solution using a fixed bed of zeolite. The experiments were carried out in two glass columns with a height of 500 mm and an internal diameter of 12 mm. The columns were filled with zeolite with particle sizes of 0.6 mm - 0.8 mm and 0.1 mm – 0.5 mm, respectively. The zeolite bed in both columns were kept constant at 115 mm (or 13 cm^3). The results showed that lead can effectively be adsorbed from a solution by means of an ion exchange process on the surface of the natural zeolite (clinoptilolite).

Section 6: Study parameters

The sorptive behaviour of heavy metals including zinc, manganese and cadmium will be studied. The effect of water hardness on the adsorptive behaviour of the heavy metals onto the mineral phases will also be studied to determine how the characteristics of the mining wastewater will affect the retentive qualities of the adsorbents. The effect of pH on the adsorption capacity of heavy metals onto the clinoptilolite will also be investigated. Furthermore, real life scenarios will be simulated to determine to what extend the soil can delay the contamination of groundwater by toxic metals by contacting real AMD and alkaline mine drainage samples with the zeolite.

Chapter 3: Methodology

3. Chapter 3: Methodology

3.1 Clinoptilolite and Chemicals

The clinoptilolite used for the experiments (VLTR Creek Clinoptilolite 0.8 – 4 mm), was ordered from ChemLite Technologies (Johannesburg, SA). The $ZnCl_2$, $Cd(NO_3)_2$, $MnCl_2$ and $Pb(NO_3)_2$ were ordered from ACE Chemicals (Johannesburg, SA). All the materials were commercial grade while stock solutions were made with distilled water.

I. Alkaline mine drainage

The real alkaline mine drainage samples that were used for various investigative experiments throughout the study was collected from the mining environments in Middelburg, SA. The analysis of the sample is given in Table 2.

Table 2: Alkaline mine drainage sample analysis

Parameter	**Unit**	**Value**
Conductivity	mS/m	430
pH	-	8.22
Temperature	°C	21
Turbidity	NTU	13.1
Calcium	mg/L	117
Magnesium	mg/L	84.5
Potassium	mg/L	14.9
Sodium	mg/L	744

II. Acid mine drainage

The acid mine drainage that was used was collected in the mining environment of Witbank, SA. The analysis of the sample is given in Table 3.

Table 3: Acid mine drainage sample analysis

Parameter	Unit	Value
pH		2.33
Temperature	°C	25
Sodium	mg/L	69.91
Calcium	mg/L	85.69
Magnesium	mg/L	46.27
Potassium	mg/L	8.9
Aluminium	mg/L	51.04
Iron	mg/L	19.03
Manganese	mg/L	7.80

3.2 Equipment and instruments

To execute the column experiments, four clear columns (height: 23 cm, diameter: 2.5 cm, made of Perspex) were used. A peristaltic pump, shaking incubator, magnetic stirrer and centrifuge were the main equipment used.

3.3 Preparation of the clinoptilolite, metal concentrations and isotherm/kinetic model studies

Activated clinoptilolite (AC) (5 kg), i.e., activated by slurrification with 5 L of 100 g/L table salt solution and baked at 110°C for 24 hrs, was used. The AC is shown in Figure 4.

For the effect of determining the initial metal concentration on adsorption for isotherm models, individual metal solutions were prepared, namely 25, 50, 75, 100, 125 and 150 mg/L. The solutions were homogeneously mixed using a magnetic stirrer (Figure 3). The solutions were poured into 250 mL Erlenmeyer flasks and 0.5g of AC was added to each flask. All the samples were put into the shaking incubator at 25°C and 160 rpm for 90 minutes; thereafter, the slurries were centrifuged at 4000 rpm for 5 minutes to recover a clear solution.

Similarly, contact time effects for kinetic models were conducted using 100 mL of 100 mg/L of individual metal solutions, in 250 mL Erlenmeyer flasks with 0.5 g of AC using a sampling regime

of 20, 40, 60, 80, 100 and 120 minutes using a shaking incubator at 25°C and 160 rpm. All samples during this step were also centrifuged at 4000 rpm for 5 minutes.

All experiments were done in triplicate.

The linear form of the Langmuir isotherm model is given in Equation [*1*].

$$\frac{C_e}{q_e} = \frac{1}{kq_m} + \frac{C_e}{q_m} \quad [1]$$

The C_e term in the equation refers to the concentration of the metal solution after adsorption has occurred (mg/L). The q_e term refers to the concentration of the metal solution at equilibrium (mg/g). q_m (mg/g) represents the Langmuir constant that is associated with the adsorption capacity. The Langmuir constant that is associated with the amount of energy that is released during the adsorption process is represented by the k term (L/mg).

The linear form of the Freundlich model is given by Equation [2].

$$\log q_e = \log k_F + \frac{1}{n}\log C_e \quad [2]$$

As described above, the C_e term refers to the concentration of the metal solution after adsorption has occurred (mg/L) and the q_e term refers to the concentration of the metal solution at equilibrium (mg/g). The k_F (mg/g) term indicates the Freundlich adsorption capacity parameter. n refers to the deviation of adsorption to linearity (Fosso-Kankeu, et al., 2016).

The adsorption rate will be determined using the pseudo-first- and pseudo-second order kinetic models. The pseudo-first order kinetic model is represented by Equation *[3].*

$$\log(q_e - q_t) = \log q_e - k_1 \frac{t}{2.303} \quad [3]$$

The pseudo-second order kinetic model is represented by Equation [4].

$$\frac{t}{q_t} = \frac{1}{k_2 q_e^2} + \frac{1}{q_e} t \quad [4]$$

The symbol k_1 refers to the first order rate constant (min^{-1}). The q_t term (mg/g) refers to the amount of metal adsorbed at time t. k_2 represents the rate constant in $(\frac{g}{mg}/min)$. t is the time in (min).

Figure 3: Magnetic stirrer

Figure 4: Activated clinoptilolite

3.4 Adsorption column studies

Ten intervals of 15 mL of each metal solution were pumped to a column at 5 mL/min using a peristaltic pump. Figure 5 indicates the pump that was used for the column experiments. Each interval filtrate was collected and sent for ICP analysis (EPA Method 6020B). The column experiments were repeated using real acid and alkaline mine drainage samples. The column setup is shown in Figure 6. All experiments were done in triplicate.

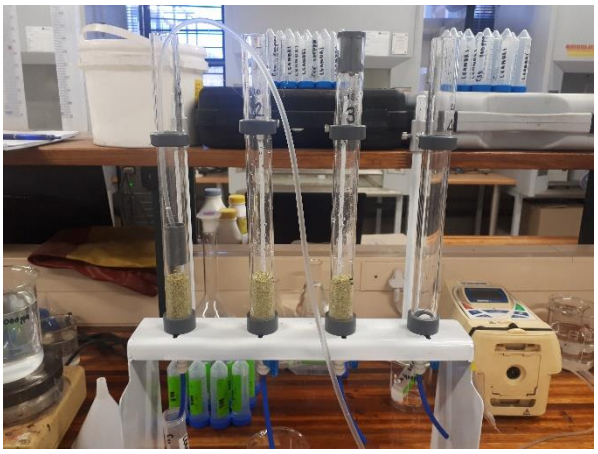

Figure 5: Column setup

Figure 6: Peristaltic pump

3.5 Testing the effect of pH

A metal solution containing zinc, manganese and cadmium was created with each metal being in a concentration of 400 mg/L. The pH of the metal solution was altered to five pH variations (namely pH of 3, 5, and 7) using hydrogen chloride to decrease the pH and sodium hydroxide to increase the pH of the solution. Lead solutions were susceptible to precipitation and was therefore excluded with a mixture of metal solutions. Columns were loaded to a height of 5 cm of AC and 10 pore volumes of each pH variation of the mixed metal solution was pumped at 5 mL/min using a peristaltic pump through a loaded column and each pore volume of filtrate was collected. The collected samples were sent for ICP analysis. The column experiments were repeated using real acid- and alkaline mine drainage samples.

3.6 Testing the effect of water hardness

A mixed metal solution containing zinc, cadmium and manganese was once again created with each metal being in a concentration of 400 mg/L. 50 mg/L, 100 mg/L, 150 mg/L and 200 mg/L of calcium and magnesium was added, respectively. Ten pore volumes of each hardness variation were used to repeat the column experiments. The collected filtrates were once again sent for ICP analyses.

3.7 Testing the effect of particle size

A particle size distribution (PSD) was manually done using 8 sieves. Figure 7 represents the sieve stack that was used to determine the PSD. The sieve aperture sizes that were used were 3350 µm, 2000 µm, 1180 µm, 500 µm, 300 µm, 212 µm, 150 µm and 106 µm. From the results obtained from the particle size distribution, 3 particle size ranges were identified to conduct experiments with (Figure 8). These ranges included particles (>1180 µm), (<1180 µm; >500 µm), and (<500 µm; >150 µm). The column experiments were repeated using the mixed metal solution and filling the columns to a height of 5 cm using the different particle size variations. The filtrates collected were sent for ICP analyses.

Figure 7: Sieve stack

Figure 8: Particle sizes of adsorbent

3.8. Testing the effect of mineral characteristics

The column was filled with a 4:1 ratio of clinoptilolite and quartz to a height of 5 cm (refer to Figure 9). The column experiments were then repeated using the mixed metal solution containing zinc, cadmium and manganese with each metal being in a concentration of 400 mg/L. The filtrates were collected and sent for ICP analyses.

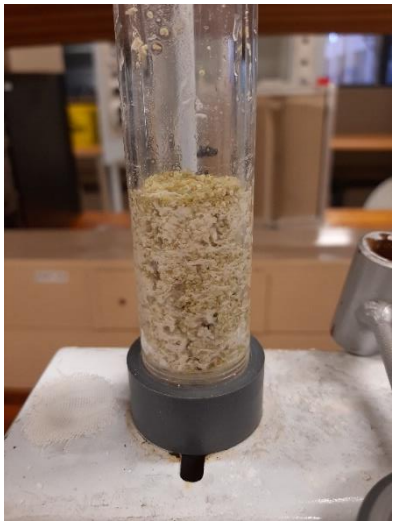

Figure 9: Clinoptilolite and Quartz filled column

Chapter 4: Results and Discussion

4. Chapter 4: Results and Discussion

All experimental data is located in Appendix A to F.

4.1 Characterisation of adsorbent

In order to characterise the adsorbent, the structural and physiochemical properties of the clinoptilolite was investigated. This was done by performing FT-IR, XRD, XRF and SEM-EDS analysis. The FT-IR pattern is reported in Figure 10.

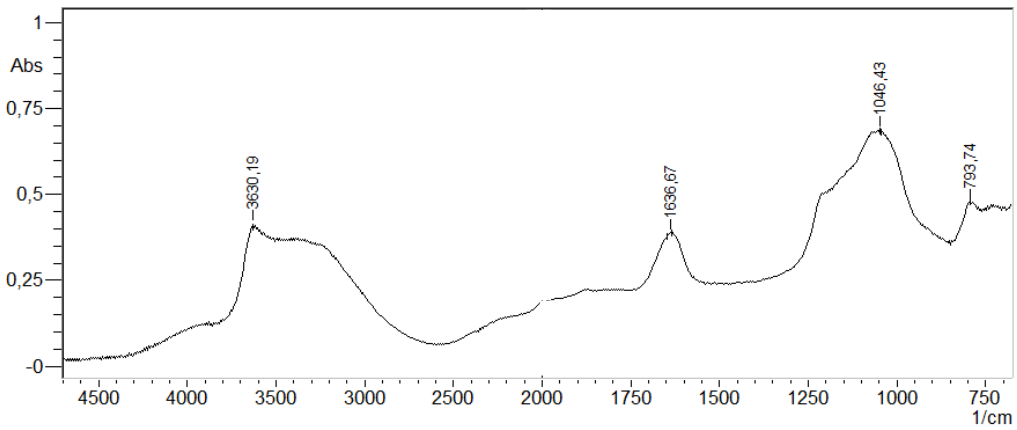

Figure 10: FT-IR analysis of clinoptilolite

The FR-IR analysis (ASTM E168) was done to determine the functional groups present in the AC. Major peaks were identified at 3360.19 cm^{-1}, 1636.67 cm^{-1} and 1046.43 cm^{-1} which indicate the presence of the O-H, C=O and C-O functional groups, respectively. All of these functional groups are responsible for the biosorption of metals (Mat Don & Yahaya, 2014).

Figure 11 reports the XRD pattern of activated clinoptilolite. The high crystallinity of the clinoptilolite was observed at the highest peak at 2Θ = 11.4°. Other peaks were identified at 2Θ

= 13°, 26.3° and 37°. It is indicated that clinoptilolite is the main mineral in the sample and that the contents of halite and heulandite are low.

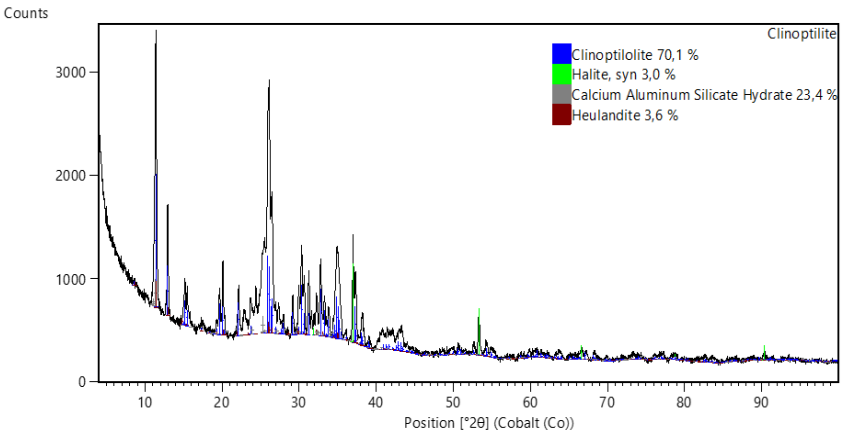

Figure 11: XRD analysis of activated clinoptilolite

XRF spectrophotometry (ASTM D6247) was used to determine the elemental composition of the clinoptilolite sample. Samples of the clinoptilolite were pulverized with a mortar and pestle to achieve the required particle size for analysis. The results are presented in Table 4.

Table 4: XRF analysis of activated clinoptilolite

	Na_2O	MgO	Al_2O_3	SiO_2	P_2O_5	K_2O	CaO	TiO_2	MnO	Fe_2O_3
	% mass	% mass	% mass	% mass	% mass	% mass	% mass	% mass	% mass	% mass
Clinoptilolite	2.96	0.84	11.92	68.18	0.21	3.69	5.23	0.12	0.06	0.94

$Al_2O_3$and SiO_2 are the most prominent compounds identified in the clinoptilolite sample, which was to be expected. Calcium and potassium are also present, but in lesser quantities.

Micrographs of the activated clinoptilolite sample obtained from SEM analysis are given in Figure 12 and Figure 13. The images show macro-pores in the structure of the clinoptilolite. The SEM analysis of the quartz sample is given in Figure 14 and Figure 15. The micrograph indicates that the quartz sample does not present any porous structure as represented by the clinoptilolite sample.

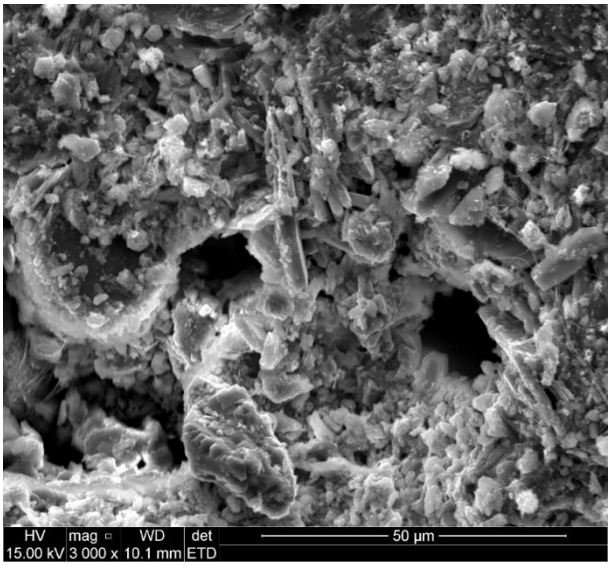

Figure 14: SEM analysis Clinoptilolite (50 µm)

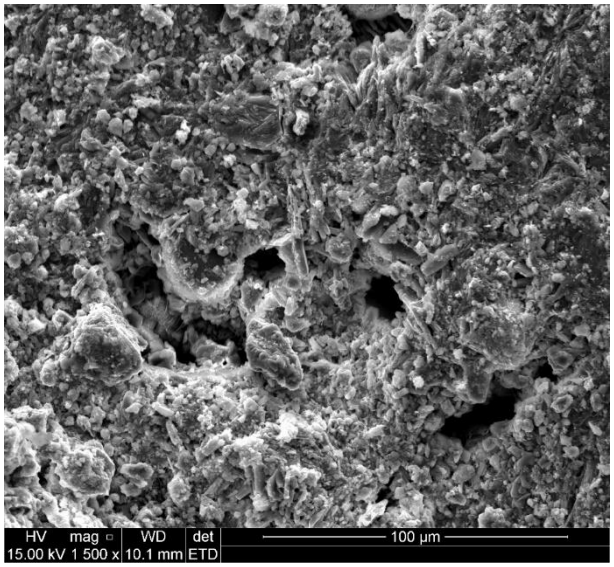

Figure 15: SEM analysis Clinoptilolite (100 µm)

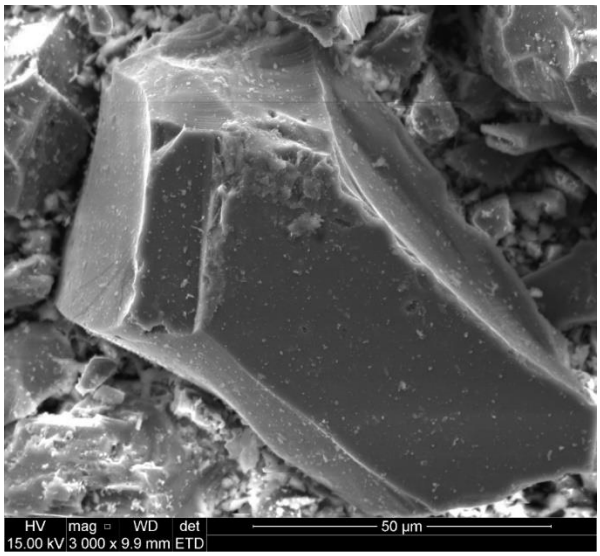

Figure 13: SEM analysis Quartz (50 µm)

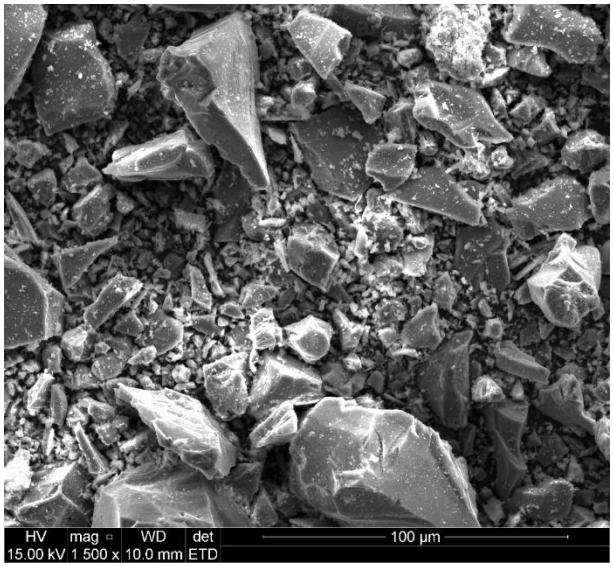

Figure 12: SEM analysis Quartz (100 µm)

EDS analysis on the clinoptilolite sample was done to get a more accurate analysis of the elemental composition of the activated clinoptilolite sample. These results are presented in Table 5. The EDS analysis results indicated that the predominate exchangeable cations of the activated clinoptilolite is sodium as the clinoptilolite was activated using table salt.

Table 5: EDS analysis

Sample	Element	Weight %
Clinoptilolite	O	42.61
	Na	11.6
	Mg	0.42
	Al	3.74
	Si	17.27
	Cl	16.18
	K	1.34
	Ca	0.49
	Fe	0.69
Quartz	O	53.19
	Al	1.08
	Si	34.68
	K	1.23

The nitrogen isotherms for clinoptilolite are shown in Figure 16. The data obtained by the BET analysis (ASTM D1993) is located in Table 6.

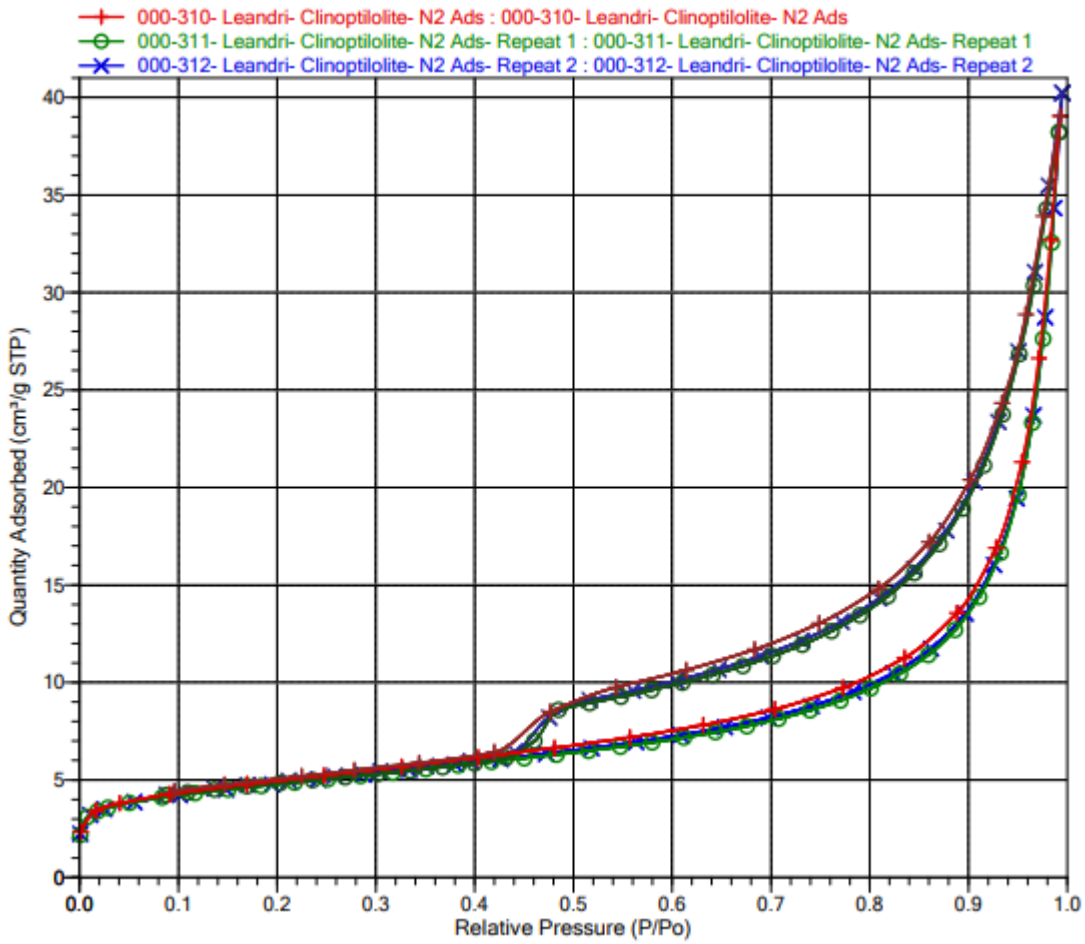

Figure 16: Nitrogen isotherm for clinoptilolite (BET)

Table 6: BET surface area, micropore area, total pore volume and average pore diameter results obtained from BET analysis

Adsorbent	BET surface area (m^2/g)	Micropore area (m^2/g)	Total pore volume (cm^3/g)	Adsorption average pore volume diameter (Å)
Activated Clinoptilolite (AC)	17.0922	3.0361	0.049754	116.436

The behaviour of the nitrogen adsorption curve in Figure 16 is similar to other reported results in literature (Kennedy, et al., 2019). Figure 16 indicates that at relatively low pressures ($\frac{P}{P_0}$ < 0.1) an

initial increase in nitrogen adsorption can be observed. The increase in the adsorption at these low pressures are expected for clinoptilolite and indicate the presence of microporosity (Kennedy, et al., 2019). The adsorption isotherm stays relatively consistent at pressure values between 0.1 < $\frac{P}{P_0}$ < 0.8. At pressure values higher than 0.8, the adsorption isotherms begin to increase quite significantly which indicate the presence of mesopores and macropores. From the curve the hysteresis loop is identified. The hysteresis loop is characteristic of clinoptilolite samples and indicate multilayer adsorption and capillary condensation that occurs within mesopores (Kennedy, et al., 2019).

In Figure 17 the particle size distribution of the clinoptilolite sample as measured using the Malvern Mastersizer Laser diffractor is given. The results obtained are given in Table 7.

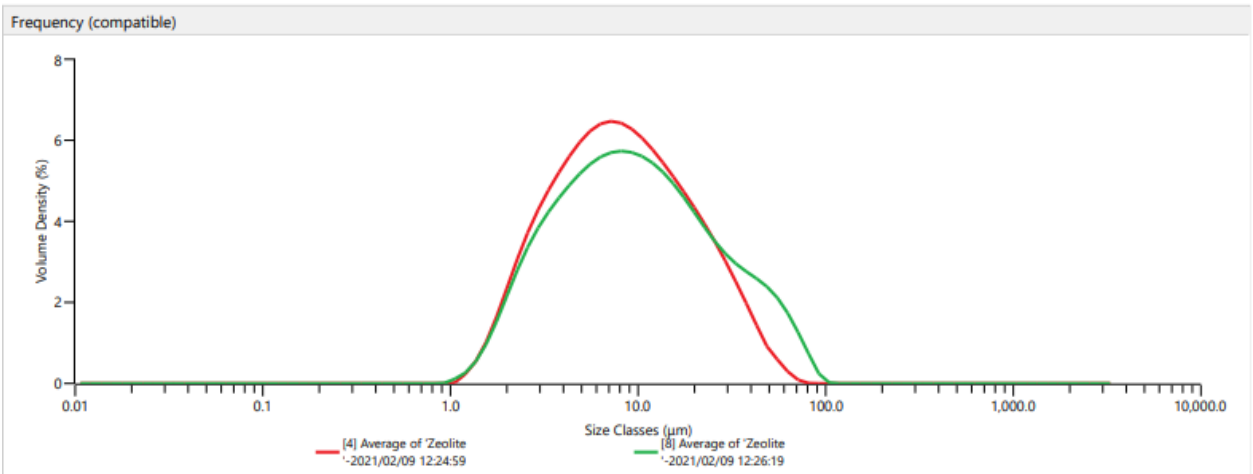

Figure 17: Malvern Mastersizer particle size distribution of the AC

Table 7: Malvern Mastersizer particle size distribution parameters

Sample	Concentration (%)	Span	Uniformity	Specific Surface Area (m^2/kg)	D[3,2] (µm)	D[4,3] (µm)	Dv(10) (µm)	Dv(50) (µm)	Dv(90) (µm)
Clinoptilolite	0.0081	2.9	0.89	1017	5.9	11.7	2.7	8.02	26.2

4.2 Isotherm studies

The Langmuir and Freundlich isotherm models were used to better understand the mechanism of the adsorption of zinc, cadmium, manganese and lead onto the surface of the clinoptilolite.

I. Zinc

Figure 18 indicates the Langmuir isotherm plot for the adsorption of zinc onto the surface of the clinoptilolite. The Langmuir plots were created by plotting C_e/q_e vs C_e.

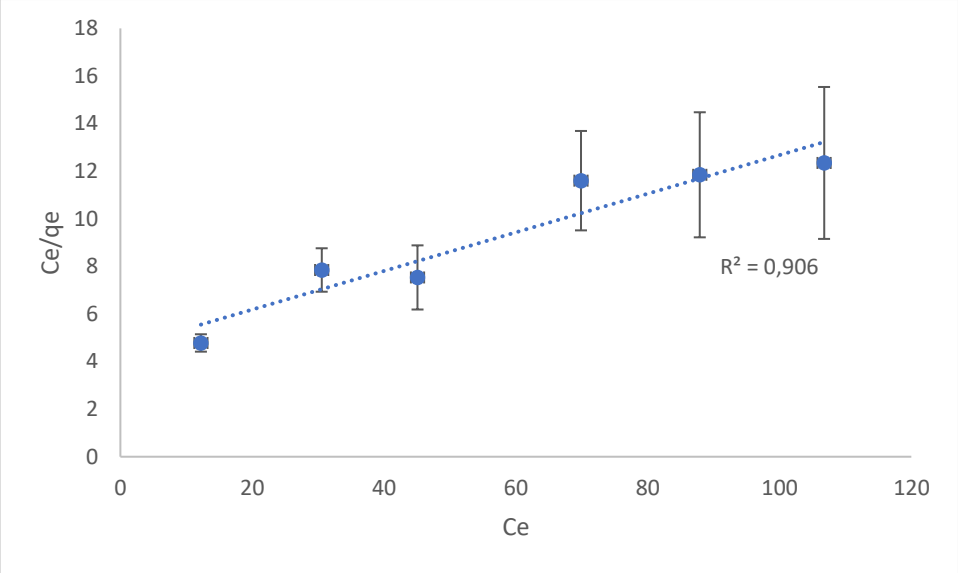

Figure 18: Zinc Langmuir isotherm plot

To construct the Freundlich isotherm plot, $\ln(q_e)$ was plotted against $\ln(C_e)$. Figure 19 indicates the Freundlich isotherm plot for the adsorption of zinc onto the surface of the clinoptilolite. It should be noted that the error bars are small and not visible on the plot.

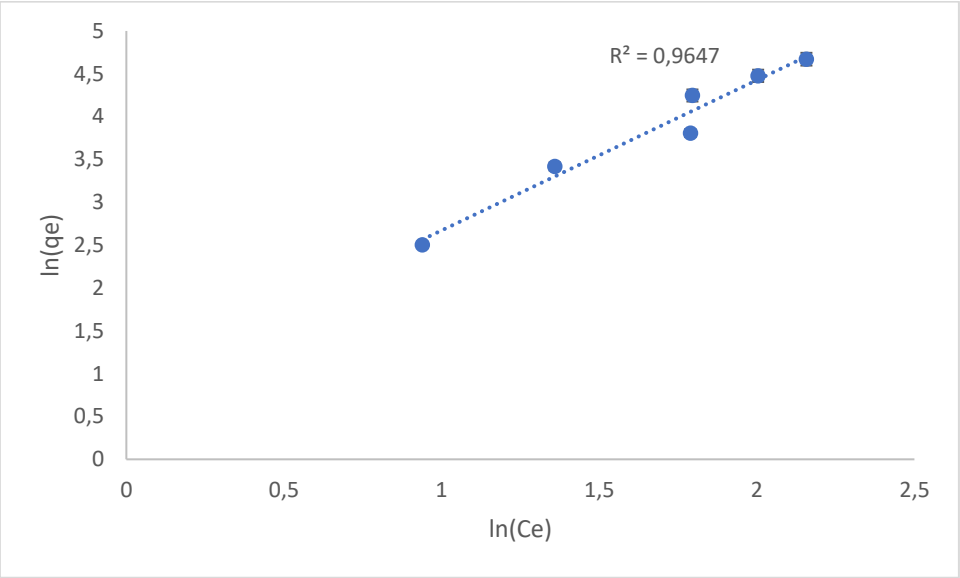

Figure 19: Zinc Freundlich isotherm plot

To determine the parameters of both of the isotherm models, the slopes and the intersects of both of the plots were calculated. The calculated parameters are indicated in Table 8. The best suited model to describe the adsorption of the zinc onto the clinoptilolite is determined by considering the coefficient of determination values (R^2). By considering these values, it is determined that the Freundlich model is the best fit as the coefficient of determination is closer to unity.

Table 8: Zinc Langmuir and Freundlich model parameters

	Langmuir				Freundlich			
Adsorbent	q_m (mg/g)	k (L/mg)	R^2	Absolute difference (%)	n	k_F	R^2	Absolute difference (%)
Clinoptilolite	12.32	0.02	0.91	9.2	1.82	0.64	0.96	3.6

II. Cadmium

The Langmuir plot for the adsorption of cadmium onto the surface of the clinoptilolite is indicated in Figure 20.

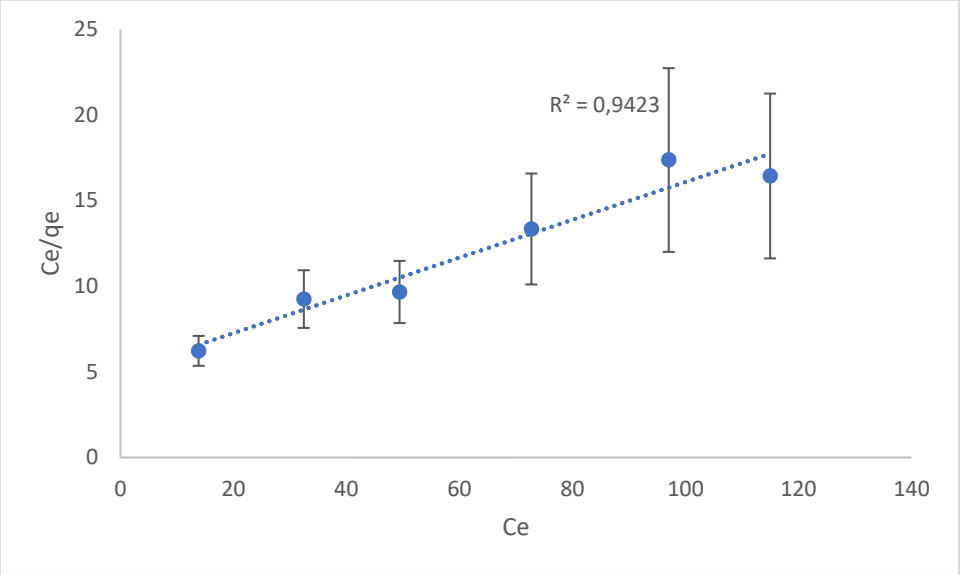

Figure 20: Cadmium Langmuir isotherm plot

The Freundlich plot for the adsorption of cadmium onto the surface of the clinoptilolite is shown in Figure 21.

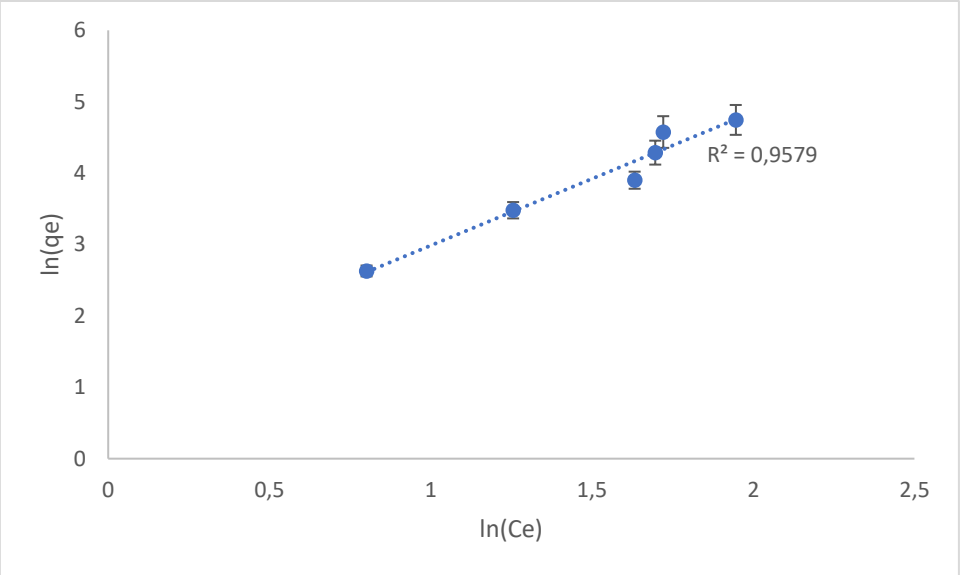

Figure 21: Cadmium Freundlich isotherm plot

The parameters of both models are located in Table 9. From these values it can be determined that the Freundlich isotherm model is best suited to describe the adsorption of the cadmium onto the surface of the clinoptilolite

Table 9: Cadmium Langmuir and Freundlich model parameters

	Langmuir				Freundlich			
Adsorbent	q_m (mg/g)	k (L/mg)	R^2	Absolute difference (%)	n	k_F	R^2	Absolute difference (%)
Clinoptilolite	9.07	0.02	0.94	6.7	2.0	0.60	0.96	3.9

III. Manganese

The Langmuir plot for the adsorption of manganese onto the surface of the clinoptilolite is indicated in Figure 22.

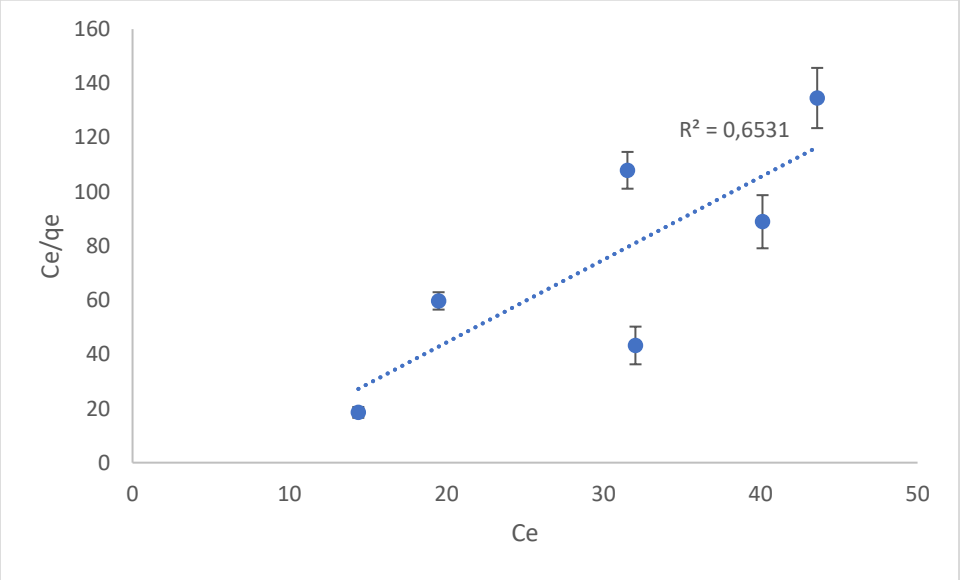

Figure 22: Manganese Langmuir isotherm plot

The Freundlich plot for the adsorption of manganese onto the surface of the clinoptilolite is shown in Figure 23.

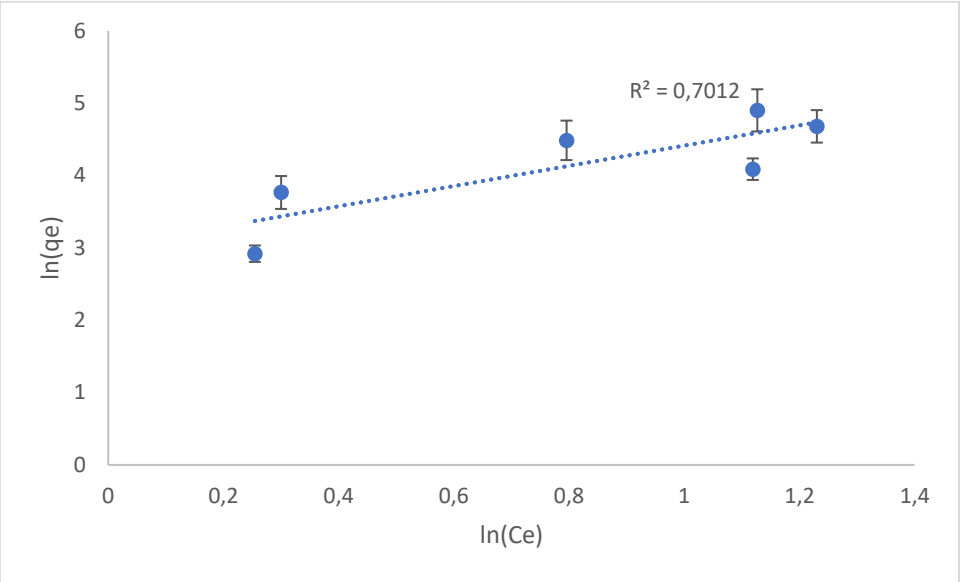

Figure 23: Manganese Freundlich isotherm plot

The parameters of both models are located in Table 10. From these values it can be determined that the Freundlich isotherm model is best suited to describe the adsorption of the manganese onto the surface of the clinoptilolite.

Table 10: Manganese Langmuir and Freundlich model parameters

	Langmuir				Freundlich			
Adsorbent	q_m (mg/g)	k (L/mg)	R^2	Absolute difference (%)	n	k_F	R^2	Absolute difference (%)
Clinoptilolite	4.68	0.02	0.65	20.5	1.99	0.28	0.70	17.6

IV. Lead

The Langmuir plot for the adsorption of lead onto the surface of the clinoptilolite is indicated in Figure 24. It should be noted that the error bars are small and not visible on the plot.

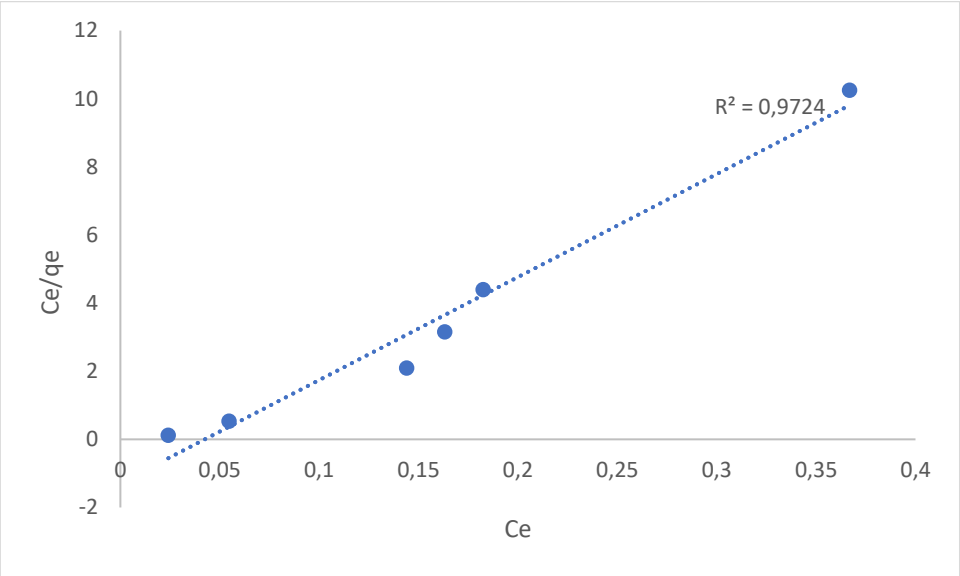

Figure 24: Lead Langmuir isotherm plot

The Freundlich plot for the adsorption of lead onto the surface of the clinoptilolite is shown in Figure 25.

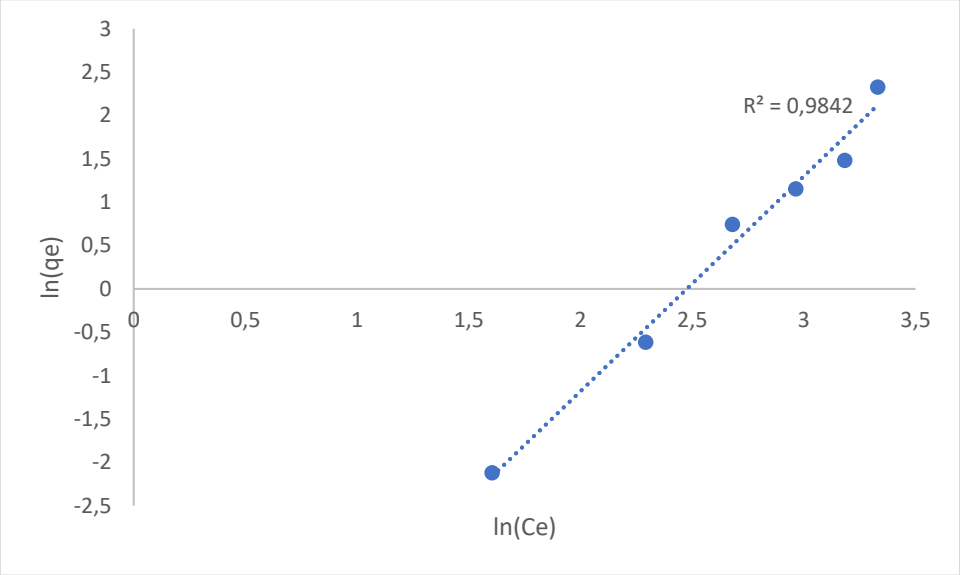

Figure 25: Lead Freundlich isotherm plot

The parameters of both models are located in Table 11.

Table 11: Lead Langmuir and Freundlich model parameters

	Langmuir				Freundlich			
Adsorbent	q_m (mg/g)	k (L/mg)	R^2	Absolute difference (%)	n	k_F	R^2	Absolute difference (%)
Clinoptilolite	31.09	0.71	0.97	17.9	2.51	11.93	0.98	2.5

From these values it can be determined that the Freundlich isotherm model is best suited to describe the adsorption of the lead onto the surface of the clinoptilolite as its coefficient of determination value is closer to unity.

The Freundlich isotherm model best described the adsorption of all of the investigated metals onto the surface of the adsorbent. Therefore, it is found that the adsorption process of zinc, cadmium, manganese and lead onto the surface of the clinoptilolite occurs through a heterogeneous binding to the surface. This implies that many layers are involved in the adsorption of the zinc.

4.3 Kinetic studies

To determine the success of the treatment of heavy metal polluted water using clinoptilolite as adsorbent, a prediction rate at which the heavy metal is adsorbed onto the surface of the clinoptilolite is determined. By conducting a kinetic study, the prediction rate as well the capacity of the adsorbent can be determined. The parameters of the kinetic models were calculated by determining the slopes and the intersects of the various plots.

I. Zinc

The pseudo-first order plot for the adsorption of zinc onto the surface of the clinoptilolite is indicated in Figure 26.

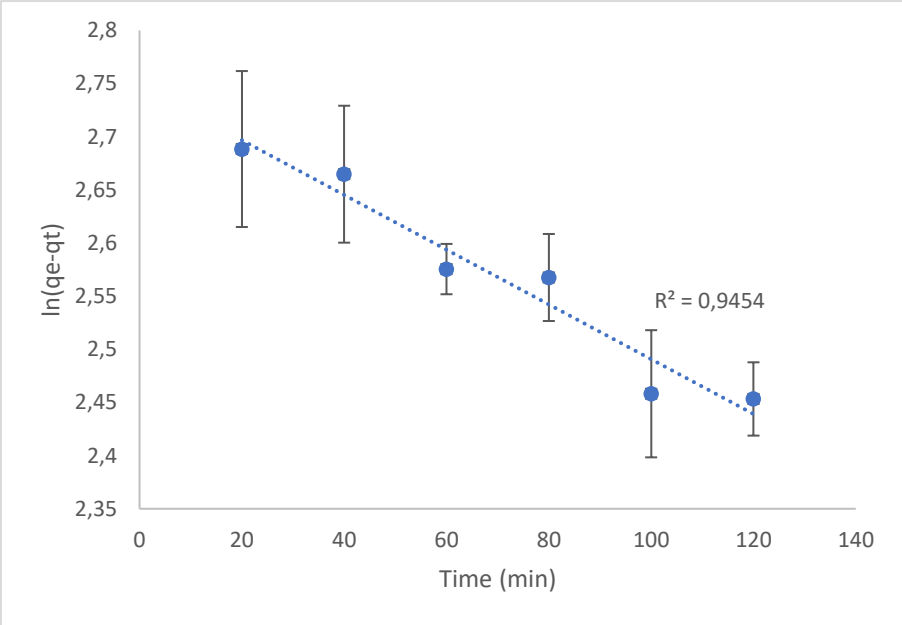

Figure 26: Zinc pseudo-first order plot

The pseudo-second order plot for the adsorption of zinc onto the surface of the clinoptilolite is indicated in Figure 27.

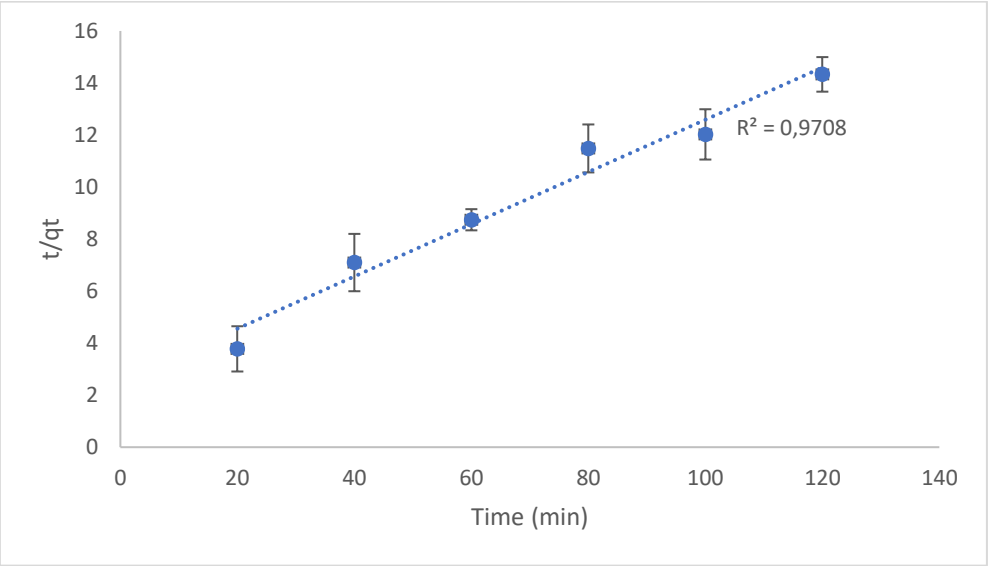

Figure 27: Zinc pseudo-second order plot

As was done with the isotherm models, the best fit kinetic model to describe the adsorption of zinc onto the surface of the clinoptilolite is determined by considering the coefficient of determination (R^2). These values are found in Table 12. By considering these values, it is determined that the pseudo-second order model is the best fit as the coefficient of determination was closer to unity.

Table 12: Zinc kinetic model parameters

	Pseudo-first order				Pseudo-second order			
Adsorbent	q_e(exp) (mg/g)	q_e(calc) (mg/g)	k_1 (min^{-1})	R^2	q_e(exp) (mg/g)	q_e(calc) (mg/g)	k_2 $(\frac{g}{mg}/min)$	R^2
Clinoptilolite	20	15.62	0.006	0.94	20	9.96	252.80	0.97

II. Cadmium

The pseudo-first order plot for the adsorption of cadmium onto the surface of the clinoptilolite is indicated in Figure 28.

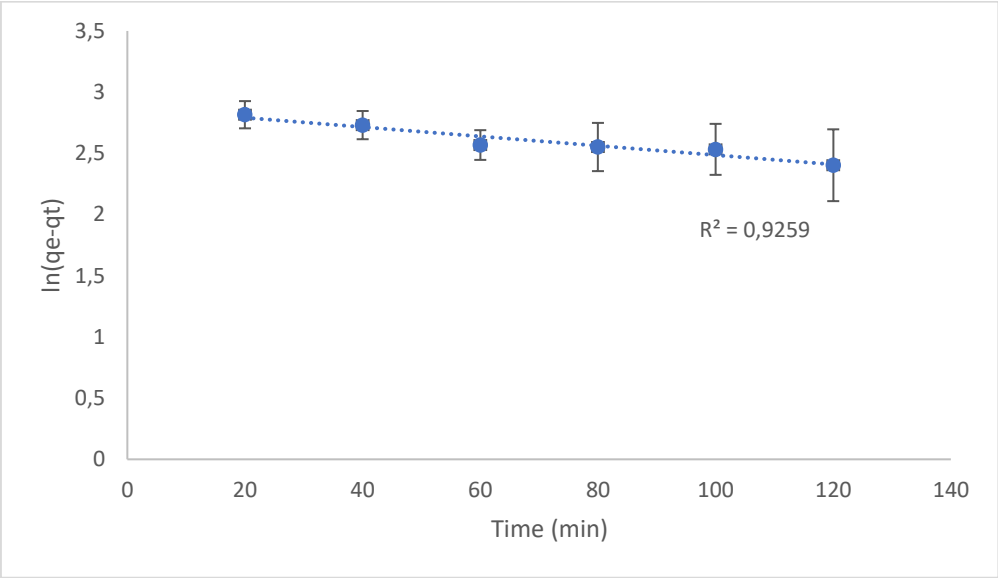

Figure 28: Cadmium pseudo-first order plot

The pseudo-second order plot for the adsorption of cadmium onto the surface of the clinoptilolite is indicated in Figure 29.

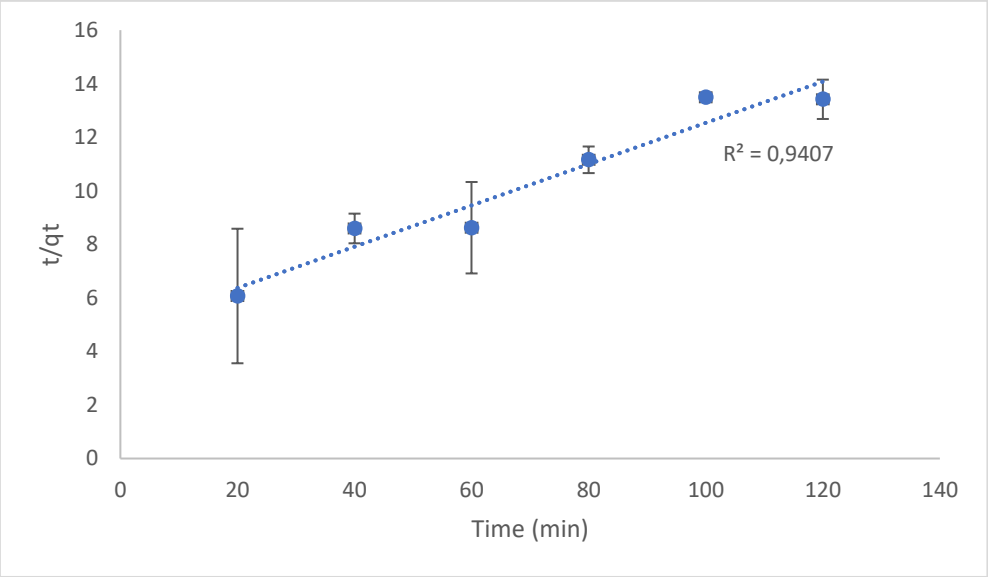

Figure 29: Cadmium pseudo-second order plot

The parameters of the kinetic models are located in Table 13. These values indicate that that the pseudo-second order model is the best fit.

Table 13: Cadmium kinetic model parameters

	Pseudo-first order				Pseudo-second order			
Adsorbent	q_e(exp) (mg/g)	q_e(calc) (mg/g)	k_1 (min^{-1})	R^2	q_e(exp) (mg/g)	q_e(calc) (mg/g)	k_2 $(\frac{g}{mg}/min)$	R^2
Clinoptilolite	20	17.59	0.008	0.92	20	12.97	812.23	0.94

III. Manganese

The pseudo-first order plot for the adsorption of manganese onto the surface of the clinoptilolite is indicated in Figure 30.

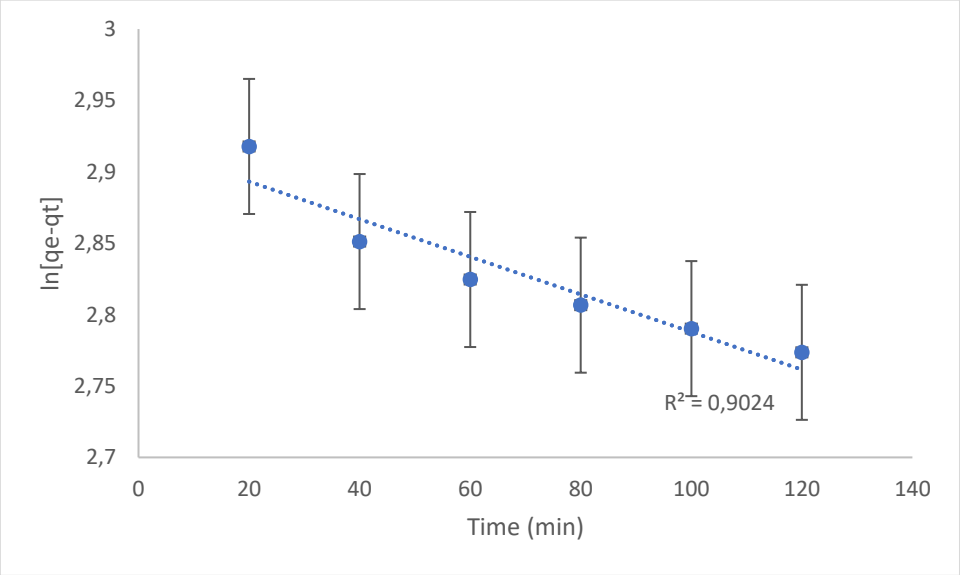

Figure 30: Manganese pseudo-first order plot

The pseudo-second order plot for the adsorption of manganese onto the surface of the clinoptilolite is indicated in Figure 31.

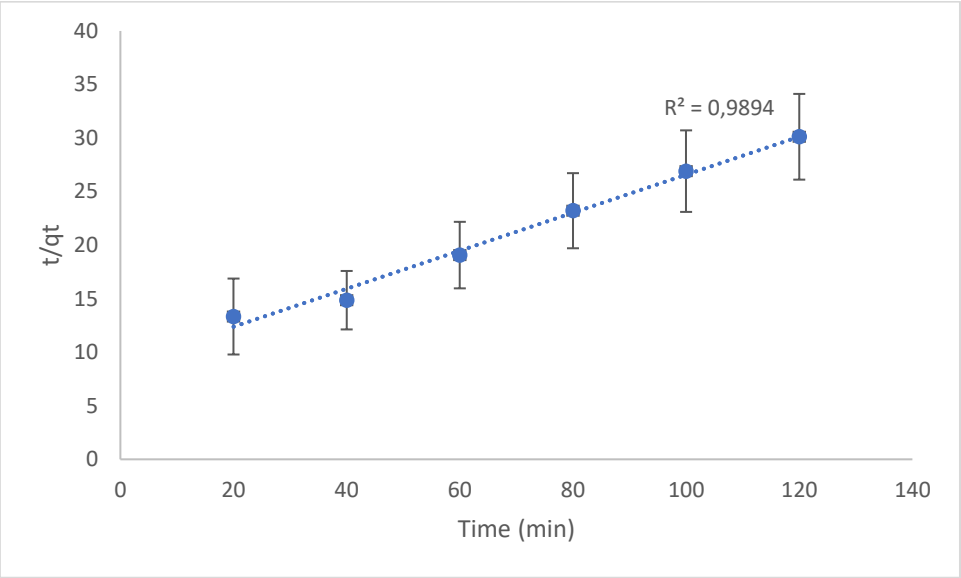

Figure 31: Manganese pseudo-second order plot

The parameters of the kinetic models are located in Table 14. The kinetic parameters above indicate that that the pseudo-second order model is the best fit.

Table 14: Manganese kinetic model parameters

	Pseudo-first order				Pseudo-second order			
Adsorbent	q_e(exp) (mg/g)	q_e(calc) (mg/g)	k_1 (min^{-1})	R^2	q_e(exp) (mg/g)	q_e(calc) (mg/g)	k_2 $(\frac{g}{mg}/min)$	R^2
Clinoptilolite	20	18.53	0.003	0.90	20	5.63	280.28	0.99

IV. Lead

The pseudo-first order plot for the adsorption of lead onto the surface of the clinoptilolite is indicated in Figure 32.

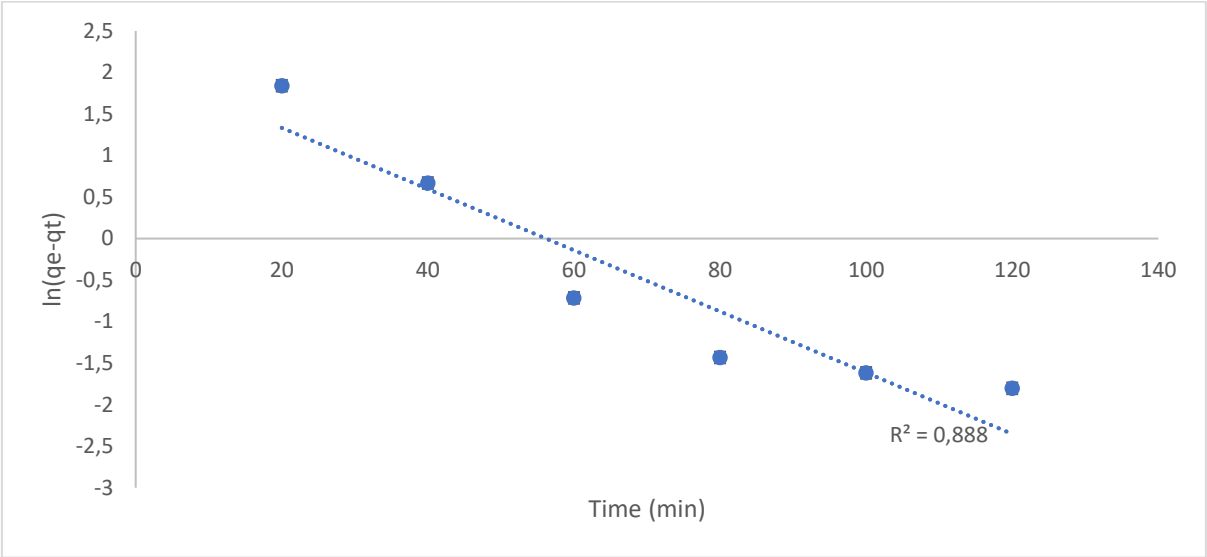

Figure 32: Lead pseudo-first order plot

The pseudo-second order plot for the adsorption of lead onto the surface of the clinoptilolite is indicated in Figure 33.

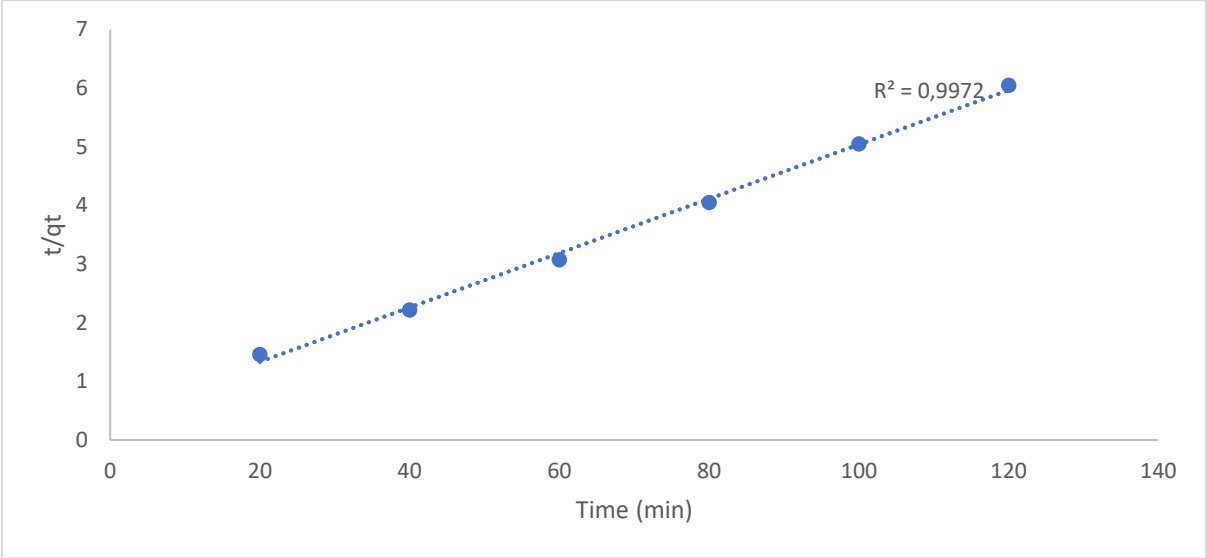

Figure 33: Lead pseudo-second order plot

The kinetic parameters of both models are located in Table 15. The parameters show that the pseudo-second order model is the best fit kinetic model to describe the adsorption.

Table 15: Lead kinetic model parameters

	Pseudo-first order				Pseudo-second order			
Adsorbent	q_e(exp) (mg/g)	q_e(calc) (mg/g)	k_1 (min^{-1})	R^2	q_e(exp) (mg/g)	q_e(calc) (mg/g)	k_2 $(\frac{g}{mg}/min)$	R^2
Clinoptilolite	20	7.93	0.08	0.89	20	21.59	190.0	0.99

The results indicated that the pseudo-second order kinetic model best describes the adsorption of all the investigated metals onto the surface of the clinoptilolite. This indicates that there is a stronger interaction between the surface of the clinoptilolite and the cadmium, manganese, zinc and lead ions.

4.4 Particle size distribution and the effect of particle size on adsorption

4.4.1 Particle size distribution (PSD)

To investigate the effect of the particle size on the adsorption capacity of the clinoptilolite, a particle size distribution of the activated clinoptilolite firstly had to be constructed. The PSD curve is given in Figure 34.

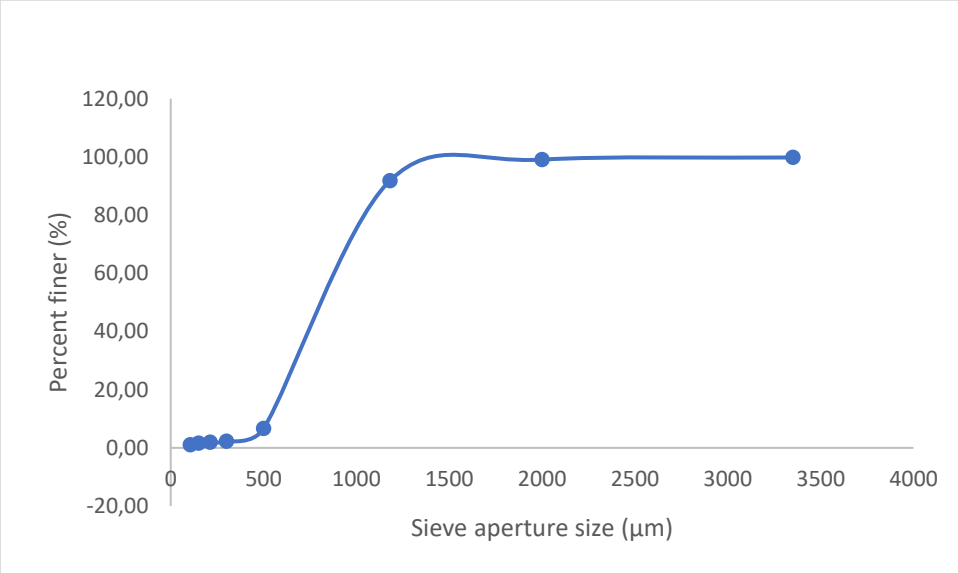

Figure 34: Clinoptilolite particle size distribution

From the above graph the d(0.1), d(0.5) and d(0.9) values were calculated. The terms d(0.1), d(0.5) and d(0.9) indicate that the portion of the particles which have diameters smaller than these values are 10 %, 50 % and 90 %, respectively. The results for these values are located in Table 16.

Table 16: PSD parameters

d(0.1)	530 µm
d(0.5)	750 µm
d(0.9)	1250 µm

Furthermore, the Rossin-Rammler as well as the Gaudin-Schumann models were applied to determine which of these two methods better suit the particle size distribution of the activated clinoptilolite. The graphs of both models are represented in Figure 35.

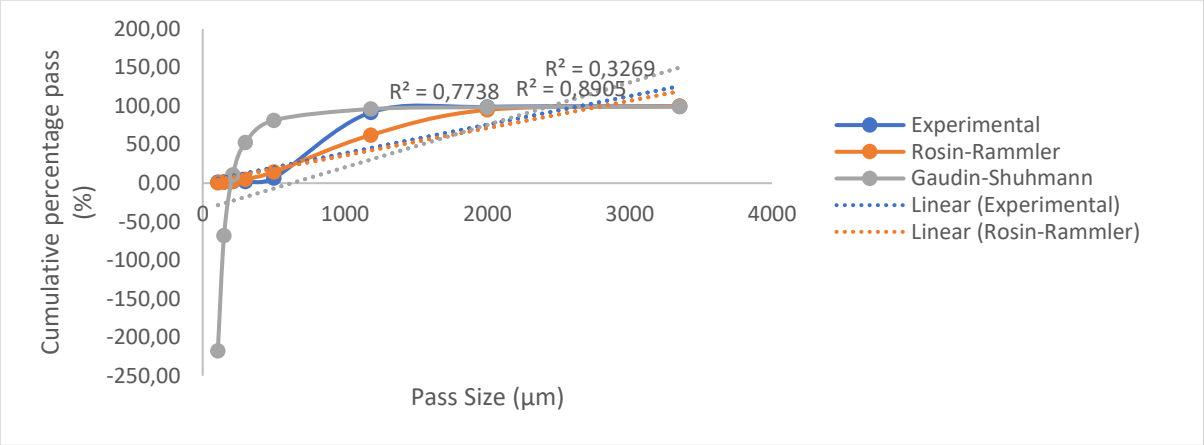

Figure 35: Rosin-Rammler and Gaudin-Shumann plots

The parameters for both the Rosin-Rammler and the Gaudin-Shumann models are given in Table 17 and Table 18, respectively. These parameters indicate that the Rosin-Rammler model is the best fit as the R^2 value for this model is closer to unity.

Table 17: Rosin-Rammler model parameters

n	d^*	R^2
2.14	1191.45	0.89

Table 18: Gaudin-Shumann model parameters

n	d^*	R^2
-1.84	198.97	0.33

4.4.2 Effect of particle size

The ranges of the particle size diameters to study the effect of particle size on the adsorption capacity of the clinoptilolite were identified as (>1180 µm); (<1180 µm,>500 µm) and (<500 µm,>150 µm). The experiments were repeated using alkaline- and acid mine drainage samples as aqueous solutions as well as a mixed metal solution.

I. Alkaline mine drainage

As the concentrations of calcium, magnesium and potassium were the highest in the sample of alkaline mine drainage that was collected, the adsorption of these ions on the different particle size ranges of clinoptilolite were studied.

The adsorption tendencies of calcium, magnesium and potassium onto the various particle size ranges of clinoptilolite are portrayed in Figure 36, Figure 37 and Figure 38, respectively.

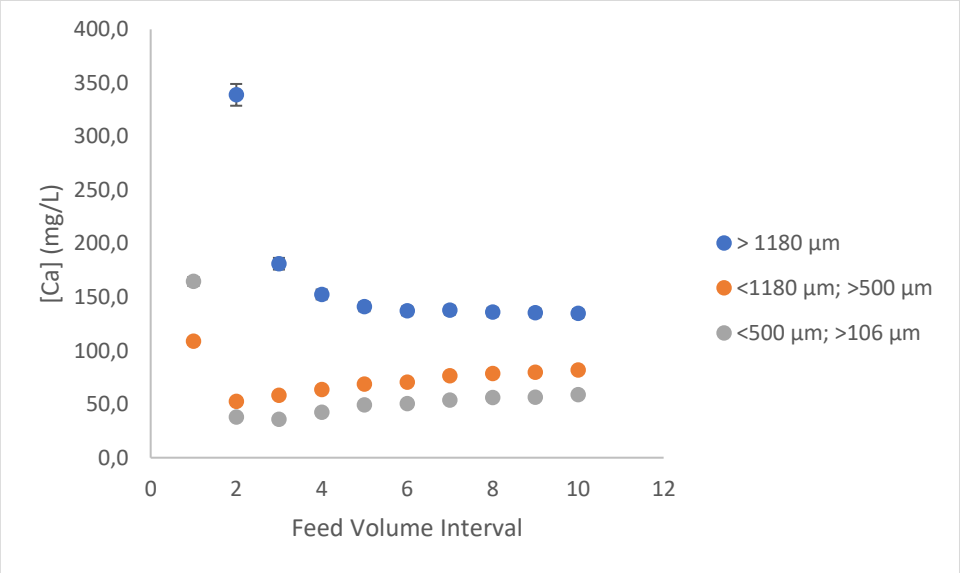

Figure 36: Calcium adsorption onto different clinoptilolite particle sizes

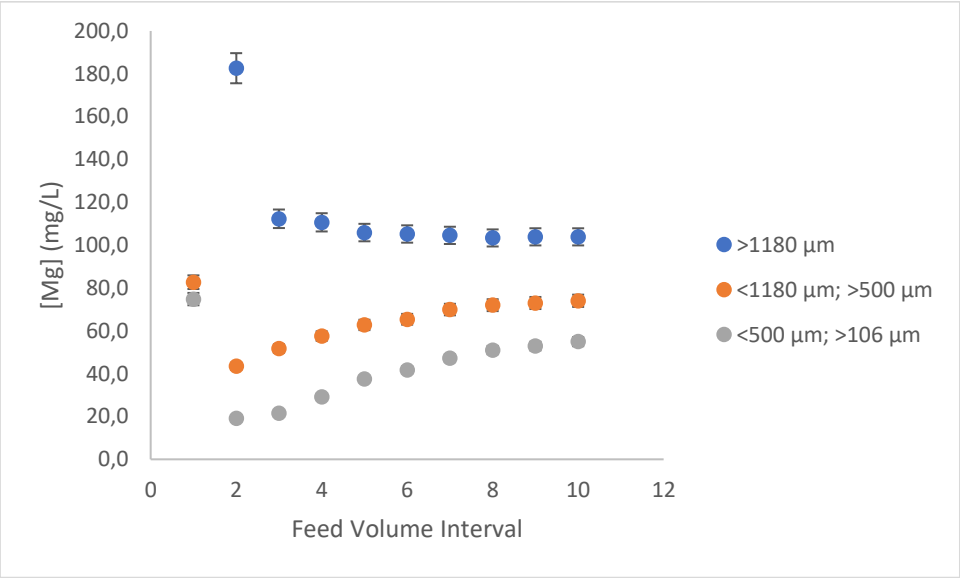

Figure 37: Magnesium adsorption onto different clinoptilolite particle sizes

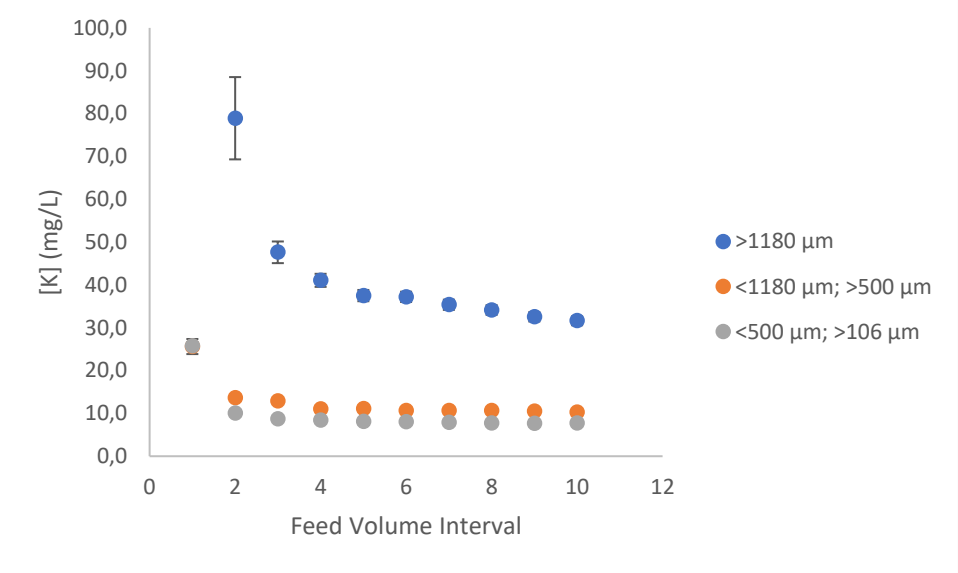

Figure 38: Potassium adsorption onto different clinoptilolite particle sizes

The graphs indicate that the adsorption of the calcium, magnesium and potassium increased with a decrease in the particle size of the sorbent.

II. Acid mine drainage

The adsorption tendencies of calcium, magnesium, potassium, aluminium, iron and manganese onto the various particle size fractions of the clinoptilolite was investigated and the results are given in Figure 39 – 44.

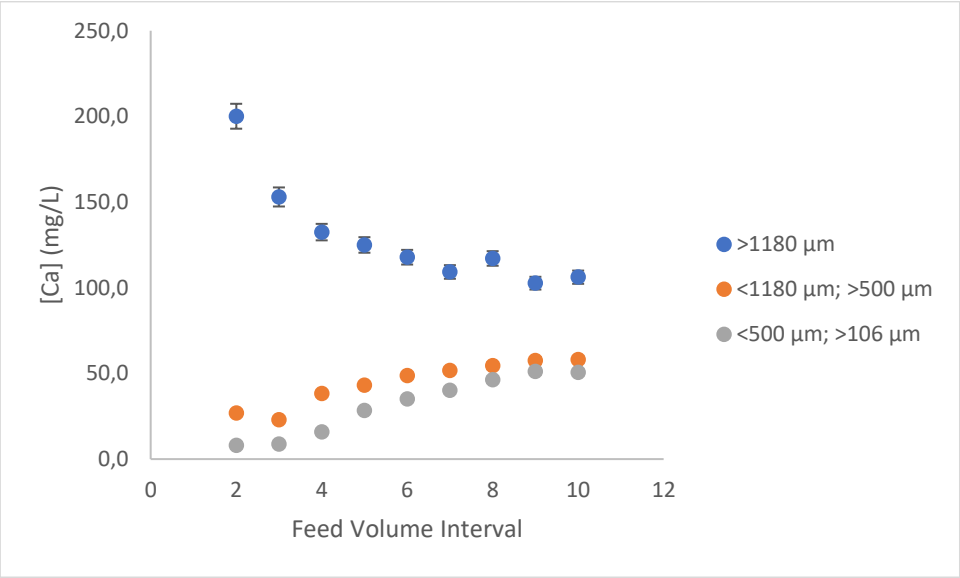

Figure 39: Adsorption of calcium in AMD onto different clinoptilolite particle sizes

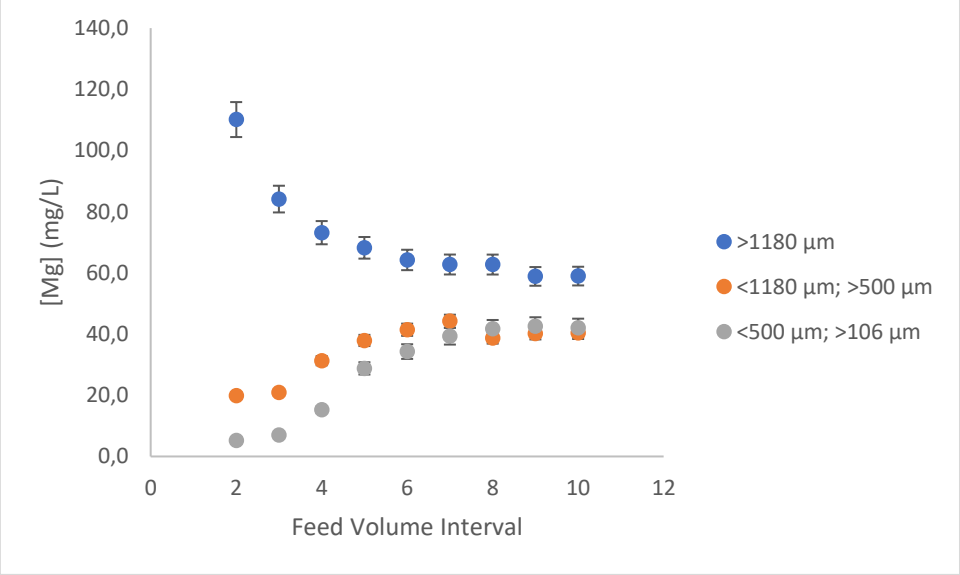

Figure 40: Adsorption of magnesium in AMD onto different clinoptilolite particle sizes

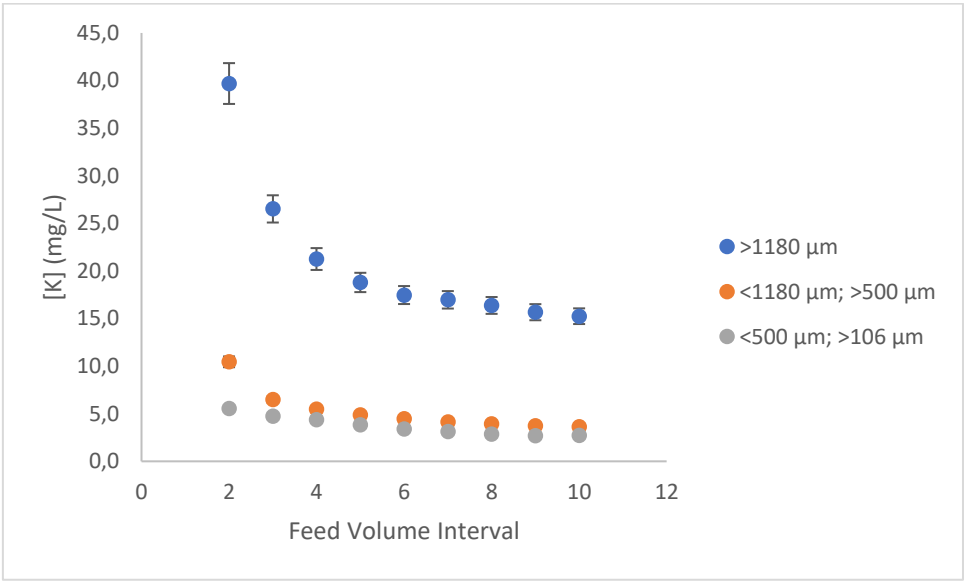

Figure 41: Adsorption of potassium in AMD onto different clinoptilolite particle sizes

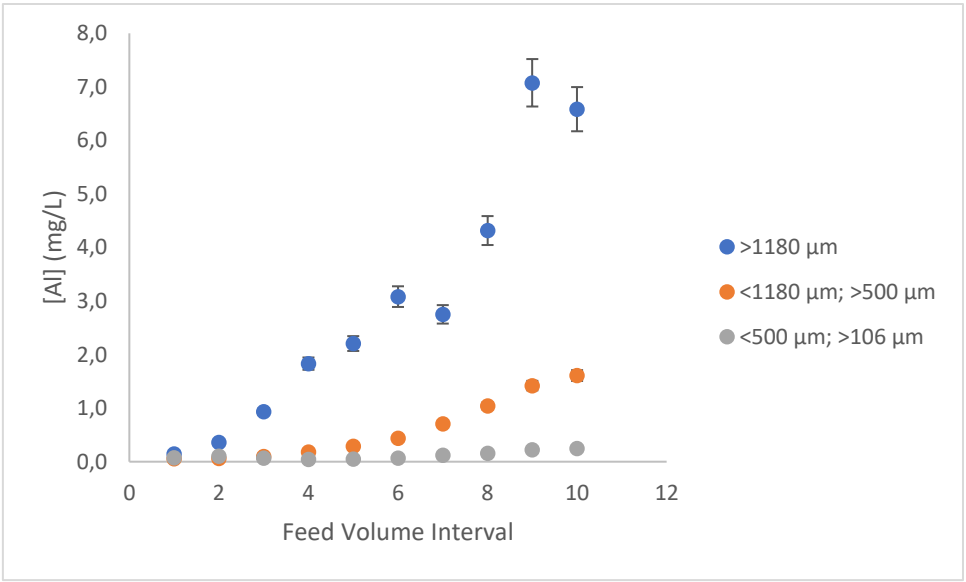

Figure 42: Adsorption of aluminium in AMD onto different clinoptilolite particle sizes

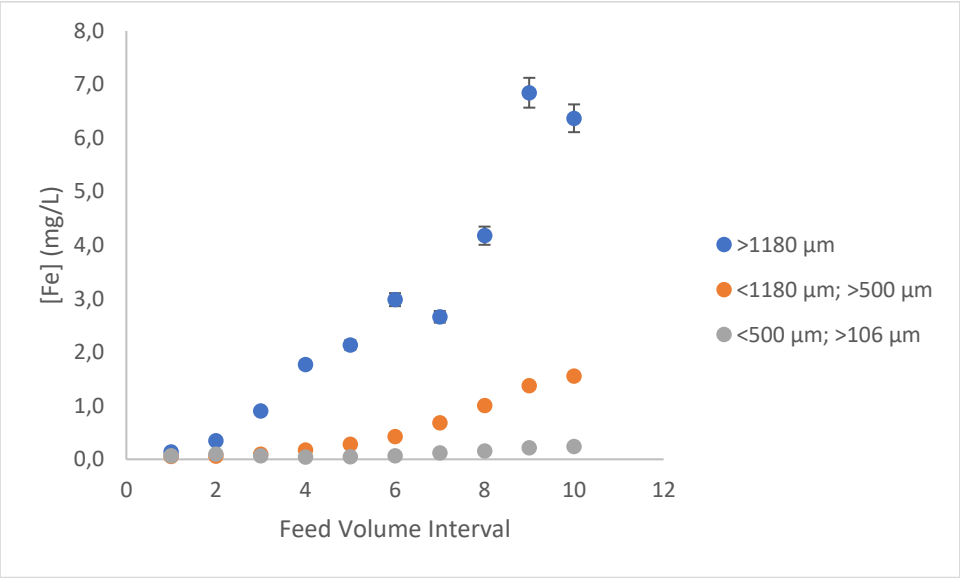

Figure 43: Adsorption of iron in AMD onto different clinoptilolite particle sizes

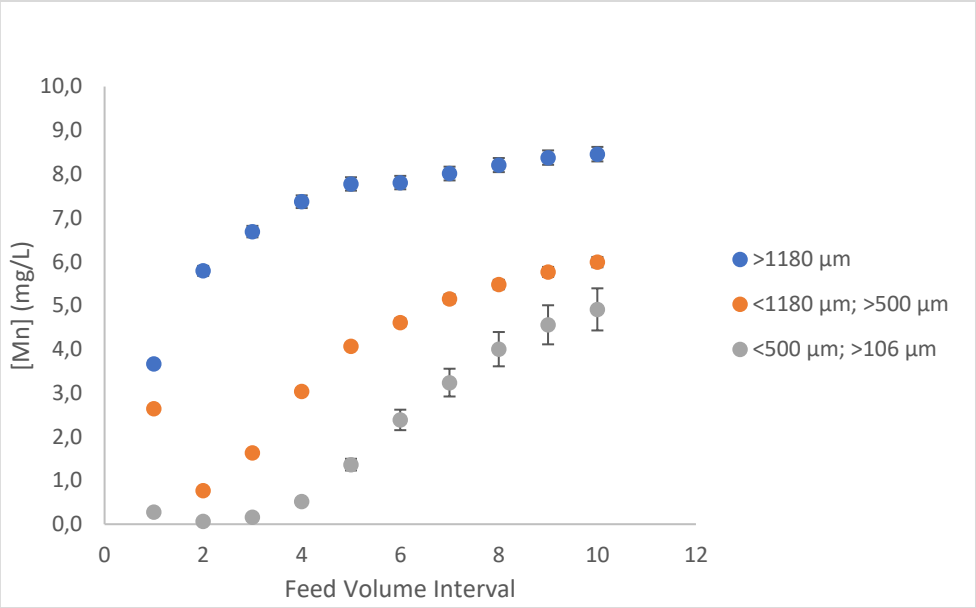

Figure 44: Adsorption of manganese in AMD onto different clinoptilolite particle sizes

The results indicated that the adsorption of all the metals investigated in the acid mine drainage sample increased with a decrease in the particle size of the adsorbent.

III. Mixed metal solution

The experiments were repeated using a mixed metal solution containing cadmium, manganese and zinc. The adsorption tendencies for all three metals onto the particle size variation of the clinoptilolite is given in Figure 45 – 47.

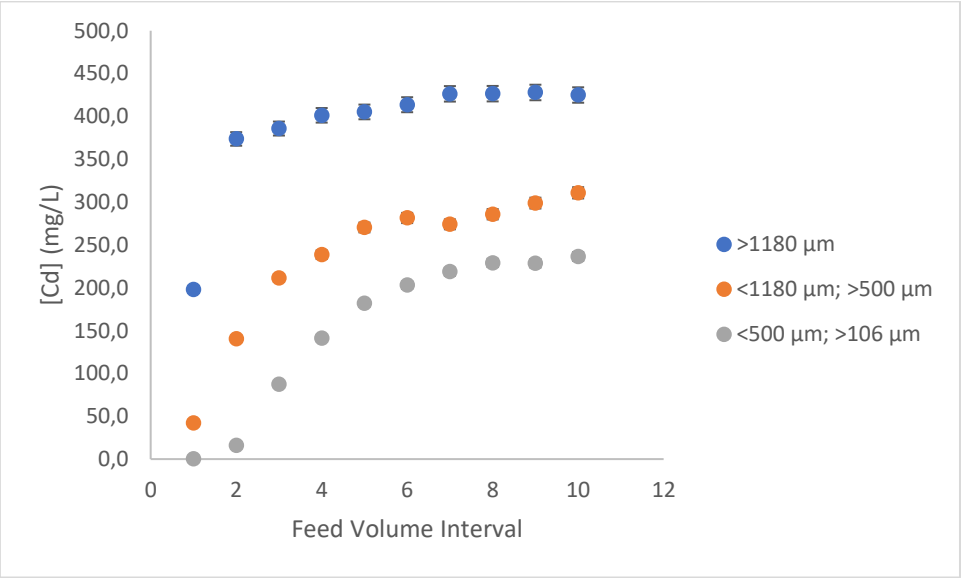

Figure 45: Adsorption of cadmium in a mixed metal solution onto different clinoptilolite particle sizes

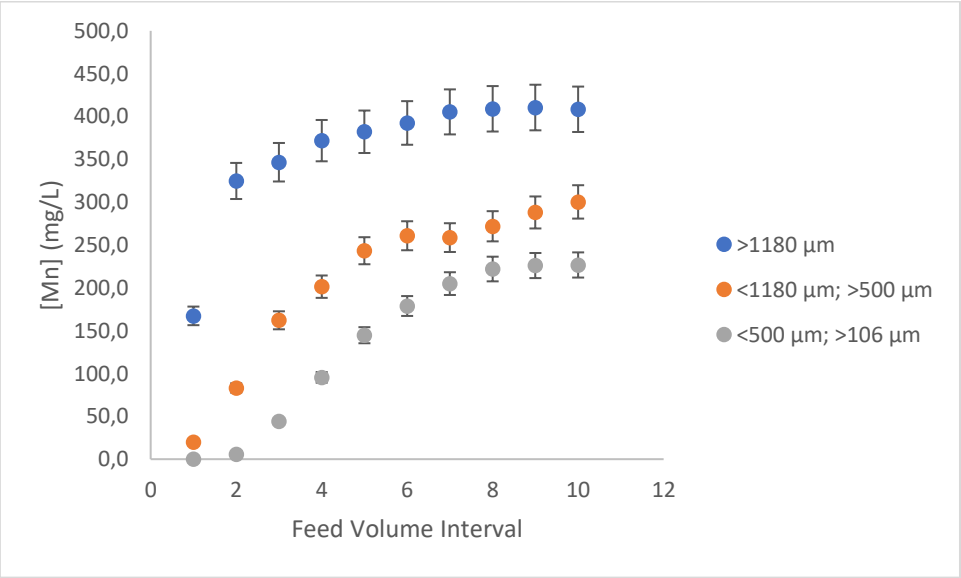

Figure 46: Adsorption of manganese in a mixed metal solution onto different clinoptilolite particle sizes

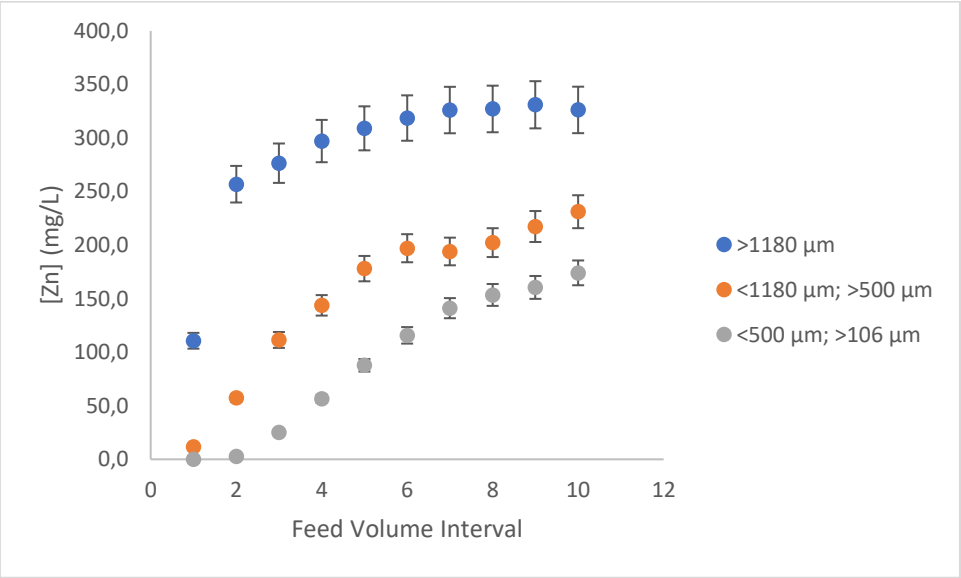

Figure 47: Adsorption of zinc in a mixed metal solution onto different clinoptilolite particle sizes

Similar to the results obtained from the experiments conducted with the alkaline- and acid mine drainage samples, the adsorption of the cadmium, manganese and zinc ions in the mixed metal solution increases with a decrease in sorbent particle size.

The results obtained from the experiments conducted to determine the effect of particle size on metals found in alkaline- and acid mine drainage and metals in the mixed metal solution is in line with the results obtained by Sprynskyy, et al., (2006). Therefore, it can be concluded that the accessibility of the adsorption centres of the sorbents are better with a decrease in sorbent fraction size.

4.5 Effect of pH

The experiments to determine the effect of pH on the adsorption of heavy metals onto the clinoptilolite was conducted with three different aqueous solutions namely alkaline mine drainage, acid mine drainage and a mixed metal solution containing cadmium, manganese and zinc. The alkaline mine drainage solution had a pH of 8.22, the acid mine drainage solution had a pH of 2.33 and the pH of the mixed metal solution was varied from pH 3 to pH 7.

I. Alkaline mine drainage

The adsorption tendencies of calcium, magnesium and potassium present in the alkaline mine drainage solutions were investigated. These tendencies are given in Figure 48.

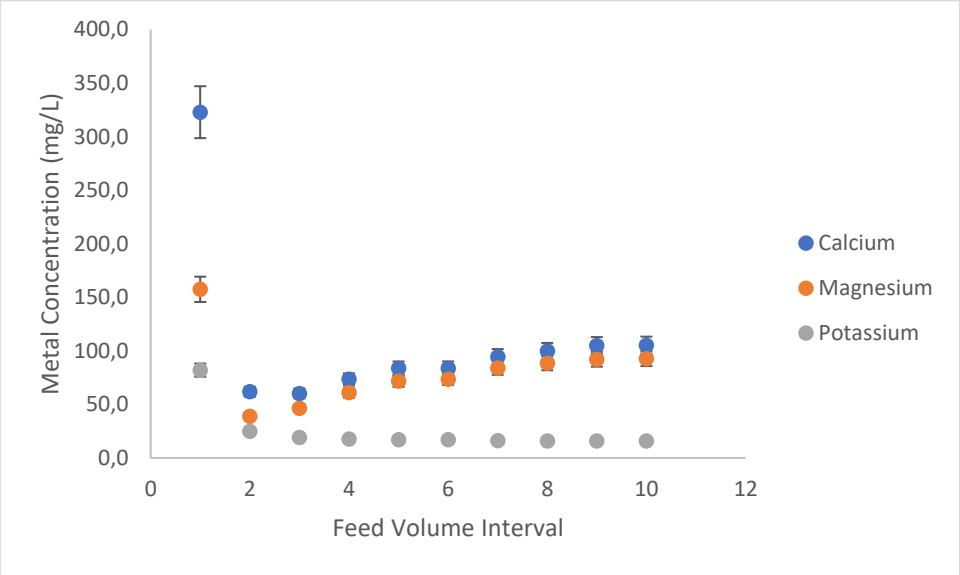

Figure 48: Adsorption Ca, Mg and K in alkaline mine drainage onto clinoptilolite

From Figure 48 it is noted that the initial adsorption of both calcium and magnesium by the clinoptilolite is quite significant until equilibrium is reached around the 8th pore volume filtrate. The affinity of the clinoptilolite for the potassium is higher than that for calcium and magnesium as the concentration of potassium consistently decreases as the pore volumes increased.

II. Acid mine drainage

The adsorption of calcium, potassium, aluminium, iron and manganese present in the acid mine drainage solution onto the clinoptilolite was studied and the results are given in Figure 49.

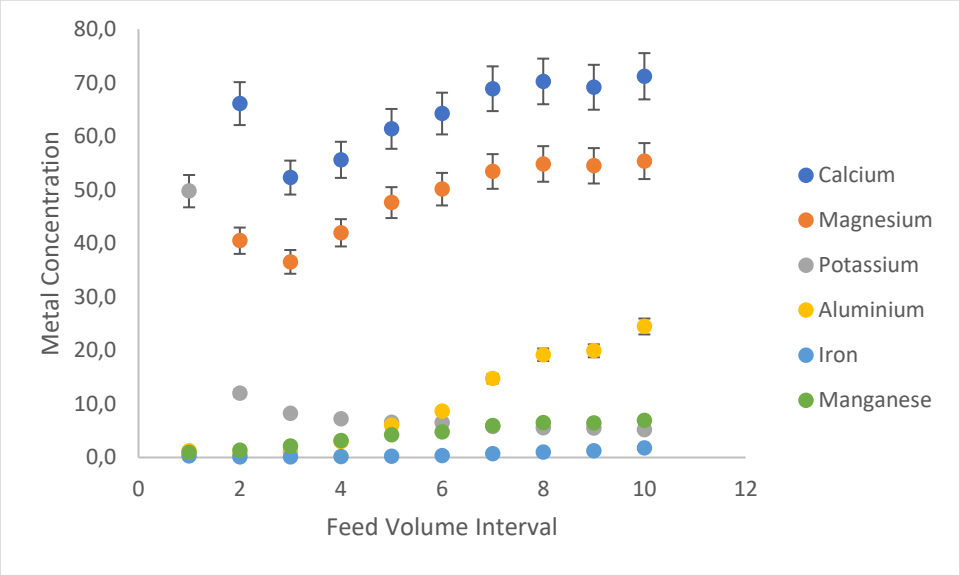

Figure 49: Adsorption of heavy metals in AMD onto clinoptilolite

The concentration of all the investigated metals present in the acid mine drainage samples ended below their initial concentration in the sample solution after 10 feed volumes were pumped through the clinoptilolite-containing column. These results indicates that the clinoptilolite is an effective adsorbent of heavy metals from industrial wastewater. This result is consistent with that found by Erdem, et al., (2004).

III. Mixed metal solution

To study the effect of pH on the adsorption of the heavy metals present in the mixed metal solution, the experiments were conducted using a mixed metal solution at pH 3, pH 5 and pH 7, respectively. The adsorption results of cadmium, manganese and zinc in a combined mixture at the different pH values are given in Figure 50 – 52.

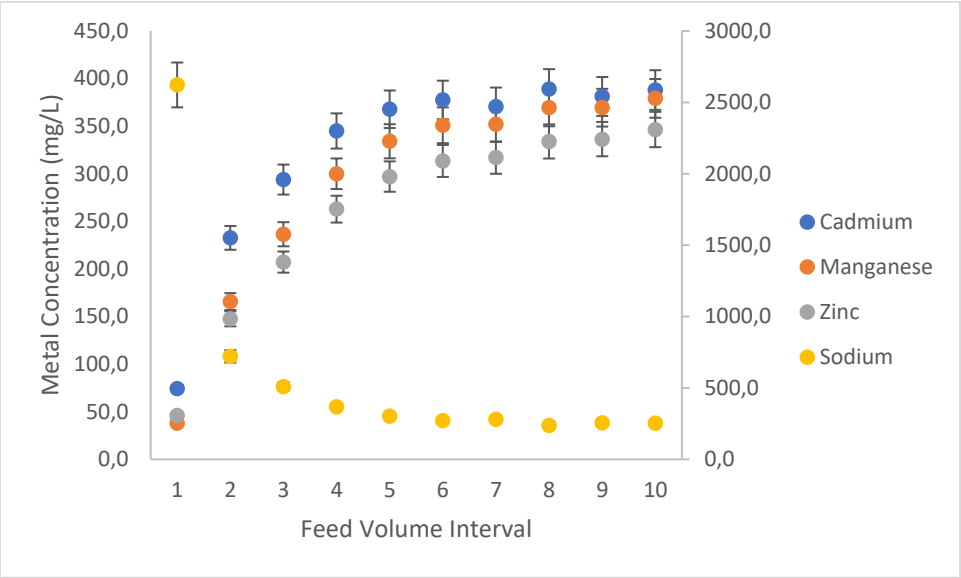

Figure 50: Filtrate of mixed metal concentrations at pH 3

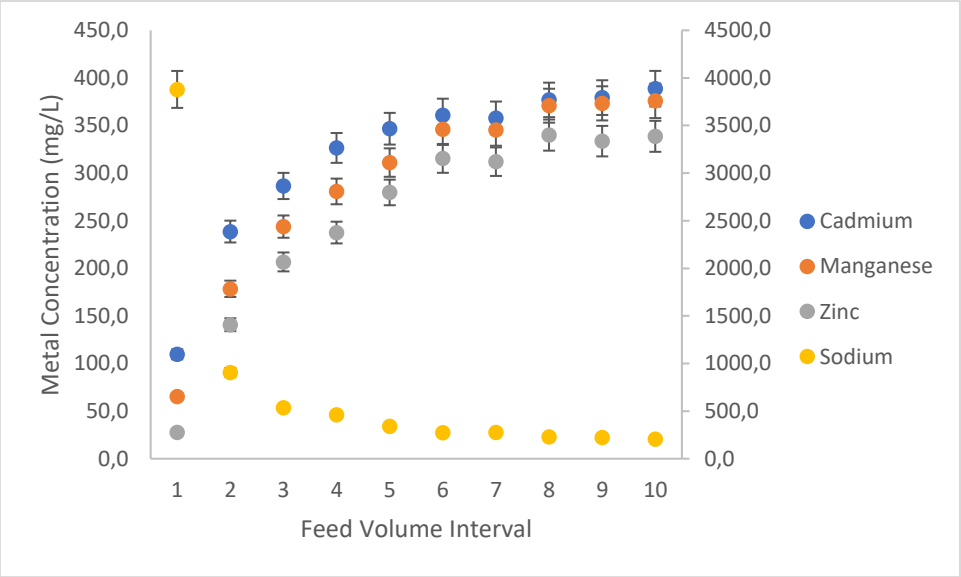

Figure 51: Filtrate of mixed metal concentrations at pH 5

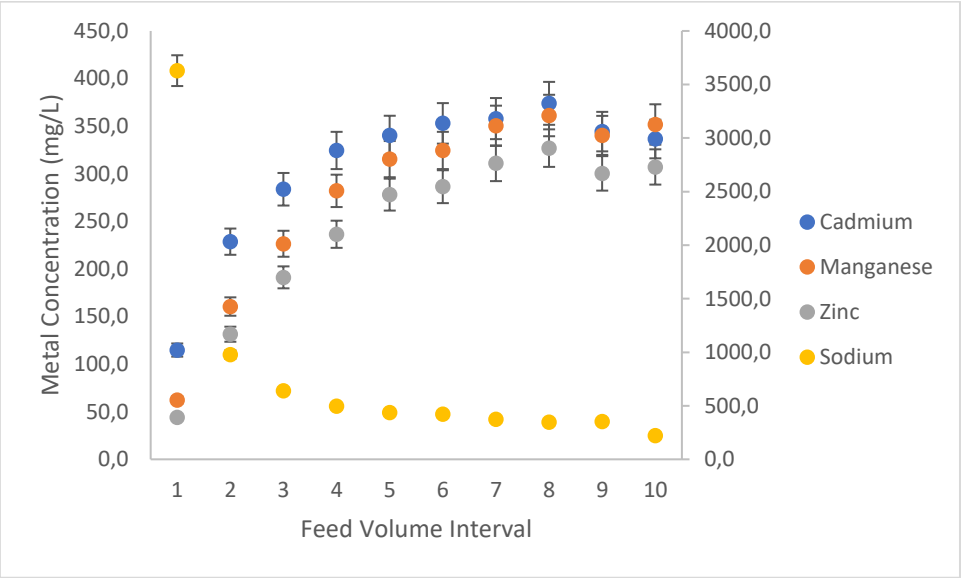

Figure 52: Filtrate of mixed metal concentrations at pH 7

At all pH variations of the mixed metal solution, the adsorption of the cadmium ion is the least effective. This result correlates to the results obtained by Erdem, et al., (2004) and is therefore likely due to the cadmium ion having the largest diameter (~0.85 nm) resulting in less cadmium ions penetrating the small diameter channels (~0.4 nm) of the adsorbent. From Figure 50 - 52 it can also be seen that the initial metal concentrations are considerably lower than that of the sodium. The amount of sodium in the filtrate decreases with an increase in pore volumes pumped to the column. This indicates that the metal ions are exchanged with the sodium ions on the surface of the clinoptilolite. This result therefore supports the ion-exchange properties of clinoptilolite stated by Zanin, et al., (2017). The influence of the variation of pH on the concentration of the individual metals are represented by Figure 53 – 55.

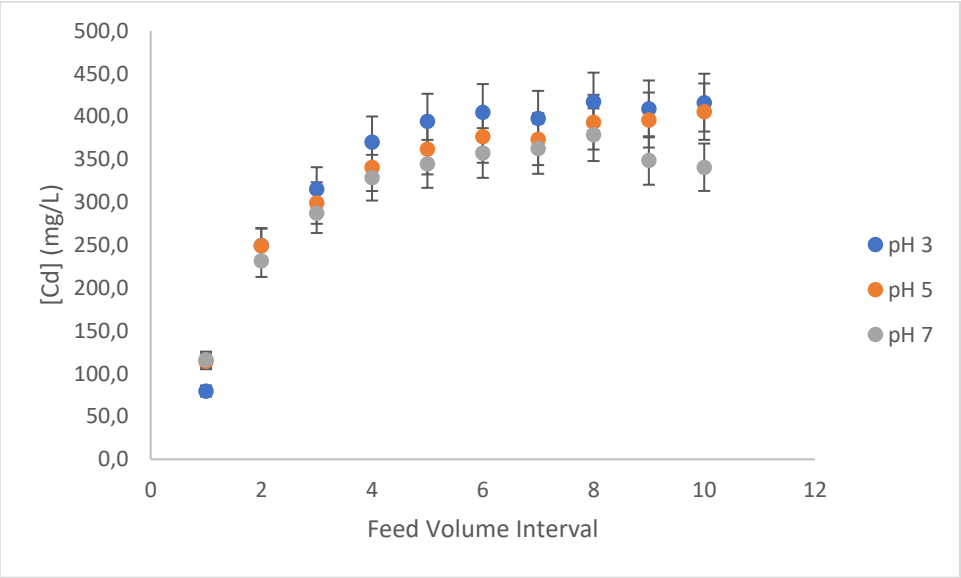

Figure 53: Influence of pH on cadmium adsorption

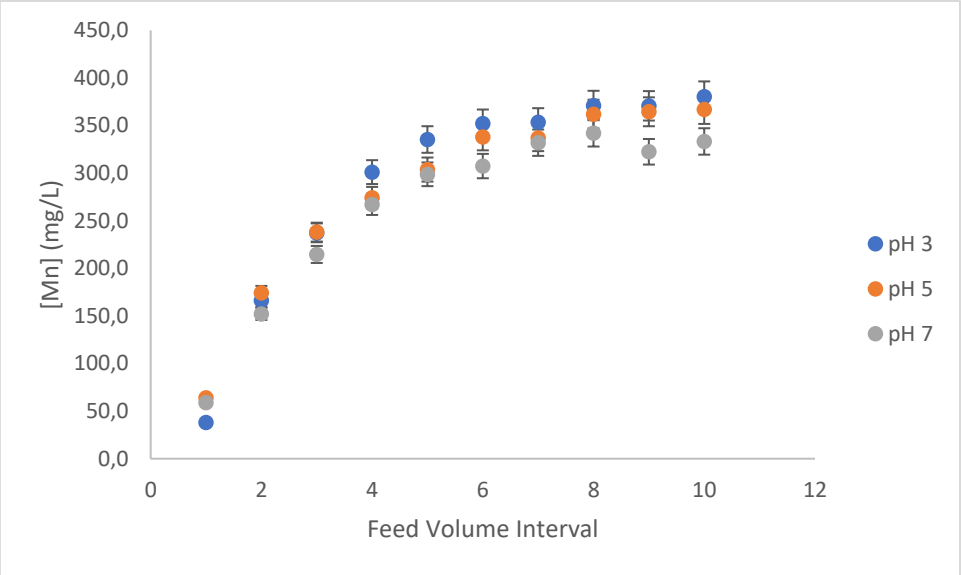

Figure 54: Influence of pH on manganese adsorption

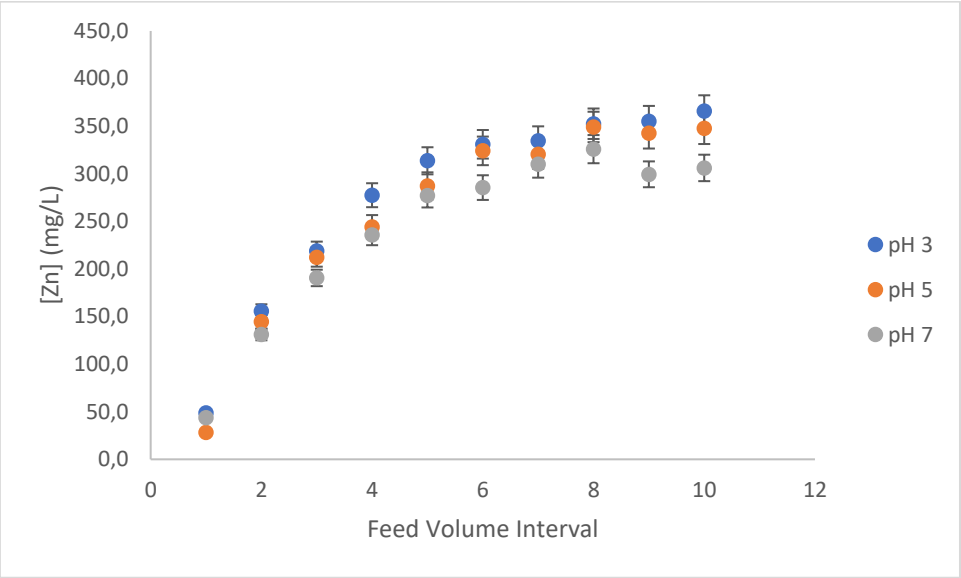

Figure 55: Influence of pH on zinc adsorption

The Figures above indicate that the adsorption of each metal is proportional to the pH of the metal solution. The decrease in adsorption of the heavy metals in the more acidic solutions are due to the heavy metal ions having to compete with a larger concentration of proton ions to bind to the surface of the clinoptilolite. The surface of the clinoptilolite is therefore saturated quicker, decreasing the opportunities for the heavy metal ions to bind to the surface of the clinoptilolite resulting in more heavy metals being present in the filtrate. In the neutral solution the concentration of the proton ions is less, resulting in the delay of surface saturation of the clinoptilolite. More heavy metal ions thus bind to the surface of the clinoptilolite causing the heavy metal concentration in the filtrate to be lower. These results correlate to the results obtained by Kithome, et al., (1999), Berber-Mendoza, et al., (2006) and Erdem, et al., (2004).

4.6 Effect of water hardness

I. Magnesium

The effect of the concentration of magnesium concerning the adsorption of cadmium, manganese and zinc onto the surface of the clinoptilolite is presented in Figure 56, Figure 57 and Figure 58, respectively. The concentration of the magnesium was varied from 50 mg/L to 200 mg/L. Figure 56 indicates that the initial cadmium concentration for the first four pore volumes of metal solution is higher with an increase in the magnesium concentration. The concentration of the cadmium ions in the filtrate in the presence of the increasing magnesium concentration did not alter

significantly with the progression of the pore volumes that transferred through the clinoptilolite. However, the adsorption of the cadmium ions did decrease with an increase in magnesium concentration.

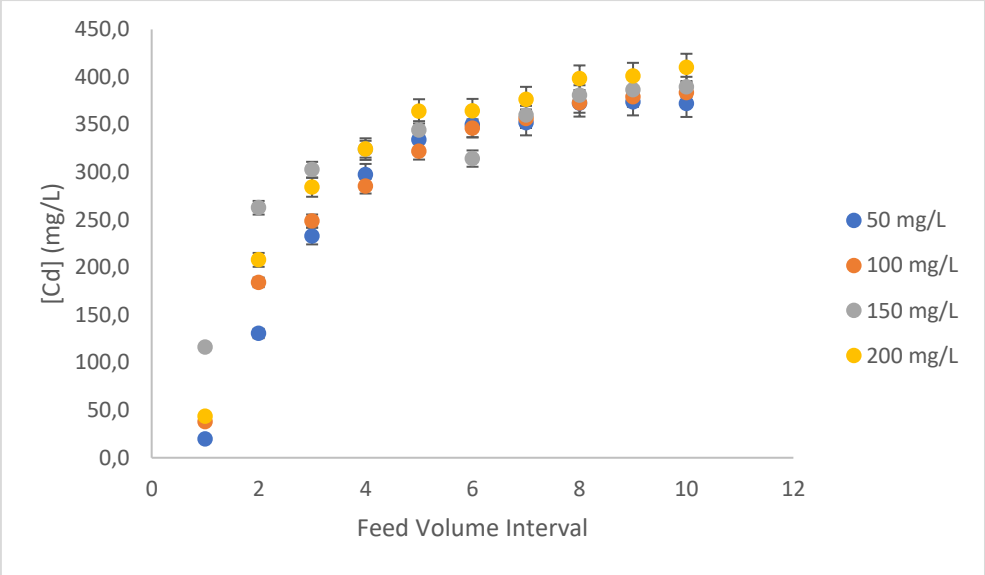

Figure 56: Influence of magnesium on cadmium adsorption

Figure 57 presents the influence of the increase in magnesium concentration on the manganese concentration in the filtrate. The initial manganese concentration of the first five pore volumes is higher with an increase in magnesium. The adsorption of the manganese ions onto the surface of the clinoptilolite did increase as the magnesium concentration decreased.

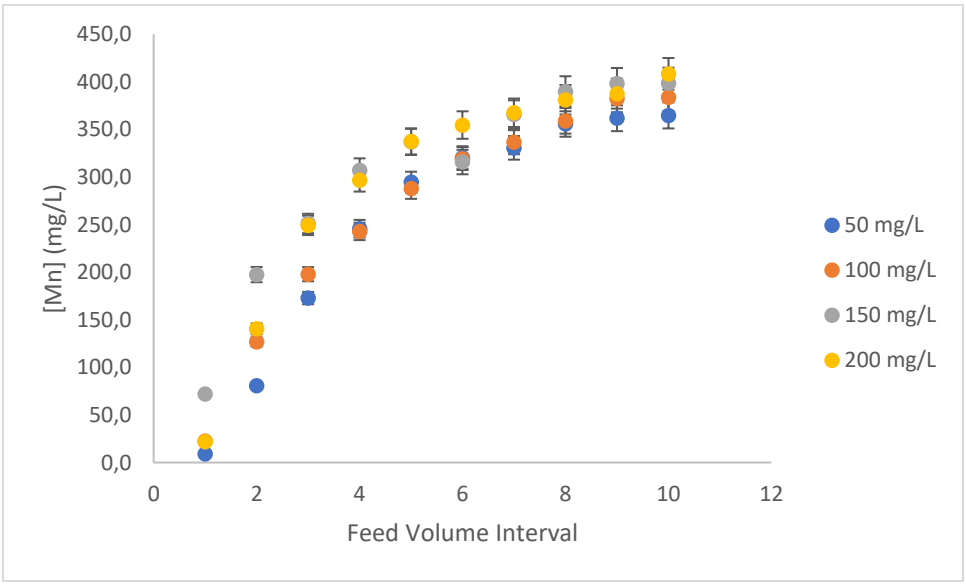

Figure 57: Influence of magnesium on manganese adsorption

The influence of the concentration of the magnesium on the adsorption of the zinc ions onto the clinoptilolite are presented in Figure 58. The zinc uptake is favoured when the magnesium concentration is lower. The increase of magnesium to a concentration of 200 mg/L resulted in a higher concentration of zinc ions being present in the filtrate. This indicates that a competitive sorption may exists between the magnesium ions and the zinc ions.

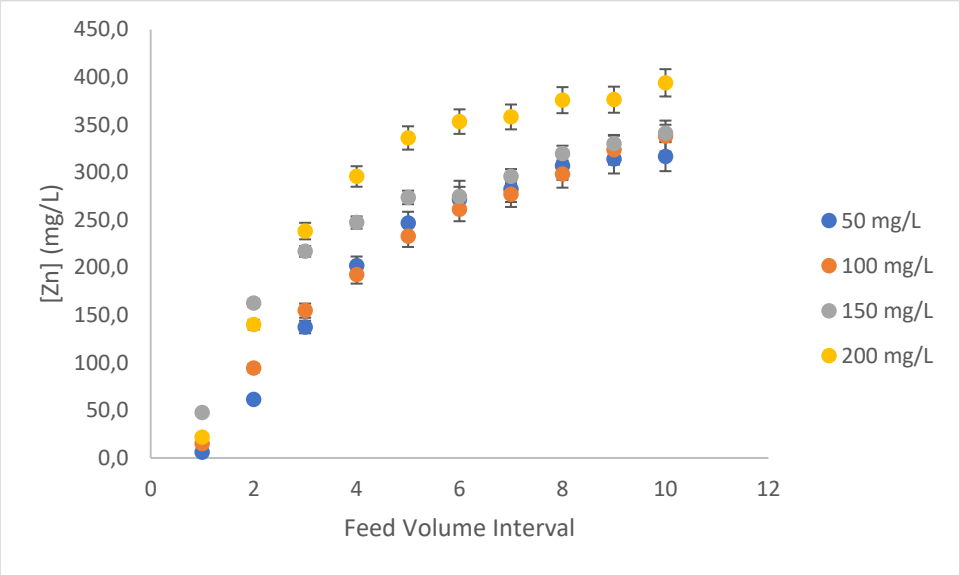

Figure 58: Influence of magnesium on zinc adsorption

II. Calcium

The effect of calcium concentration on the adsorption of cadmium, manganese and zinc is represented in Figure 59 – 61.

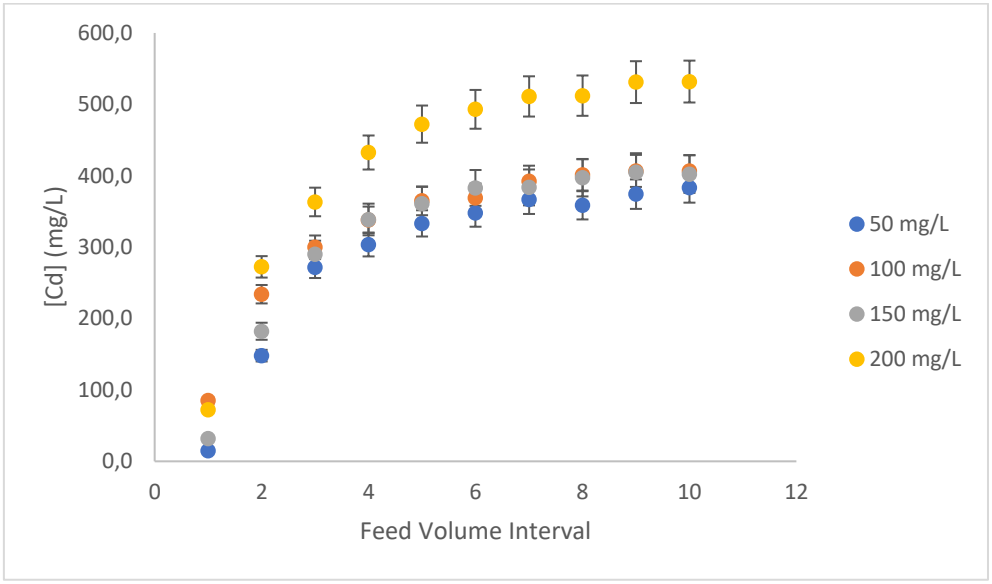

Figure 59: Influence of calcium on cadmium adsorption

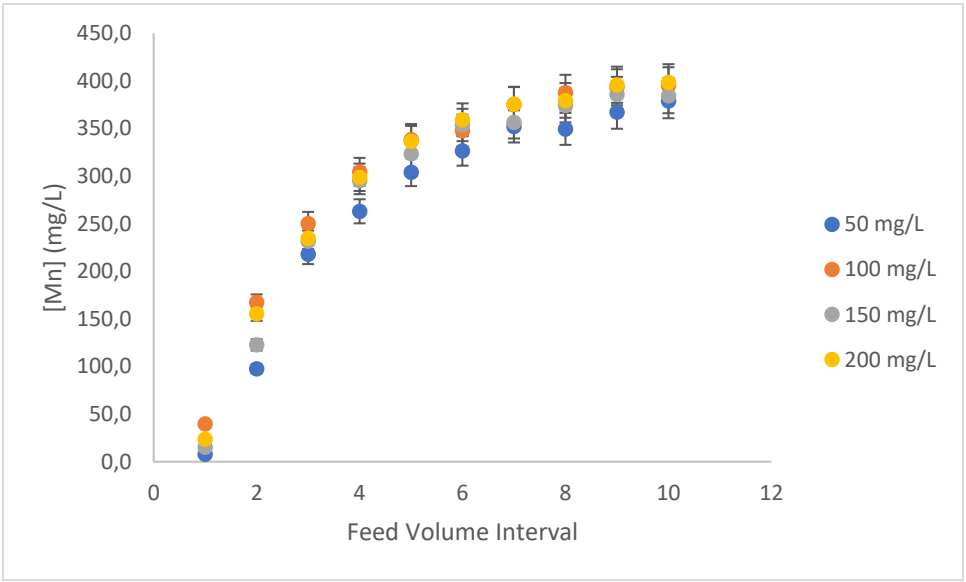

Figure 60: Influence of calcium on manganese adsorption

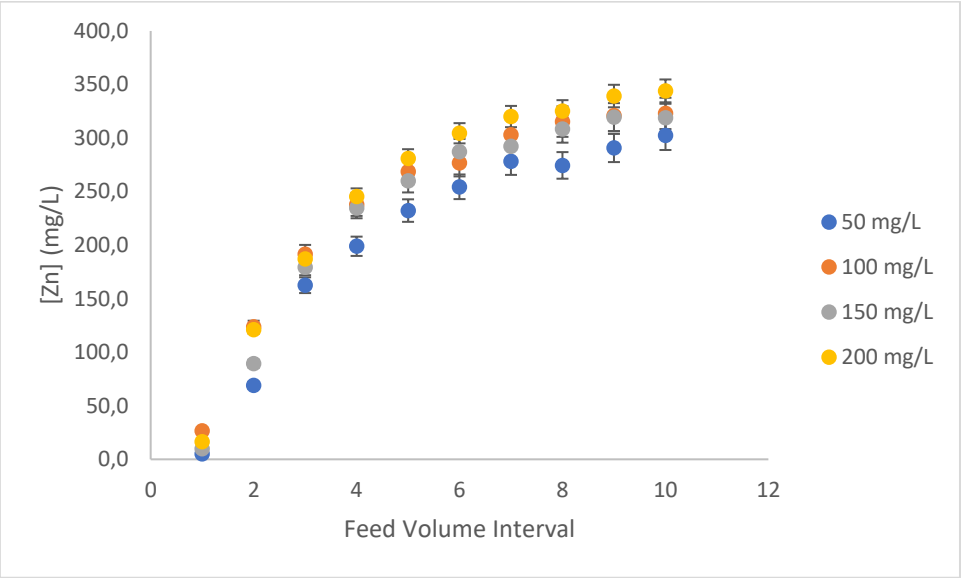

Figure 61: Influence of calcium on zinc adsorption

From the Figures above it can be seen that the increase in calcium concentration had a large effect on the cadmium adsorption and a lesser effect on the adsorption of the manganese and the zinc onto the surface of the clinoptilolite. It is, however, important to note that the adsorption of all the heavy metals increased as the concentration of the calcium ions decreased. This indicates that the heavy metals have to compete with the increase in calcium ions to bind to the surface of the clinoptilolite. Therefore, as the concentration of the calcium ions increase, the concentration of the heavy metals in the filtrate will increase. This result is similar to that found by Dyer, et al., (2018) and Martins & Boaventura (2004).

4.7 Effect of mineral characteristics

I. Alkaline mine drainage

To study the effect of mineral characteristics on the adsorption of calcium, magnesium and potassium present in alkaline mine drainage, the adsorption of these ions onto the clinoptilolite and onto a clinoptilolite-quartz mixture was investigated. Figure 62 presents the adsorption onto the two sorption compositions.

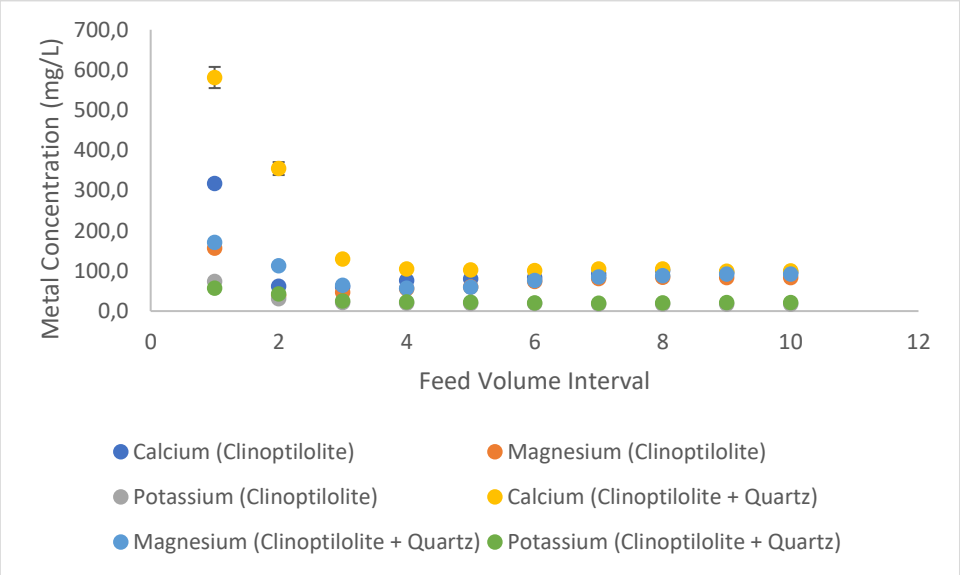

Figure 62: Adsorption of Ca, Mg and K onto clinoptilolite and onto a clinoptilolite and quartz mixture

The adsorption of the calcium, magnesium and potassium ions are better when clinoptilolite is the only mineral phase available for adsorption. This result correlates to the results obtained by Haile & Fuerhacker (2018). However, a larger difference in adsorption capacity was expected due to the quartz consisting of a no sorption capacity. The smaller difference in final metal concentrations in the filtrates of the two sorption compositions are likely due to the difference in particle sizes of the two minerals used. The particle size of the clinoptilolite ranged from 0.8 – 4 mm, whilst the quartz was in powder form with a particle size of less than 106 µm. The smaller particle size of the quartz likely reduced the flowrate of the alkaline mine drainage through the column contents, resulting in a higher residence time of the aqueous solution inside the column. The higher residence time resulted in more metal ions to be exposed to the sorptive clinoptilolite.

II. Acid mine drainage

The adsorption of calcium, magnesium, potassium, aluminium, iron and manganese present in the acid mine drainage sample onto the different sorptive composites were investigated. Figure 63 and Figure 64 present the adsorption of these metals onto the clinoptilolite and clinoptilolite-quartz sorptive minerals, respectively.

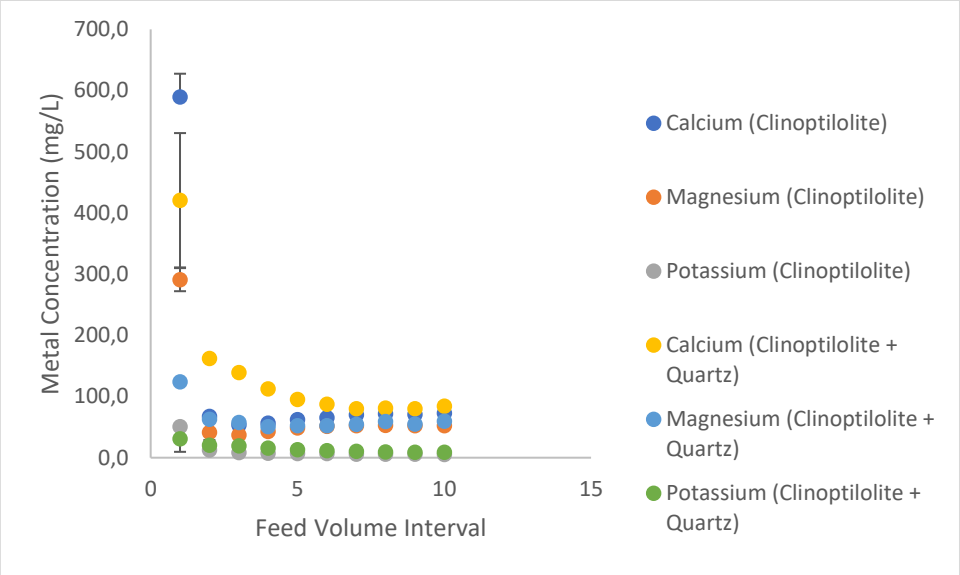

Figure 63: Adsorption of Ca, Mg, K in AMD onto clinoptilolite and onto a clinoptilolite and quartz mixture

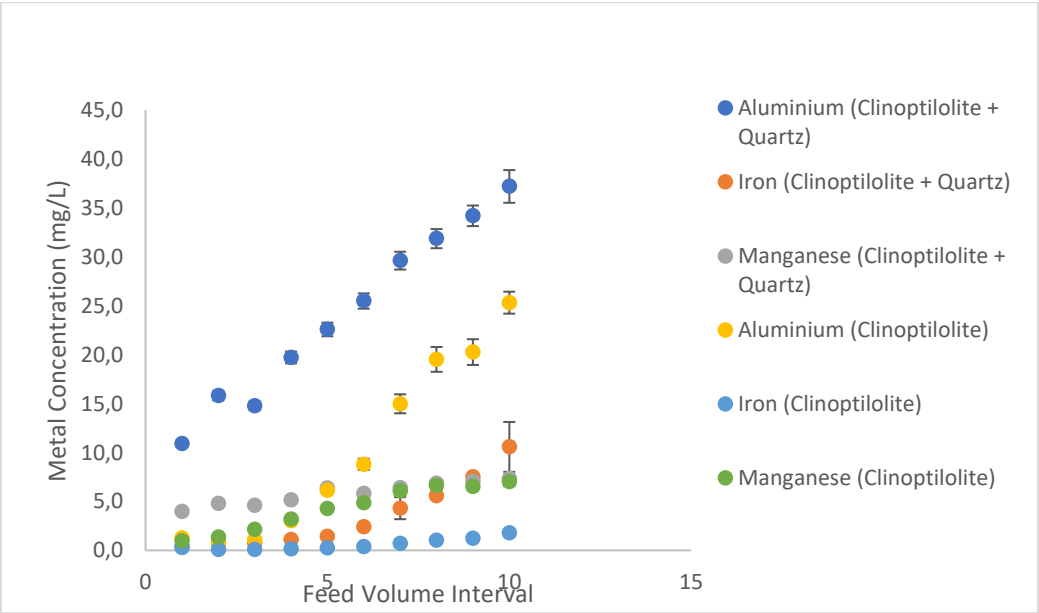

Figure 64: Adsorption of Al, Fe and Mn in AMD onto clinoptilolite and onto a clinoptilolite and quartz mixture

All of the analysed metals indicated better adsorption onto the clinoptilolite mineral phase. The adsorption of the calcium and magnesium ions onto the clinoptilolite and the clinoptilolite-quartz mineral phases did not differ significantly. Similar to experiments conducted with the alkaline mine drainage, this result is likely due to the increase in the residence time of the acid mine drainage solution inside of the column due to restrictive flow caused by the small particle size of the quartz, clogging the free flow of the water. The adsorption of the potassium, aluminium, iron and manganese indicated a larger difference in adsorption onto the different mineral phases. The clinoptilolite mineral phase resulted in higher adsorption of these ions. This result is similar to the results found by Haile & Fuerhacker (2018).

III. Mixed metal solution

Cadmium, manganese and zinc were the metals analysed to determine the effect of minerals characteristics on the adsorption of a mixed metal solution. Figure 65 presents the adsorption of these metals onto the clinoptilolite and clinoptilolite-quartz sorptive minerals.

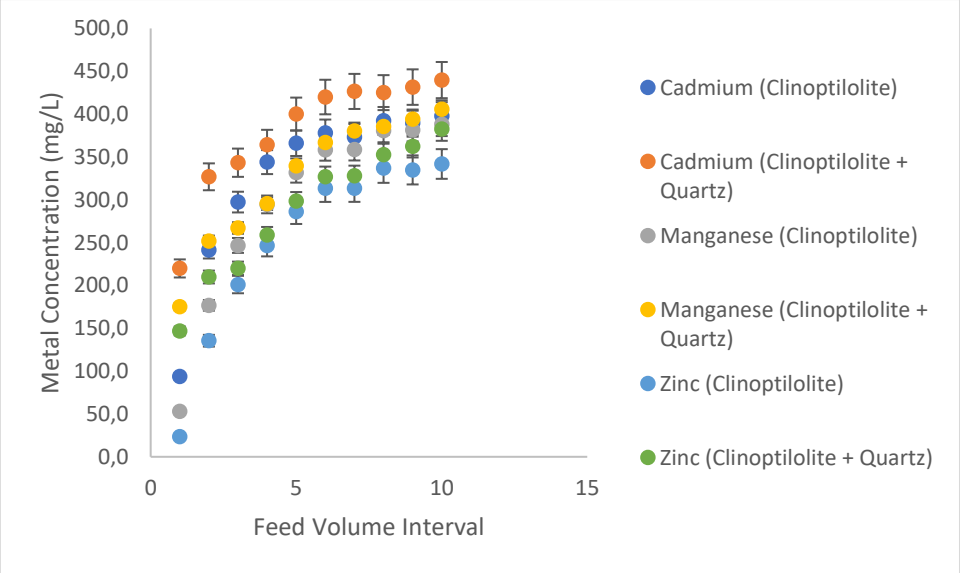

Figure 65: Adsorption of Cd, Mn, Zn onto clinoptilolite and onto a clinoptilolite and quartz mixture

The figure above indicates that the adsorption of the cadmium-, manganese- and zinc ions are improved when clinoptilolite is the only mineral phase present in the column. These results indicate that the quartz has a low adsorption capacity and can therefore inhibit the adsorption of

the heavy metals onto the surface of the clinoptilolite. The small adsorption capacity of quartz is likely due to its perfect crystalline structure and non-porous surface. This result correlates with that found by Haile & Fuerhacker (2018).

Chapter 5: Conclusion and Recommendations

5. Chapter 5: Conclusion and Recommendations

5.1 Conclusion

This study investigated the sorptive nature of the natural zeolite, clinoptilolite, on the heavy metal removal of industrial effluents. The effect of aqueous solution properties including pH and water hardness on the adsorption capacity of the clinoptilolite was also investigated. Finally, the effect of the quartz impurity on the adsorption of the heavy metals onto the surface of the clinoptilolite was also determined.

Characterisation of the clinoptilolite included FT-IR, SEM-EDS, XRD and XRF analysis. Regarding the surface characterisation of the clinoptilolite, the FT-IR analysis indicated the presence of the O-H, C=O and the C-O functional groups present on the clinoptilolite and the SEM analysis indicated the porous surface of the zeolite. The presence of these functional groups in junction with the porous surface of the clinoptilolite, indicates the zeolite as a suitable adsorbent of heavy metals. The XRD analysis indicated that the high crystallinity of the clinoptilolite was observed at the highest peak at 2Θ = 11.4°. XRF spectrophotometry was used to determine the elemental composition of the clinoptilolite sample and the results indicated that $Al_2O_3$and SiO_2 are the most prominent compounds identified in the clinoptilolite sample. The BET analysis indicated the presence of micro-porosity, mesopores and macropores.

It was found that the Freundlich isotherm model and the Pseudo-second order kinetic models better described the adsorption of the cadmium, zinc, manganese and lead onto the surface of the clinoptilolite. The result of the Freundlich isotherm model being the best fit for the adsorption of all the investigated heavy metals, indicates that the adsorption process of the heavy metals occurs onto a heterogeneous surface and therefore, many layers are involved in the adsorption process. The Pseudo-second order kinetic model fit, implies that the surface adsorption, that involves chemisorption, is the rate-limiting step.

The results further indicate that the ion exchange process occurs between the sodium cations on the surface of the clinoptilolite and the heavy metal cations in the aqueous solutions. However, it was indicated that the adsorption of the heavy metals decreased when the pH of the aqueous solutions decreased. The decrease in adsorption of the heavy metals in the more acidic solutions are due to the heavy metal ions having to compete with a larger concentration of proton ions to bind to the surface of the clinoptilolite resulting in the surface of the clinoptilolite reaching

saturation at an accelerated pace and more heavy metals being present in the filtrate. Adsorption of the heavy metals were favoured at a neutral pH environment as the experimental results indicated a competitive reaction between the heavy metal ions and the increased calcium and magnesium ions present in the alkaline solutions.

Lastly it is concluded that the adsorption of the investigated heavy metal ions is favoured when clinoptilolite is the only mineral phase present, with the adsorption of the heavy metals decreasing with the presence of quartz. The low adsorption capacity of the quartz is likely due to its reduced adsorption sites due to its perfect crystalline structure and non-porous surface.

5.2 Recommendations

It will be advisable to investigate the regeneration of the clinoptilolite after heavy metal adsorption for future study.

References

Abollino, O. & Barberis, R., 2002. Distribution and mobility of metals in contaminated sites. Chemometric investigation of pollutant profiles. *Environmental Pollution,* 119(2), pp. 177-193.

Agbenyeky, E., Muzenda, E. & Msibi, A., 2016. Chemical alterations in three clayey soils from percolation and interaction with acid mine drainage (AMD). *South African Journal of Chemical Engineering,* 21(21), pp. 28-36.

Akcil, A. & Koldas, S., 2006. Acid Mine Drainage: causes, treatment and case studies. *Cleaner Production,* 5(13), pp. 1139-1145.

Akimkhan, A., 2012. Structural and Ion-Exchange Properties of Natural Zeolite. In: Kilislioglu, ed. *Ion Exchange Technologies.* Rijeka: InTech.

Appelo, C. & Postma, D., 2010. *Geochemistry, Groundwater and Pollution, 2nd edition.* Amsterdam: A.A Balkema Publishers.

Awadh, H., 2013. Assessment of the potential nickel and lead in the road-side dust in the Karkh city along the highway between Ramadi and Rutba, West of Iraq. *Environmental Science Toxicology Journal,* 1(7), pp. 126-135.

Baker, H., Massadeh, A. & Younes, H., 2009. Natural Jordanian zeolite: removal of heavy metal ions from water samples using column and batch methods. *Environmental Monitoring and Assessment,* Volume 157, pp. 319-330.

Banks, D. et al., 2002. Alkaline mine drainage from metal sulphide and coal mines: examples from Svalbard and Siberia. *Geological Society, 198,* pp. 287-296.

Baran, A. & Tarnawski, M., 2015. Assessment of heavy metals mobility and toxicity in contaminated sediments by sequential extraction and a battery of bioassays. *Ecotoxicology,* 24(6), p. 1279–1293.

Berber-Mendoza, M., Leyva-Ramos, R. & Alonso-Davila, P., 2006. Effect of pH and temperature on the ion-exchange isotherm of Cd(II) and Pb(II) on clinoptilolite. *Journal of Chemical Technology and Biotechnology,* 81(6), pp. 966-973.

Blowes, D., Ptacek, C., Jambor, J. & Weisener, C., 2003. The Geochemistry of Acid Mine Drainage. *Treatise on Geochemistry.*

Butler, L., Lall, U. & Bonnafous, L., 2017. Cumalative heavy metal contamination in mining areas of the Rimac, Peru basin. *Hydrology and Earth Sciences,* 21(4), pp. 135-145.

Can, O., Balkose, D. & Ulku, S., 2010. Batch and column studies on heavy metal removal using a local zeolitic tuff. *Desalination,* Volume 259, pp. 17-21.

Charki, A., Kazemian, H. & Kazemeini, M., 2010. Optimized experimental design for natural clinoptilolite zeeolite ball mill to produce nano powders. *Powder Technology,* 203(2010), pp. 389-396.

Chen, W.-H., Peng, J. & T.Bi, X., 2015. A state-of-the-art review of biomass torrefaction, densificationand applications. *Renewable and Sustainable Energy Reviews,* 1(44), pp. 847-866.

Cosgrove, W. & Loucks, D., 2015. *Water management: Current and future challenges andresearch directions,* Montreal: AGU Publications.

Cotruvo, J. et al., 2011. *World Health Organisation: Background document for development of.* [Online] Available at: https://www.who.int/water_sanitation_health/dwq/chemicals/hardness.pdf

Dharmappa, H., Sivakumar, M. & Singh, R., 1995. *The toxicity of Cu and Zn increased with decreasing water hardness. Results.* Dnver, American Institute of Htdrology.

Diale, P., Muzenda, E. & Zimba, J., 2011. *A Study of South African Natural Zeolites.* San Francisco, WCECS.

Donnenfeld, Z., Crookes, C. & Hedden, S., 2018. *A delicate balance, water scarcity in South Africa,* s.l.: Institute for security studies.

Dube, A. et al., 2001. Adsorption and Migration of Heavy Metals in Soil. *Polish Journal of Environmental Studies,* 10(1), pp. 1-10.

Duruibe, J., Ogwuegbu, M. & Egwurugwu, J., 2007. Heavy metal pollution and human biotoxic effects. *International Journal of Physical Sciences,* 2(5), pp. 112-118.

Dyer, A. et al., 2018. The use of columns of the zeolite clinoptilolite in the remediation of aqueous nuclear waste streams. *Journal of Radioanalytical and Nuclear Chemistry,* 318(2018), pp. 2473-2491.

Erdem, E., Karapinar, N. & Donat, R., 2004. The removal of heavy metal cations by natural zeolites. *Journal of Colloid and Interface Science,* pp. 309-314.

Fick, G., Mirgaux, O., Neau, P. & Patisson, F., 2014. Using Biomass for Pig Iron Production: A Technical,Environmental and Economical Assessment. *Waste Biomass Valor,* Issue 5, pp. 43-55.

Fosso-Kankeu, E., Waanders, F. & Fourie, C., 2016. Adsorption of Congo Red by surfactant-impregnated bentonite clay. *Desalination and Water Treatment,* 57(57), pp. 27663-27671.

Fosso-Kankeu, E., Waanders, F. & Fourie, C., 2016. Adsorption of Congo Red by surfactant-impregnated bentonite clay. *Desalination and Water Treatment.*

Fosso-Kankeu, E., Waanders, F. & Fourie, C., 2016. Adsorption of Congo Red by surfactant-impregnated bentonite clay. *Desalination and Water Treatment,* 57(57), pp. 858-866.

Gil, M., García, R., C, P. & Rubiera, F., 2015. Grindability and combustion behavior of coal and torrefied biomass blends. *Bioresour,* pp. 205-212.

Goienaga, N. & Madariaga, J., 2015. Recrystallization and stability of Zn and Pb minerals on their migration to groundwater in soils affected by Acid Mine Drainage under CO2 rich atmospheric waters. *Chemosphere,* Volume 119, pp. 727-733.

Gray, N., 1997. Environmental impact and remediation of acid mine drainage: a management problem. *Environmental Geology,* 30(1), pp. 62-71.

Gyamfi, E., Appiah-Adjei, E. & Adjei, K. A., 2019. Potential heavy metal pollution of soil and water resources from artisanal mining in Kokoteasua, Ghana. *Groundwater for Sustainable Development,* pp. 1-2.

Gyamfi, E., Appiah-Adjei, E. & Adjei, K. A., 2019. Potential heavy metal pollution of soil and water resources from artisanal mining in Kokoteasua, Ghana. *Groundwater for Sustainable Development,* 8(4), pp. 450-456.

Haile, T. & Fuerhacker, M., 2018. Simultaneous Adsorption of Heavy Metals from Roadway Stormwater Runoff Using Different Filter Media in Column Studies. *Water,* 10(9), p. 1160.

Huang, H., Yan, B., Xiao, X. & Yang, L., 2009. Ammonium Removal From Aqueous Solutions by Using Natural Chinese (Chende) Zeolite as Adsorbent. *Journal of hazardous materials,* 175(1-3), pp. 247-252.

Inglezakis, V., 2005. The concept of "capacity" in zeolite ion-exchange systems. *Journal of Colloid and Interface Science,* 281(1), pp. 68-79.

Ismail, A. et al., 2010. Synthesis, optimization and characterization of zeolite A and its ion-exchange properties. *Colloids and Surfaces A: Physiochemical and Engineering Aspects,* 366(1-3), pp. 80-87.

Jhariya, D. & Khan, R., 2016. *Impact of Mining Activity on Water Resources: An overview study.* Raipur, National Seminar on Recent Practices & Innovations in Mining Industry.

Johnson, R. et al., 2016. *Column Testing and 1D Reactive Transport Modeling To Evaluate Uranium Plume Presistance Processes.* Freiberg, s.n., pp. 652-659.

Kearney, L., 2012. *Mining and minerals in South Africa.* [Online]
Available at: https://www.brandsouthafrica.com/investments-immigration/business/economy/mining-and-minerals-in-south-africa

Kithome, M., Paul, J., Lavkulich, L. & Bomke, A., 1999. Effect of pH on ammonium adsorption by natural Zeolite clinoptilolite. *Communications in Soil Science and Plant Analysis,* 30(9-10), pp. 1417-1430.

Kumari, S., Udayabhanu, G. & Prasad, B., 2010. Studies on environmental impact of acid mine drainage generation and its treatment: An appraisal. *Indian Journal of Environmental Protection 30(11),* pp. 953-967.

Kumar, V. et al., 2019. Global evaluation of heavy metal content in surface water bodies: A meta-analysis using heavy metal pollution indices and multivariate statistical analyses. *Chemosphere,* Volume 236.

Liao, J. & Wei, C., 2016. Distribution and migration of heavy metals in soil and crops affected by acid mine drainage: Public health implications in Guangdong Province, China. *Ecotoxicology and Environmental Safety,* Volume 124, pp. 460-469.

Liu, F., Qiao, X., Zhou, L. & Zang, J., 2018. Migration and Fate of Acid Mine Drainage Pollutants in Calcareous Soil. *International Journal of Environmental Research and Public Health,* 15(8), p. 1759.

Li, Y. et al., 2019. Removal of Zn2+, Pb2+, Cd2+, and Cu2+ from aqueous solution by synthetic clinoptilolite. *Microporous and Mesoporous Materials,* Volume 273, pp. 203-211.

Lucia, T. & McBride, B., 1982. MOBILITY AND EXTRACTABILITY OF CADMIUM. *Soil Science.*

Luis, A. et al., 2009. Impact of Acid Mine Drainage (AMD) on Water Quality, Stream Sediments and Periphytic Diatom Communities in the Surrounding Streams of Aljustrel Mining Area (Portugal). *Water, Air and Soil Pollution,* 2009(200), pp. 147-167.

Mamba, B. et al., 2009. Metal adsorption capabilities of clinoptilolite and selected strains of bacteria from mine water. *Physics and Chemistry of the Earth, Parts A/B/C,* 34(13-16), pp. 830-840.

Martins, R. & Boaventura, R., 2004. Cadmium(II) and zinc(II) adsorption by the aquatic moss Fontinalis antipyretica: effect of temperature, pH and water hardness. *Water Research,* 38(3), pp. 693-699.

Minerals Council South Africa, 2021. *Minerals Council South Africa.* [Online]
Available at: https://www.mineralscouncil.org.za/sa-

mining#:~:text=In%202018%20the%20mining%20sector,up%20to%20nine%20indirect%20dependants [Accessed 11 May 2021].

Mining in Africa, 2017. *Mining in Africa.* [Online]
Available at: https://miningafrica.net/mining-countries-africa/south-africa/#:~:text=Mining%20in%20South%20Africa%20started,also%20in%20the%20Northern%20Cape. [Accessed 11 May 2021].

Mnisi, N., 2020. *WATER SCARCITY IN SOUTH AFRICA: A RESULT OF PHYSICAL OR ECONOMIC FACTORS?.* [Online]
Available at: https://hsf.org.za/publications/hsf-briefs/water-scarcity-in-south-africa-a-result-of-physical-or-economic-factors#_ftnref2

Modoi, O., Roba, C., Torok, Z. & Ozunu, A., 2014. ENVIRONMENTAL RISKS DUE TO HEAVY METAL POLLUTION OF. *Environmental Engineering and Managemnet Journal, Volume 13 no 9,* pp. 2325-2336.

Munnik, V., 2020. *The Social and Environmental Consequences of Coal mining in South Africa,* The Netherlands: Environmental Monotoring Group.

Natarajan, K., 2018. Microbial Aspects of Acid Mine Drainage—Mining Environmental Pollution and Control. *Biotechnology of Metals,* 18(6), pp. 1352-1360.

Obiri-Nyarko, F., Kwiatkowska-Malina, J., Malina, G. & Kasela, T., 2015. Geochemical modelling for predicting the long-termperformance of zeolite-PRB to treat leadcontaminated groundwater. *Journal of Contaminant Hydrology,* 2015(177-178), pp. 76-84.

Otieno, F. & Ochieng, G., 2004. Water management tools as a means of averting a possible water scarcity in South Africa by the year 2025. *Water SA,* 30(5), pp. 120-124.

Panayotova, M. & Velikov, B., 2003. Influence of Zeolite Transformation in a Homoionic Form on the Removal of Some Heavy Metal Ions from Wastewater. *Journal of Environmental Science and Health, Part A,* 38(3), pp. 545-554.

Pandey, P. & Sharma, S., 2017. Removal of Cr(VI) and Pb(II) from Wastewater by ZeoliteNaX in Fixed Bed Column. *Water Conservation Science and Engineering,* Volume 2, pp. 61-65.

Prikryl, J., Jain, A., Turner, D. & Pabalan, R., 2001. Uranium sorption behaviour on silica mineral mixtures. In: *Mining and Hydrogeology.* s.l.:s.n., pp. 515-524.

Prikryl, J., Jain, A., Turner, D. & Pabalan, R., 2001. Uranium sorption behaviour on silica mineral mixtures. *Contaminant Hydrology,* pp. 241-253.

Rijsberman, R. F., 2005. Water scarcity: Fact or fiction?. *Agricultural water management,* 80(1-3), pp. 5-22.

Risjberman, F., 2005. Water scarcity: Fact or fiction?. *Agricultural Water Management,* 80(2006), pp. 5-22.

Romano, N. et al., 2020. The effects of water hardness on the growth, metabolic indicators and stress resistance of largemouth bass Micropterus salmoides. *Aquaculture,* 527(2020), pp. 1-6.

Roodbol, A., 2020. *South Africa approaching physical water scarcity by 2025.* [Online]
Available at: https://www.esi-africa.com/event-news/south-africa-approaching-physical-water-scarcity-by-2025/

Sankhla, M. et al., 2016. Heavy metals contamination in water and their hazardous effect on human health- A review. *International Journal of Currebt Microbiology and Applied Sciences,* 5(10), pp. 759-766.

Sherry, H., 2003. Ion Exchange. In: S. Auerbach, K. Carrado & P. Dutta, eds. *Handbook of Zeolite Structure and Technology.* New York: Marcel Dekker Inc..

Sprynskyy, M., Buszewski, B., Terzyk, A. & Namiesnik, J., 2006. Study of the selection mechanism of heavy metal adsorption on clinoptilolite. *Journal of Colloid and Interface Science,* Volume 304, pp. 21-28.

Sprynskyy, M., Golembiewski, R., Trykowski, G. & Buszewski, B., 2010. Heterogeneity and hierarchy of clinoptilolite porosity. *Journal of Physics and Chemistry of Solids,* 71(9), pp. 1269-1277.

Stefanakis, A., Zouzias, D. & Marsellos, A., 2015. *Groundwater Pollution: Human and Natural Sources and Risks.* 1st ed. s.l.:Studium Press LLC.

Tiruta-Barna, L., 2008. Using PHREEQC for modelling and simulation of dynamic leaching tests and scenarios. *Journal of Hazardous Materials,* 157(2-3), pp. 525-533.

USGS, 2021. *Hardness of Water.* [Online]
Available at: https://www.usgs.gov/special-topic/water-science-school/science/hardness-water?qt-science_center_objects=0#qt-science_center_objects
[Accessed 24 May 2021].

USGS, 2021. *Hardness of Water.* [Online]
Available at: https://www.usgs.gov/special-topic/water-science-school/science/hardness-water?qt-science_center_objects=0#qt-science_center_objects
[Accessed 04 July 2021].

Vukojevic Medvidovic, N., Peric, J. & Trgo, M., 2006. Column performance in lead removal from aqueous solutions by fixed bed of natural zeolite–clinoptilolite. *Separation and Purification Technology,* 49(3), pp. 237-244.

Wan Zuhairi, W., Samsudin, A. & Ridwan, N., 2008. *The Retention Characteristics of Heavy Metals in Natural Soils using Soil Column Experiment.* s.l., s.n., pp. 2405-2411.

Wang, Z. et al., 2018. Silica oxide encapsulated natural zeolite for high efficiency remocal of low concentration heavy metals in water. *Colloids and Surfaces A.*

Xu, Y. & Usher, B., 2006. *Groundwater pollution in Africa.* 1 ed. Leiden: Taylor & Francis/Balkema.

Zamzow, M. & Murphy, J., 2006. Removal of Metal Cations from Water Using Zeolites. *Seperation Science and Technology,* 27(14), pp. 1969-1984.

Zanin, E. et al., 2017. Adsorption of heavy metals from wastewater graphic industry using clinoptilolite zeolite as adsorbent. *Process Safety and Environmental Protection,* Volume 105, pp. 194-200.

Zanin, W. et al., 2017. Adsorption of heavy metals from wastewater graphic industry using clinoptilolite zeolite as adsorbent. *Process Safety and Environmental Protection,* Volume 105, pp. 194-200.

Zeledon-Toruno, Z., Lao-Luque, C. & Sole-Sardans, M., 2005. Nickel and copper removal from aqueous solution by an immature coal (leonardite): effect of pH, contact time and water hardness. *Journal of Chemical Technology & Biotechnology,* 80(6).

Zhang, J., Yuan, J.-W., Sheng, C.-D. & Xu, Y.-Q., 2000. Characterization of coals utilized in power stations of China. *Fuel,* pp. 95-102.

Appendix A

A.1.1: Isotherm study raw experimental data: Zinc_REV1

C_0 (mg/L)	C_e (mg/L)	q_e (mg/g)	Freundlich		Langmuir	
			$\ln(q_e)$	$\ln(C_e)$	C_e/q_e	C_e
25	12.2	2.6	0.9	2.5	4.8	12.2
50	30.5	3.9	1.4	3.4	7.8	30.5
75	45.1	6.0	1.8	3.8	7.5	45.1
100	69.9	6.0	1.8	4.2	11.6	69.9
125	87.9	7.4	2.0	4.5	11.8	87.9
150	106.8	8.6	2.2	4.7	12.3	106.8

A.1.2: Isotherm study raw experimental data: Zinc_REV2

C_0 (mg/L)	C_e (mg/L)	q_e (mg/g)	Freundlich		Langmuir	
			$\ln(q_e)$	$\ln(C_e)$	C_e/q_e	C_e
25	11.6	2.7	1.0	2.5	4.3	11.6
50	29.0	4.2	1.4	3.4	6.9	29.0
75	42.8	6.4	1.9	3.8	6.7	42.8
100	66.4	6.7	1.9	4.2	9.9	66.4
125	83.5	8.3	2.1	4.4	10.1	83.5
150	101.4	9.7	2.3	4.6	10.4	101.4

A.1.3: Isotherm study raw experimental data: Zinc_REV3

C_0 (mg/L)	C_e (mg/L)	q_e (mg/g)	Freundlich		Langmuir	
			$\ln(q_e)$	$\ln(C_e)$	C_e/q_e	C_e
25	11.6	2.7	1.0	2.5	4.3	11.6
50	29.0	4.2	1.4	3.4	6.9	29.0
75	42.8	6.4	1.9	3.8	6.7	42.8

100	66.4	6.7	1.9	4.2	9.9	66.4
125	83.5	8.3	2.1	4.4	10.1	83.5
150	101.4	9.7	2.3	4.6	10.4	101.4

A.2.1: Isotherm study raw experimental data: Manganese_REV1

C_0 (mg/L)	C_e (mg/L)	q_e (mg/g)	Freundlich		Langmuir	
			$\ln(q_e)$	$\ln(C_e)$	C_e/q_e	C_e
25	18.6	1.3	0.3	2.9	14.4	18.6
50	43.3	1.4	0.3	3.8	32.0	43.3
75	59.7	3.1	1.1	4.1	19.5	59.7
100	88.9	2.2	0.8	4.5	40.1	88.9
125	107.9	3.4	1.2	4.7	31.5	107.9
150	134.6	3.1	1.1	4.9	43.6	134.6

A.2.2: Isotherm study raw experimental data: Manganese_REV2

C_0 (mg/L)	C_e (mg/L)	q_e (mg/g)	Freundlich		Langmuir	
			$\ln(q_e)$	$\ln(C_e)$	C_e/q_e	C_e
25	17.3	1.5	0.4	2.8	11.1	17.3
50	40.2	2.0	0.7	3.7	20.6	40.2
75	55.5	3.9	1.4	4.0	14.2	55.5
100	82.7	3.5	1.2	4.4	23.9	82.7
125	100.3	4.9	1.6	4.6	20.3	100.3
150	125.2	5.0	1.6	4.8	25.2	125.2

A.2.3: Isotherm study raw experimental data: Manganese_REV3

C_0 (mg/L)	C_e (mg/L)	q_e (mg/g)	Freundlich		Langmuir	
			$\ln(q_e)$	$\ln(C_e)$	C_e/q_e	C_e
25	17.1	1.6	0.5	2.8	10.8	17.1

50	39.8	2.0	0.7	3.7	19.5	39.8
75	54.9	4.0	1.4	4.0	13.7	54.9
100	81.8	3.6	1.3	4.4	22.5	81.8
125	99.3	5.1	1.6	4.6	19.3	99.3
150	123.8	5.2	1.7	4.8	23.6	123.8

A.3.1: Isotherm study raw experimental data: Cadmium_REV1

C_0 (mg/L)	C_e (mg/L)	q_e (mg/g)	Freundlich		Langmuir	
			$\ln(q_e)$	$\ln(C_e)$	C_e/q_e	C_e
25	13.9	2.2	0.8	2.6	6.2	13.9
50	32.5	3.5	1.3	3.5	9.2	32.5
75	49.4	5.1	1.6	3.9	9.7	49.4
100	72.7	5.5	1.7	4.3	13.3	72.7
125	97.1	5.6	1.7	4.6	17.4	97.1
150	115	7.0	1.9	4.7	16.4	115

A.3.2: Isotherm study raw experimental data: Cadmium_REV2

C_0 (mg/L)	C_e (mg/L)	q_e (mg/g)	Freundlich		Langmuir	
			$\ln(q_e)$	$\ln(C_e)$	C_e/q_e	C_e
25	13.2	2.4	0.9	2.6	5.6	13.2
50	30.8	3.8	1.3	3.4	8.0	30.8
75	46.9	5.6	1.7	3.8	8.4	46.9
100	69.1	6.2	1.8	4.2	11.2	69.1
125	92.2	6.6	1.9	4.5	14.1	92.2
150	109.3	8.2	2.1	4.7	13.4	109.3

A.3.3: Isotherm study raw experimental data: Cadmium_REV3

			Freundlich	Langmuir

C_0 (mg/L)	C_e (mg/L)	q_e (mg/g)	$\ln(q_e)$	$\ln(C_e)$	C_e/q_e	C_e
25	14.8	2.0	0.7	2.7	7.3	14.8
50	34.7	3.1	1.1	3.5	11.4	34.7
75	52.9	4.4	1.5	4.0	12.0	52.9
100	77.8	4.4	1.5	4.4	17.5	77.8
125	103.8	4.2	1.4	4.6	24.5	103.8
150	123.1	5.4	1.7	4.8	22.8	123.1

A.4.1: Isotherm study raw experimental data: Lead_REV1

C_0 (mg/L)	C_e (mg/L)	q_e (mg/g)	Freundlich		Langmuir	
			$\ln(q_e)$	$\ln(C_e)$	C_e/q_e	C_e
25	0.6	4.9	1.6	-0.5	0.1	0.6
50	0.4	9.9	2.3	-1.0	0.0	0.4
75	0.6	14.9	2.7	-0.5	0.0	0.6
100	1.5	19.7	3.0	0.4	0.1	1.5
125	5.3	23.9	3.2	1.7	0.2	5.3
150	3.9	29.2	3.4	1.3	0.1	3.9

A.4.2: Isotherm study raw experimental data: Lead_REV2

C_0 (mg/L)	C_e (mg/L)	q_e (mg/g)	Freundlich		Langmuir	
			$\ln(q_e)$	$\ln(C_e)$	C_e/q_e	C_e
25	0.5	4.9	1.6	-0.7	0.1	0.5
50	0.7	9.9	2.3	-0.4	0.1	0.7
75	0.9	14.8	2.7	-0.2	0.1	0.9
100	1.4	19.7	3.0	0.3	0.1	1.4
125	4.6	24.1	3.2	1.5	0.2	4.6
150	4.3	29.1	3.4	1.5	0.1	4.3

A.4.3: Isotherm study raw experimental data: Lead_REV3

C_0 (mg/L)	C_e (mg/L)	q_e (mg/g)	Freundlich		Langmuir	
			$\ln(q_e)$	$\ln(C_e)$	C_e/q_e	C_e
25	0.7	4.9	1.6	-0.4	0.1	0.7
50	0.8	9.8	2.3	-0.2	0.1	0.8
75	1.0	14.8	2.7	0.0	0.1	1.0
100	2.5	19.5	3.0	0.9	0.1	2.5
125	4.6	24.1	3.2	1.5	0.2	4.6
150	4.9	29.0	3.4	1.6	0.2	4.9

Appendix B

B.1.1: Kinetic study raw experimental data: Zinc_REV1

Time (min)	C_0 (mg/L)	C_t (mg/L)	$C_0 - C_t$ (mg/L)	q_e (mg/g)	q_t (mg/g)	t/q_t (g.min/mg)	Pseudo-first order		Pseudo-second order	
							Time (min)	$\ln(q_e - q_t)$	Time (min)	t/q_t
20	100	68.8	31.2	20	6.2	3.2	20	2.6	20	3.2
40	100	75.5	24.5	20	4.9	8.2	40	2.7	40	8.2
60	100	64.4	35.6	20	7.1	8.4	60	2.6	60	8.4
80	100	68.2	31.8	20	6.4	12.6	80	2.6	80	12.6
100	100	59.5	40.5	20	8.1	12.4	100	2.5	100	12.4
120	100	59.5	40.5	20	8.1	14.8	120	2.5	120	14.8

B.1.2: Kinetic study raw experimental data: Zinc_REV2

Time (min)	C_0 (mg/L)	C_t (mg/L)	$C_0 - C_t$ (mg/L)	q_e (mg/g)	q_t (mg/g)	t/q_t (g.min/mg)	Pseudo-first order		Pseudo-second order	
							Time (min)	$\ln(q_e - q_t)$	Time (min)	t/q_t
20	100	79.5	20.5	20	4.1	4.9	20	2.8	20	4.9
40	100	73.2	26.8	20	5.4	7.5	40	2.7	40	7.5

60	100	67.4	32.6	20	6.5	9.2	60	2.6	60	9.2
80	100	63.0	37.0	20	7.4	10.8	80	2.5	80	10.8
100	100	54.6	45.5	20	9.1	11.0	100	2.4	100	11.0
120	100	55.9	44.1	20	8.8	13.6	120	2.4	120	13.6

B.1.3: Kinetic study raw experimental data: Zinc_REV3

Time (min)	C_0 (mg/L)	C_t (mg/L)	$C_0 - C_t$ (mg/L)	q_e (mg/g)	q_t (mg/g)	t/q_t (g.min/mg)	Pseudo-first order		Pseudo-second order	
							Time (min)	$\ln(q_e - q_t)$	Time (min)	t/q_t
20	100	72.4	27.6	20	5.5	3.6	20	2.7	20	3.6
40	100	66.7	33.3	20	6.7	6.0	40	2.6	40	6.0
60	100	65.2	34.8	20	7.0	8.6	60	2.6	60	8.6
80	100	64.3	35.7	20	7.1	11.2	80	2.6	80	11.2
100	100	61.2	38.8	20	7.8	12.9	100	2.5	100	12.9
120	100	59.0	41.0	20	8.2	14.6	120	2.5	120	14.6

B.2.1: Kinetic study raw experimental data: Cadmium_REV1

Time							Pseudo-first order	Pseudo-second order

(min)	C_0 (mg/L)	C_t (mg/L)	$C_0 - C_t$ (mg/L)	q_e (mg/g)	q_t (mg/g)	t/q_t (g.min/mg)	Time (min)	$\ln(q_e - q_t)$	Time (min)	t/q_t
20	100	78.9	21.1	20	4.2	4.7	20	2.8	20	4.7
40	100	78.4	21.6	20	4.3	9.3	40	2.8	40	9.3
60	100	74.6	25.4	20	5.1	11.8	60	2.7	60	11.8
80	100	66.5	33.5	20	6.7	11.9	80	2.6	80	11.9
100	100	62.9	37.1	20	7.4	13.5	100	2.5	100	13.5
120	100	51.1	48.9	20	9.8	12.3	120	2.3	120	12.3

B.2.2: Kinetic study raw experimental data: Cadmium_REV2

Time (min)	C_0 (mg/L)	C_t (mg/L)	$C_0 - C_t$ (mg/L)	q_e (mg/g)	q_t (mg/g)	t/q_t (g.min/mg)	Pseudo-first order		Pseudo-second order	
							Time (min)	$\ln(q_e - q_t)$	Time (min)	t/q_t
20	100	82.2	17.8	20	3.6	5.6	20	2.8	20	5.6
40	100	75.9	24.1	20	4.8	8.3	40	2.7	40	8.3
60	100	73.5	26.5	20	5.3	11.3	60	2.7	60	11.3
80	100	63.5	36.5	20	7.3	11.0	80	2.5	80	11.0
100	100	63.8	36.2	20	7.2	13.8	100	2.5	100	13.8

120	100	56.3	43.7	20	8.7	13.7	120	2.4	120	13.7

B.2.3: Kinetic study raw experimental data: Cadmium_REV3

Time (min)	C_0 (mg/L)	C_t (mg/L)	$C_0 - C_t$ (mg/L)	q_e (mg/g)	q_t (mg/g)	t/q_t (g.min/mg)	Pseudo-first order		Pseudo-second order	
							Time (min)	$\ln(q_e - q_t)$	Time (min)	t/q_t
20	100	89.4	10.6	20	2.1	9.5	20	2.9	20	9.5
40	100	75.9	24.1	20	4.8	8.3	40	2.7	40	8.3
60	100	65.2	34.8	20	7.0	8.6	60	2.6	60	8.6
80	100	64.8	35.2	20	7.0	11.4	80	2.6	80	11.4
100	100	63.6	36.4	20	7.3	13.7	100	2.5	100	13.7
120	100	54.2	45.8	20	9.2	13.1	120	2.4	120	13.1

B.3.1: Kinetic study raw experimental data: Manganese_REV1

Time (min)	C_0 (mg/L)	C_t (mg/L)	$C_0 - C_t$ (mg/L)	q_e (mg/g)	q_t (mg/g)	t/q_t (g.min/mg)	Pseudo-first order		Pseudo-second order	
							Time (min)	$\ln(q_e - q_t)$	Time (min)	t/q_t
20	100	92.5	7.5	20	1.5	13.3	20	2.9	20	13.3
40	100	86.5	13.5	20	2.7	14.9	40	2.9	40	14.9

60	100	84.3	15.7	20	3.1	19.1	60	2.8	60	19.1
80	100	82.8	17.2	20	3.4	23.2	80	2.8	80	23.2
100	100	81.4	18.6	20	3.7	26.9	100	2.8	100	26.9
120	100	80.1	19.9	20	4.0	30.1	120	2.8	120	30.1

B.3.2: Kinetic study raw experimental data: Manganese_REV2

Time (min)	C_0 (mg/L)	C_t (mg/L)	$C_0 - C_t$ (mg/L)	q_e (mg/g)	q_t (mg/g)	t/q_t (g.min/mg)	Pseudo-first order		Pseudo-second order	
							Time (min)	$\ln(q_e - q_t)$	Time (min)	t/q_t
20	100	88.8	11.2	20	2.2	8.9	20	2.9	20	8.9
40	100	83.1	16.9	20	3.4	11.8	40	2.8	40	11.8
60	100	80.9	19.1	20	3.8	15.7	60	2.8	60	15.7
80	100	79.5	20.5	20	4.1	19.5	80	2.8	80	19.5
100	100	78.2	21.8	20	4.4	22.9	100	2.7	100	22.9
120	100	76.9	23.1	20	4.6	25.9	120	2.7	120	25.9

B.3.3: Kinetic study raw experimental data: Manganese_REV3

Time							Pseudo-first order	Pseudo-second order

(min)	C_0 (mg/L)	C_t (mg/L)	$C_0 - C_t$ (mg/L)	q_e (mg/g)	q_t (mg/g)	t/q_t (g.min/mg)	Time (min)	$\ln(q_e - q_t)$	Time (min)	t/q_t
20	100	84.2	15.8	20	3.2	6.3	20	2.8	20	6.3
40	100	78.8	21.2	20	4.2	9.4	40	2.8	40	9.4
60	100	76.7	23.3	20	4.7	12.9	60	2.7	60	12.9
80	100	75.3	24.7	20	4.9	16.2	80	2.7	80	16.2
100	100	74.1	25.9	20	5.2	19.3	100	2.7	100	19.3
120	100	72.9	27.1	20	5.4	22.1	120	2.7	120	22.1

B.4.1: Kinetic study raw experimental data: Lead_REV1

Time (min)	C_0 (mg/L)	C_t (mg/L)	$C_0 - C_t$ (mg/L)	q_e (mg/g)	q_t (mg/g)	t/q_t (g.min/mg)	Pseudo-first order		Pseudo-second order	
							Time (min)	$\ln(q_e - q_t)$	Time (min)	t/q_t
20	100	30.2	69.8	20	14.0	1.4	20	1.8	20	1.4
40	100	9.4	90.6	20	18.1	2.2	40	0.6	40	2.2
60	100	2.4	97.6	20	19.5	3.1	60	-0.8	60	3.1
80	100	1.1	98.9	20	19.8	4.0	80	-1.5	80	4.0
100	100	1.0	99.0	20	19.8	5.0	100	-1.7	100	5.0
120	100	0.8	99.2	20	19.8	6.0	120	-1.8	120	6.0

B.4.2: Kinetic study raw experimental data: Lead_REV2

Time (min)	C_0 (mg/L)	C_t (mg/L)	$C_0 - C_t$ (mg/L)	q_e (mg/g)	q_t (mg/g)	t/q_t (g.min/mg)	Pseudo-first order		Pseudo-second order	
							Time (min)	$\ln(q_e - q_t)$	Time (min)	t/q_t
20	100	34.7	65.3	20	13.1	1.5	20	1.9	20	1.5
40	100	10.7	89.3	20	17.9	2.2	40	0.8	40	2.2
60	100	2.7	97.3	20	19.5	3.1	60	-0.6	60	3.1
80	100	1.3	98.7	20	19.7	4.1	80	-1.3	80	4.1
100	100	1.1	98.9	20	19.8	5.1	100	-1.5	100	5.1
120	100	0.9	99.1	20	19.8	6.1	120	-1.7	120	6.1

B.4.3: Kinetic study raw experimental data: Lead_REV3

Time (min)	C_0 (mg/L)	C_t (mg/L)	$C_0 - C_t$ (mg/L)	q_e (mg/g)	q_t (mg/g)	t/q_t (g.min/mg)	Pseudo-first order		Pseudo-second order	
							Time (min)	$\ln(q_e - q_t)$	Time (min)	t/q_t
20	100	31.5	68.5	20	13.7	1.5	20	1.8	20	1.5
40	100	9.8	90.2	20	18.0	2.2	40	0.7	40	2.2
60	100	2.4	97.6	20	19.5	3.1	60	-0.7	60	3.1

80	100	1.2	98.8	20	19.8	4.0	80	-1.4	80	4.0
100	100	1.0	99.0	20	19.8	5.1	100	-1.6	100	5.1
120	100	0.8	99.2	20	19.8	6.0	120	-1.8	120	6.0

Appendix C

C.1.1: Particle size distribution table

Sieve aperture size (µm)	Mass of clinoptilolite retained on each sieve (g)	Percent of mass retained above each sieve (%)	Cumulative percent retained (%)	Percent finer (%)
3350	0.9	0.1	0.1	99.8
2000	3.6	0.7	0.9	99.0
1180	36.2	7.2	8.2	91.7
500	424.4	85.1	93.3	6.6
300	21.9	4.4	97.7	2.2
212	1.7	0.3	98.1	1.8
150	1.3	0.2	98.3	1.6
106	2.6	0.5	98.9	1.0

Pan	5.3	1.0	100	0.0
Total	498.4	100		
Mass Loss	1.5			

C.1.2: Rosslin-Rammler raw data

Pass size (µm)	Cumulative percentage pass (%)	ln(d)	ln(-ln(1-Y^-))	-Y^- (%)	Parameters	
Top	100				n	2.1
3350	99.8	8.1	1.8	99.9	d^*	1191.4
2000	99.0	7.6	1.5	95.1		
1180	97.7	7.0	0.9	62.4		
500	6.6	6.2	-2.6	14.4		
300	2.2	5.7	-3.7	5.1		
212	1.8	5.3	-3.9	2.4		
150	1.6	5.0	-4.1	1.1		
106	1.0	4.6	-4.5	0.5		

C.1.3: Gaudin-Schumann raw data

Pass size (µm)	Cumulative percentage pass (%)	ln(d)	ln(-ln(1-Y^-))	-Y^- (%)	Parameters	
Top	100				n	-1.8
3350	99.8	8.1	-6.2	99.4	d^*	198.9
2000	99.0	7.6	-4.6	98.5		
1180	97.7	7.0	-2.5	96.1		
500	6.6	6.2	-0.1	81.9		
300	2.2	5.7	-0.02	52.9		
212	1.8	5.3	-0.02	10.9		
150	1.6	5.0	-0.02	-67.9		
106	1.0	4.6	-0.01	-217.6		

C.2.1: Effect of particle size: Alkaline mine drainage (Calcium)

	REV1			REV2			REV3		
Feed Volume interval	PSD 1	PSD 2	PSD 3	PSD 1	PSD 2	PSD 3	PSD 1	PSD 2	PSD 3
1	1924,8	108,9	165,1	1867,1	105,7	160,2	1982,6	111,1	168,4
2	338,8	52,7	37,9	328,7	51,1	36,7	349,0	53,8	38,6
3	181,1	58,5	36,0	175,7	56,7	35,0	186,6	59,7	36,8
4	152,5	63,7	42,4	147,9	61,8	41,1	157,0	65,0	43,3
5	141,0	68,9	49,4	136,7	66,8	48,0	145,2	70,2	50,4
6	137,1	70,7	50,6	133,0	68,6	49,1	141,2	72,1	51,6
7	137,8	76,7	54,0	133,6	74,4	52,4	141,9	78,2	55,1
8	135,9	78,8	56,3	131,9	76,4	54,7	140,0	80,4	57,5
9	135,2	80,1	56,7	131,2	77,7	55,0	139,3	81,7	57,8
10	134,6	82,2	59,0	130,6	79,8	57,2	138,7	83,9	60,1

C.2.2: Effect of particle size: Alkaline mine drainage (Magnesium)

	REV1			REV2			REV3		
Feed Volume interval	PSD 1	PSD 2	PSD 3	PSD 1	PSD 2	PSD 3	PSD 1	PSD 2	PSD 3
1	840.8	84.1	76.1	790.4	79.1	71.5	849.2	85.0	76.8
2	185.7	44.2	19.5	174.6	41.5	18.4	187.6	44.6	19.7
3	114.2	52.6	21.9	107.4	49.4	20.6	115.4	53.1	22.2
4	112.5	58.5	29.6	105.8	55.0	27.9	113.7	59.1	29.9
5	107.7	63.8	38.2	101.2	60.0	35.9	108.7	64.5	38.5
6	107.0	66.5	42.5	100.6	62.5	39.9	108.1	67.2	42.9
7	106.3	71.1	48.0	100.0	66.8	45.1	107.4	71.8	48.5
8	105.1	73.2	51.9	98.8	68.8	48.8	106.2	73.9	52.4
9	105.6	74.2	53.8	99.3	69.8	50.6	106.7	75.0	54.3
10	105.6	75.3	55.9	99.3	70.8	52.5	106.7	76.0	56.4

C.2.3: Effect of particle size: Alkaline mine drainage (Potassium)

	REV1			REV2			REV3		
Feed Volume interval	PSD 1	PSD 2	PSD 3	PSD 1	PSD 2	PSD 3	PSD 1	PSD 2	PSD 3
1	301.2	26.3	25.9	308.2	26.9	26.5	289.2	23.6	24.9
2	79.4	13.7	10.1	81.2	14.0	10.4	76.2	13.2	9.7
3	47.9	13.0	8.8	49.0	13.3	9.0	46.0	12.5	8.4
4	41.3	11.1	8.4	42.2	11.3	8.6	39.6	10.6	8.1
5	37.7	11.2	8.2	38.6	11.4	8.3	36.2	10.7	7.8
6	37.4	10.8	8.1	38.3	11.0	8.3	35.9	10.3	7.7
7	35.6	10.7	7.9	36.4	10.9	8.1	34.1	10.3	7.6
8	34.3	10.7	7.8	35.1	10.9	8.0	33.0	10.3	7.5
9	32.7	10.6	7.7	33.5	10.8	7.9	31.4	10.2	7.4
10	31.8	10.3	7.8	32.5	10.6	8.0	30.5	9.9	7.5

C.3.1: Effect of particle size: Acid mine drainage (Calcium)

	REV1			REV2			REV3		
Feed Volume interval	PSD 1	PSD 2	PSD 3	PSD 1	PSD 2	PSD 3	PSD 1	PSD 2	PSD 3
1	700.9	492.1	50.9	651.8	457.7	47.3	679.9	477.4	49.4
2	207.0	2727	8.2	192.5	25.7	7.6	200.8	26.9	8.0
3	158.3	23.8	9.0	147.2	22.1	8.4	153.5	23.0	8.8
4	137.0	39.5	16.4	127.4	36.7	15.3	132.9	38.3	15.9
5	129.3	44.6	29.3	120.2	41.5	27.3	125.4	43.3	28.5
6	121.9	50.4	36.4	113.4	46.8	33.8	118.2	48.8	35.3
7	113.0	53.5	41.4	105.1	49.8	38.5	109.6	51.9	40.2
8	121.1	56.3	47.9	112.7	52.4	44.6	117.5	54.6	46.5
9	106.2	59.4	53.0	98.8	55.3	49.2	103.0	57.7	51.4
10	109.8	60.1	52.4	102.1	55.9	48.7	106.5	58.3	50.8

C.3.2: Effect of particle size: Acid mine drainage (Magnesium)

	REV1			REV2			REV3		
Feed Volume interval	PSD 1	PSD 2	PSD 3	PSD 1	PSD 2	PSD 3	PSD 1	PSD 2	PSD 3
1	362,5	244,1	32,0	391,5	263,7	34,6	355,3	241,7	30,1
2	107,9	19,4	5,2	116,6	21,0	5,6	105,8	19,3	4,9
3	82,5	20,5	6,9	89,1	22,1	7,5	80,8	20,3	6,5
4	71,7	30,6	15,1	77,4	33,0	16,3	70,3	30,3	14,2
5	66,9	37,0	28,6	72,2	40,0	30,9	65,5	36,7	26,9
6	63,0	40,5	34,1	68,0	43,7	36,8	61,7	40,1	32,0
7	61,5	43,2	39,0	66,4	46,6	42,2	60,3	42,8	36,7
8	61,5	37,9	41,4	66,4	40,9	44,7	60,3	37,5	38,9
9	57,7	39,3	42,2	62,3	42,4	45,6	56,5	38,9	39,7
10	57,8	39,4	41,8	62,4	42,6	45,2	56,6	39,0	39,3

C.3.3: Effect of particle size: Alkaline mine drainage (Potassium)

	REV1			REV2			REV3		
Feed Volume interval	PSD 1	PSD 2	PSD 3	PSD 1	PSD 2	PSD 3	PSD 1	PSD 2	PSD 3
1	120,3	63,5	17,6	110,6	58,4	16,2	122,7	64,7	17,9
2	40,5	10,7	5,7	37,3	9,8	5,2	41,3	10,9	5,8
3	27,1	6,6	4,8	24,9	6,1	4,4	27,6	6,7	4,9
4	21,7	5,6	4,4	20,0	5,1	4,1	22,1	5,7	4,5
5	19,2	5,0	3,9	17,6	4,6	3,6	19,6	5,1	4,0
6	17,8	4,6	3,5	16,4	4,2	3,2	18,2	4,7	3,5
7	17,3	4,2	3,2	15,9	3,9	2,9	17,7	4,3	3,2
8	16,7	4,0	2,9	15,4	3,7	2,7	17,0	4,1	3,0
9	16,0	3,8	2,8	14,7	3,5	2,5	16,3	3,9	2,8
10	15,6	3,7	2,8	14,3	3,4	2,6	15,9	3,8	2,8

C.3.4: Effect of particle size: Acid mine drainage (Aluminium)

	REV1			REV2			REV3		
Feed Volume interval	PSD 1	PSD 2	PSD 3	PSD 1	PSD 2	PSD 3	PSD 1	PSD 2	PSD 3
1	0,1	0,1	0,1	0,1	0,1	0,1	0,2	0,1	0,1
2	0,3	0,1	0,1	0,3	0,1	0,1	0,4	0,1	0,1
3	0,9	0,1	0,1	0,9	0,1	0,1	1,0	0,1	0,1
4	1,8	0,2	0,0	1,7	0,2	0,0	2,0	0,2	0,0
5	2,1	0,3	0,0	2,1	0,3	0,0	2,4	0,3	0,1
6	3,0	0,4	0,1	2,9	0,4	0,1	3,3	0,5	0,1
7	2,7	0,7	0,1	2,6	0,7	0,1	2,9	0,8	0,1
8	4,2	1,0	0,2	4,1	1,0	0,2	4,6	1,1	0,2
9	6,9	1,4	0,2	6,8	1,4	0,2	7,6	1,5	0,2
10	6,4	1,6	0,2	6,3	1,5	0,2	7,1	1,7	0,3

C.3.5: Effect of particle size: Acid mine drainage (Iron)

	REV1			REV2			REV3		
Feed Volume interval	PSD 1	PSD 2	PSD 3	PSD 1	PSD 2	PSD 3	PSD 1	PSD 2	PSD 3
1	0,2	0,1	0,1	0,1	0,1	0,1	0,1	0,1	0,1
2	0,4	0,1	0,1	0,3	0,1	0,1	0,4	0,1	0,1
3	1,0	0,1	0,1	0,9	0,1	0,1	0,9	0,1	0,1
4	2,0	0,2	0,0	1,7	0,2	0,0	1,8	0,2	0,0
5	2,4	0,3	0,1	2,0	0,3	0,0	2,2	0,3	0,0
6	3,3	0,5	0,1	2,9	0,4	0,1	3,1	0,4	0,1
7	2,9	0,8	0,1	2,5	0,7	0,1	2,8	0,7	0,1
8	4,6	1,1	0,2	4,0	1,0	0,1	4,3	1,0	0,2
9	7,6	1,5	0,2	6,5	1,3	0,2	7,1	1,4	0,2
10	7,1	1,7	0,3	6,1	1,5	0,2	6,6	1,6	0,2

C.3.7: Effect of particle size: Acid mine drainage (Manganese)

	REV1			REV2			REV3		
Feed Volume interval	PSD 1	PSD 2	PSD 3	PSD 1	PSD 2	PSD 3	PSD 1	PSD 2	PSD 3
1	3,6	2,6	0,3	3,7	2,7	0,3	3,7	2,6	0,3
2	5,7	0,7	0,1	5,9	0,8	0,1	5,8	0,8	0,1
3	6,6	1,6	0,1	6,8	1,7	0,2	6,7	1,6	0,2
4	7,2	3,0	0,5	7,5	3,1	0,5	7,4	3,0	0,6
5	7,6	4,0	1,3	7,9	4,1	1,3	7,8	4,1	1,5
6	7,7	4,5	2,2	8,0	4,7	2,3	7,8	4,6	2,6
7	7,9	5,0	3,0	8,2	5,3	3,1	8,0	5,1	3,6
8	8,0	5,4	3,7	8,4	5,6	3,9	8,2	5,5	4,4
9	8,2	5,7	4,2	8,5	5,9	4,4	8,4	5,8	5,1
10	8,3	5,9	4,5	8,6	6,1	4,7	8,5	6,0	5,5

C.4.1: Effect of particle size: Mixed metal solution (Cadmium)

	REV1			REV2			REV3		
Feed Volume interval	PSD 1	PSD 2	PSD 3	PSD 1	PSD 2	PSD 3	PSD 1	PSD 2	PSD 3
1	201,4	42,8	0,2	193,4	41,1	0,2	199,4	42,4	0,2
2	380,0	142,9	16,2	364,8	137,2	15,6	376,2	141,4	16,1
3	392,4	215,1	88,8	376,7	206,5	85,3	388,5	212,9	88,0
4	408,1	242,6	143,5	391,8	232,9	137,8	404,0	240,2	142,1
5	412,1	274,9	185,0	395,6	263,9	177,6	408,0	272,2	183,1
6	420,7	286,2	206,4	403,8	274,8	198,1	416,4	283,4	204,3
7	433,6	278,6	222,4	416,2	267,5	213,5	429,2	275,9	220,2
8	433,8	290,6	232,9	416,4	279,0	223,6	429,4	287,7	230,6
9	435,2	303,9	232,3	417,8	291,7	223,1	430,8	300,8	230,0
10	432,2	316,1	240,5	414,9	303,4	230,9	427,8	312,9	238,1

C.4.2: Effect of particle size: Mixed metal solution (Manganese)

	REV1			REV2			REV3		
Feed Volume interval	PSD 1	PSD 2	PSD 3	PSD 1	PSD 2	PSD 3	PSD 1	PSD 2	PSD 3
1	166,7	19,7	0,1	178,4	21,1	0,1	156,7	18,5	0,1
2	323,7	82,9	5,8	346,3	88,7	6,2	304,2	77,9	5,5
3	345,5	161,6	44,1	369,7	172,9	47,2	324,7	151,9	41,5
4	370,6	200,7	95,2	396,5	214,8	101,8	348,4	188,7	89,5
5	380,9	242,5	144,2	407,6	259,5	154,3	358,1	228,0	135,6
6	391,2	259,9	178,2	418,6	278,1	190,7	367,7	244,3	167,5
7	404,0	257,8	204,3	432,3	275,8	218,6	379,8	242,3	192,0
8	407,6	271,0	221,3	436,2	289,9	236,7	383,2	254,7	208,0
9	409,1	287,1	225,3	437,8	307,1	241,0	384,6	269,8	211,8
10	407,1	299,3	226,0	435,6	320,3	241,8	382,6	281,4	212,4

C.4.3: Effect of particle size: Mixed metal solution (Zinc)

	REV1			REV2			REV3		
Feed Volume interval	PSD 1	PSD 2	PSD 3	PSD 1	PSD 2	PSD 3	PSD 1	PSD 2	PSD 3
1	108,2	11,6	0,1	104,9	11,2	0,1	119,0	12,7	0,1
2	251,1	56,0	2,7	243,5	54,3	2,7	276,2	61,6	3,0
3	270,2	108,9	24,5	262,1	105,7	23,8	297,2	119,8	27,0
4	290,4	140,5	55,3	281,7	136,3	53,6	319,5	154,6	60,8
5	302,0	174,0	85,8	293,0	168,8	83,2	332,2	191,4	94,4
6	311,4	192,6	113,1	302,1	186,9	109,7	342,6	211,9	124,4
7	318,7	189,7	137,9	309,2	184,0	133,8	350,6	208,6	151,7
8	319,7	197,7	150,0	310,1	191,8	145,5	351,7	217,5	165,0
9	323,5	212,5	156,9	313,8	206,1	152,2	355,9	233,7	172,6
10	318,8	225,9	170,1	309,3	219,2	165,0	350,7	248,5	187,2

Appendix D

D.1.1: Effect of water hardness (Magnesium): Cadmium_REV1

Feed Volume Interval	50 mg/L Mg	100 mg/L Mg	150 mg/L Mg	200 mg/L Mg
1	20.5	39.1	119.8	43.3
2	136.0	190.0	270.8	207.2
3	242.6	256.5	312.0	283.2
4	309.9	294.2	334.2	323.2
5	348.1	332.0	354.9	362.7
6	364.3	356.8	324.0	363.0
7	366.6	367.2	371.0	375.2
8	387.9	384.2	392.7	396.9
9	389.3	390.7	398.4	399.5
10	387.5	395.5	401.6	408.7

D.1.2: Effect of water hardness (Magnesium): Cadmium_REV2

Feed Volume Interval	50 mg/L Mg	100 mg/L Mg	150 mg/L Mg	200 mg/L Mg
1	19.1	37.1	113.8	42.0
2	126.5	180.5	257.2	201.0
3	225.6	243.7	296.4	274.7
4	288.2	279.5	317.5	313.5
5	323.7	35.4	337.1	351.8
6	338.8	339.0	307.8	352.2
7	340.9	348.8	352.4	364.0
8	360.7	364.9	373.1	385.0
9	362.0	371.2	378.5	387.5
10	360.4	375.7	381.6	396.4

D.1.3: Effect of water hardness (Magnesium): Cadmium_REV3

Feed Volume Interval	50 mg/L Mg	100 mg/L Mg	150 mg/L Mg	200 mg/L Mg
1	19.5	37.5	115.0	45.0
2	129.2	182.4	259.9	215.5
3	230.5	246.2	299.5	294.5
4	294.4	282.4	320.8	336.1
5	330.7	318.7	340.7	377.2
6	346.1	342.5	311.1	377.6
7	348.2	352.5	356.2	390.2
8	368.5	368.8	377.0	412.8
9	369.8	375.1	382.5	415.5
10	368.1	379.6	385.6	425.0

D.2.1: Effect of water hardness (Magnesium): Manganese_REV1

Feed Volume Interval	50 mg/L Mg	100 mg/L Mg	150 mg/L Mg	200 mg/L Mg
1	9.7	23.5	72.3	22.0
2	84.1	132.0	198.8	141.4
3	180.0	206.1	252.8	250.8
4	255.9	252.9	309.2	298.7
5	306.7	299.8	339.2	339.6
6	333.6	332.6	317.8	356.9
7	344.4	350.6	368.1	369.9
8	370.5	374.0	392.5	383.7
9	376.8	398.2	401.0	390.2
10	379.9	399.8	401.3	411.1

D.2.2: Effect of water hardness (Magnesium): Manganese_REV2

Feed Volume Interval	50 mg/L Mg	100 mg/L Mg	150 mg/L Mg	200 mg/L Mg
1	9.0	21.8	68.7	20.9
2	78.2	122.8	188.8	134.4
3	167.4	191.7	240.2	238.2
4	238.0	235.2	293.7	283.8
5	285.3	278.8	322.2	322.6
6	310.3	309.3	301.9	339.1
7	320.3	326.0	349.7	351.4
8	344.5	347.8	372.9	364.5
9	350.4	370.4	380.9	370.7
10	353.3	371.8	381.2	390.5

D.2.3: Effect of water hardness (Magnesium): Manganese_REV3

Feed Volume Interval	50 mg/L Mg	100 mg/L Mg	150 mg/L Mg	200 mg/L Mg
1	9.2	22.3	74.5	22.7
2	79.9	125.4	204.7	145.7
3	171.0	195.8	260.4	258.3
4	243.1	240.3	318.4	307.7
5	291.4	284.8	349.3	349.8
6	316.9	316.0	327.3	367.6
7	327.2	333.0	379.2	381.0
8	351.9	355.3	404.3	395.2
9	357.9	378.3	413.0	401.9
10	360.9	379.8	413.3	423.4

D.3.1: Effect of water hardness (Magnesium): Zinc_REV1

Feed Volume Interval	50 mg/L Mg	100 mg/L Mg	150 mg/L Mg	200 mg/L Mg
1	6.0	15.2	49.1	22.0
2	62.6	96.0	167.3	141.4
3	139.9	157.4	223.1	240.8
4	205.4	195.7	254.2	298.7
5	251.0	236.8	281.3	339.6
6	276.4	265.7	255.7	356.9
7	287.2	281.7	304.1	361.9
8	312.1	303.4	328.7	379.7
9	319.3	329.3	339.2	380.2
10	321.9	343.9	350.7	398.1

D.3.2: Effect of water hardness (Magnesium): Zinc_REV2

Feed Volume Interval	50 mg/L Mg	100 mg/L Mg	150 mg/L Mg	200 mg/L Mg
1	5.6	14.1	46.6	20.9
2	58.2	89.3	158.9	134.4
3	130.1	146.4	211.9	228.7
4	191.0	182.0	241.5	283.8
5	233.4	220.2	267.2	322.6
6	257.0	247.1	281.2	339.1
7	267.1	262.0	288.9	343.8
8	290.2	282.1	312.2	360.7
9	296.9	306.2	322.2	361.2
10	299.4	319.8	333.2	378.2

D.3.3: Effect of water hardness (Magnesium): Zinc_REV3

Feed Volume Interval	50 mg/L Mg	100 mg/L Mg	150 mg/L Mg	200 mg/L Mg
1	6,1	15,5	47,5	22,5
2	63,8	97,9	162,1	144,3
3	142,7	160,5	216,2	245,6
4	209,5	199,6	246,3	304,7
5	256,0	241,5	272,6	346,4
6	281,9	271,0	286,9	364,1
7	293,0	287,4	294,6	369,1
8	318,3	309,4	318,5	387,3
9	325,7	335,8	328,7	387,8
10	328,3	350,8	339,8	406,1

D.4.1: Effect of water hardness (Calcium): Cadmium_REV1

Feed Volume Interval	50 mg/L Mg	100 mg/L Mg	150 mg/L Mg	200 mg/L Mg
1	4.8	84.2	31.5	71.6
2	146.6	231.8	179.2	269.7
3	269.0	296.8	285.3	359.7
4	300.7	334.8	333.2	428.3
5	330.0	361.2	354.9	467.7
6	344.4	365.2	376.7	488.1
7	363.1	388.6	377.4	506.1
8	355.0	397.4	390.6	507.1
9	370.5	402.8	398.4	525.9
10	379.6	402.5	395.7	526.7

D.4.2: Effect of water hardness (Calcium): Cadmium_REV2

Feed Volume Interval	50 mg/L Mg	100 mg/L Mg	150 mg/L Mg	200 mg/L Mg
1	14.3	80.8	30.3	68.7
2	140.7	222.5	172.0	258.9
3	258.3	285.0	273.9	345.3
4	288.7	321.4	319.9	411.1
5	316.8	346.8	340.7	448.9
6	330.6	350.6	361.6	468.6
7	348.5	373.1	362.3	485.8
8	340.8	381.5	374.9	486.8
9	355.7	386.7	382.5	504.9
10	364.5	386.4	379.9	505.6

D.4.3: Effect of water hardness (Calcium): Cadmium_REV3

Feed Volume Interval	50 mg/L Mg	100 mg/L Mg	150 mg/L Mg	200 mg/L Mg
1	15.9	90.1	34.3	76.6
2	156.8	248.0	195.3	288.6
3	287.8	317.6	311.0	384.9
4	321.8	358.2	363.2	458.3
5	353.1	386.5	386.9	500.4
6	368.5	390.7	410.6	522.3
7	388.5	415.8	411.3	541.5
8	379.9	425.3	425.7	542.6
9	396.5	431.0	434.3	562.7
10	406.2	430.7	431.4	563.5

D.5.1: Effect of water hardness (Calcium): Manganese_REV1

Feed Volume Interval	50 mg/L Mg	100 mg/L Mg	150 mg/L Mg	200 mg/L Mg
1	8.0	40.4	15.5	24.2
2	99.1	170.5	124.8	158.1
3	221.7	254.6	235.6	238.6
4	267.5	309.7	300.2	303.8
5	309.3	344.2	329.1	342.3
6	332.2	353.7	359.7	365.2
7	358.2	381.8	362.7	.82.2
8	355.6	394.4	380.8	386.0
9	373.7	400.0	392.3	402.7
10	385.4	402.1	391.1	405.2

D.5.2: Effect of water hardness (Calcium): Manganese_REV2

Feed Volume Interval	50 mg/L Mg	100 mg/L Mg	150 mg/L Mg	200 mg/L Mg
1	7.4	37.6	14.4	22.5
2	92.2	158.6	116.0	147.0
3	206.2	236.8	219.1	221.9
4	248.8	288.0	279.2	282.5
5	287.6	320.1	306.1	318.3
6	308.9	329.0	334.5	339.7
7	333.1	355.1	337.3	355.4
8	330.7	366.8	354.1	358.9
9	347.5	372.0	364.8	347.5
10	358.4	373.9	363.7	376.8

D.5.3: Effect of water hardness (Calcium): Manganese_REV3

Feed Volume Interval	50 mg/L Mg	100 mg/L Mg	150 mg/L Mg	200 mg/L Mg
1	81	41.2	15.8	24.7
2	101.	173.9	127.3	161.3
3	226.2	259.7	240.3	243.4
4	272.8	315.9	306.2	309.9
5	315.5	351.1	335.7	349.1
6	338.8	360.8	366.9	372.5
7	365.4	389.5	370.0	389.8
8	362.7	402.3	388.4	393.7
9	381.1	408.0	400.1	410.7
10	393.1	410.1	398.9	413.3

D.6.1: Effect of water hardness (Calcium): Zinc_REV1

Feed Volume Interval	50 mg/L Mg	100 mg/L Mg	150 mg/L Mg	200 mg/L Mg
1	5.2	26.8	9.7	15.8
2	69.4	124.3	88.2	116.9
3	163.1	192.2	176.9	180.6
4	199.6	238.9	231.6	236.7
5	233.1	269.5	256.5	270.9
6	255.4	277.6	283.6	293.7
7	279.1	304.3	288.5	308.8
8	275.4	316.4	304.3	313.8
9	291.7	322.1	315.3	327.2
10	303.6	324.1	314.7	331.9

D.6.2: Effect of water hardness (Calcium): Zinc_REV2

Feed Volume Interval	50 mg/L Mg	100 mg/L Mg	150 mg/L Mg	200 mg/L Mg
1	5.0	25.4	9.5	16.6
2	66.0	118.0	86.4	122.7
3	155.0	182.6	173.4	189.7
4	189.6	226.9	227.0	248.5
5	221.4	256.0	251.4	284.5
6	242.6	263.7	277.9	308.4
7	265.2	289.0	282.7	324.2
8	261.6	300.6	298.2	329.5
9	277.1	306.0	309.0	343.6
10	288.4	307.9	308.4	348.5

D.6.3: Effect of water hardness (Calcium): Zinc_REV3

Feed Volume Interval	50 mg/L Mg	100 mg/L Mg	150 mg/L Mg	200 mg/L Mg
1	5.4	27.8	10.2	16.7
2	72.2	129.2	93.5	123.9
3	169.7	199.9	187.5	191.5
4	207.6	248.4	245.5	250.9
5	242.4	280.3	271.9	287.2
6	265.6	288.7	300.6	311.3
7	290.3	316.4	305.8	327.3
8	286.4	329.1	322.6	332.6
9	303.4	335.0	334.2	346.9
10	315.7	337.1	333.6	351.8

Appendix E

E.1.1: Effect of water pH: Alkaline mine drainage_REV1

Feed Volume Interval	Ca mg/L	Mg mg/L	K mg/L	Na mg/L
1	317.6	154.9	80.7	3589.4
2	60.8	38.4	24.4	1036.0
3	56.3	45.8	19.0	794.7
4	72.2	59.9	17.5	722.4
5	82.4	70.5	16.8	682.4
6	82.5	72.5	16.7	668.3
7	93.0	82.6	16.0	635.6
8	98.3	87.1	15.7	622.8
9	103.3	90.7	15.7	607.3
10	103.6	91.2	15.5	600.7

E.1.2: Effect of water pH: Alkaline mine drainage_REV2

Feed Volume Interval	Ca mg/L	Mg mg/L	K mg/L	Na mg/L
1	301.7	147.1	76.6	3409.9
2	57.8	36.5	23.2	984.2
3	56.3	43.5	18.0	754.9
4	68.6	56.9	16.7	686.2
5	78.3	67.0	16.0	648.2
6	78.3	68.9	15.9	634.8
7	88.4	78.4	15.2	603.8
8	93.3	82.7	14.9	591.6
9	98.1	86.1	14.9	577.0
10	98.4	86.7	14.8	570.6

E.1.3: Effect of water pH: Alkaline mine drainage_REV3

Feed Volume Interval	Ca mg/L	Mg mg/L	K mg/L	Na mg/L
1	349.3	170.4	88.7	3948.3
2	66.9	42.2	26.8	1139.6
3	65.2	50.3	20.9	874.1
4	79.5	65.9	19.3	794.6
5	90.7	77.6	18.5	750.6
6	90.7	79.8	18.4	735.1
7	102.3	90.8	17.7	699.1
8	108.1	95.8	17.2	685.0
9	113.6	99.7	17.3	668.1
10	114.0	100.3	17.1	660.7

E.2.1: Effect of water pH: Acid mine drainage_REV1

Feed Volume Interval	Ca mg/L	Mg mg/L	K mg/L	Al mg/L	Fe mg/L	Mn mg/L
1	583.4	288.1	50.1	1.2	0.3	1.0
2	66.5	40.8	12.1	0.6	0.1	1.3
3	52.6	36.8	8.3	1.1	0.1	2.1
4	56.0	42.2	7.3	3.0	0.2	3.2
5	61.8	47.9	6.6	6.1	0.2	4.2
6	64.7	50.4	6.5	8.7	0.4	4.8
7	69.3	53.8	5.8	14.8	0.7	6.0
8	70.7	55.2	5.6	19.3	1.0	6.6
9	69.6	54.8	5.5	20.1	1.2	6.5
10	71.7	55.7	5.2	24.6	1.8	6.9

E.2.2: Effect of water pH: Acid mine drainage_REV2

Feed Volume Interval	Ca mg/L	Mg mg/L	K mg/L	Al mg/L	Fe mg/L	Mn mg/L
1	542.6	267.9	46.6	1.2	0.3	0.9
2	61.9	37.9	11.2	0.6	0.1	1.2
3	48.9	34.2	7.7	1.0	0.1	2.0
4	52.0	39.3	6.8	2.8	0.1	2.9
5	57.5	44.6	6.2	5.7	0.2	3.9
6	60.1	46.9	6.1	8.1	0.3	4.5
7	64.5	50.0	5.4	13.8	0.7	5.6
8	65.8	51.3	5.2	18.0	1.0	6.1
9	64.7	51.0	5.1	18.7	1.1	6.0
10	66.7	51.8	4.9	22.9	1.6	6.5

E.2.3: Effect of water pH: Acid mine drainage_REV3

Feed Volume Interval	Ca mg/L	Mg mg/L	K mg/L	Al mg/L	Fe mg/L	Mn mg/L
1	612.6	302.5	52.6	1.3	0.3	1.0
2	69.9	42.8	12.7	0.7	0.1	1.4
3	55.3	38.6	8.7	1.1	0.1	2.2
4	58.8	44.4	7.6	3.1	0.2	3.3
5	64.9	50.3	7.0	6.4	0.3	4.4
6	67.9	53.0	6.9	9.1	0.4	5.1
7	72.8	56.5	6.1	15.6	0.7	6.3
8	74.2	57.9	5.9	20.3	1.1	6.9
9	73.1	57.6	5.8	21.1	1.3	6.8
10	75.3	58.5	5.5	25.9	1.9	7.3

E.3.1: Effect of water pH: Mixed metal solution (pH3)_REV1

Feed Volume Interval	Cd mg/L	Mn mg/L	Zn mg/L	Na mg/L
1	77.6	39.8	48.2	2604.7
2	243.2	173.2	154.3	716.5
3	307.2	247.2	216.6	506.3
4	360.6	313.6	274.7	356.7
5	384.4	349.3	310.5	300.0
6	394.6	366.8	327.7	269.6
7	387.5	368.2	331.3	377.6
8	406.6	386.5	349.1	235.3
9	398.4	386.1	351.6	254.6
10	405.5	396.3	262.2	251.2

E.3.2: Effect of water pH: Mixed metal solution (pH3)_REV2

Feed Volume Interval	Cd mg/L	Mn mg/L	Zn mg/L	Na mg/L
1	75.3	38.6	46.7	2474.5
2	235.9	168.0	149.6	680.7
3	298.0	239.7	210.1	481.0
4	349.7	304.2	266.5	347.4
5	372.9	338.8	301.2	285.0
6	382.8	355.8	317.8	256.1
7	375.9	357.2	321.4	263.7
8	394.4	374.9	338.6	223.6
9	386.5	374.5	341.1	241.9
10	393.3	384.5	351.3	238.6

E.3.3: Effect of water pH: Mixed metal solution (pH3)_REV3

Feed Volume Interval	Cd mg/L	Mn mg/L	Zn mg/L	Na mg/L
1	69.8	35.9	43.4	2787.1
2	218.9	155.9	138.8	766.7
3	276.5	222.4	194.9	541.7
4	324.5	282.2	247.2	391.3
5	346.0	314.3	279.5	321.0
6	355.2	330.1	294.9	288.5
7	348.7	331.4	298.2	297.1
8	366.0	347.8	314.2	251.8
9	358.6	347.5	316.5	272.4
10	365.0	356.7	326.0	268.8

E.4.1: Effect of water pH: Mixed metal solution (pH5)_REV1

Feed Volume Interval	Cd mg/L	Mn mg/L	Zn mg/L	Na mg/L
1	111.5	66.5	28.1	3879.2
2	242.6	181.5	143.1	905.8
3	291.4	247.9	210.2	535.6
4	332.0	285.5	241.6	461.2
5	352.5	316.4	284.4	339.6
6	366.9	352.1	320.8	274.0
7	364.0	351.2	317.3	278.2
8	383.3	377.1	345.7	231.1
9	385.7	379.6	339.2	223.0
10	395.3	382.3	344.4	206.3

E.4.2: Effect of water pH: Mixed metal solution (pH5)_REV2

Feed Volume Interval	Cd mg/L	Mn mg/L	Zn mg/L	Na mg/L
1	103.8	61.8	26.1	3685.2
2	225.7	168.8	133.1	860.5
3	271.0	230.6	195.5	508.8
4	308.7	265.5	224.7	438.1
5	327.8	294.2	264.5	322.6
6	341.3	327.5	298.4	260.3
7	338.6	326.6	295.1	264.3
8	356.5	350.7	321.5	219.5
9	358.7	353.0	315.5	211.9
10	367.6	355.5	320.3	196.0

E.4.3: Effect of water pH: Mixed metal solution (pH5)_REV3

Feed Volume Interval	Cd mg/L	Mn mg/L	Zn mg/L	Na mg/L
1	113.7	67.8	28.7	4073.1
2	247.5	185.1	146.0	951.1
3	297.2	252.9	214.4	562.4
4	338.6	291.2	246.4	484.2
5	359.5	322.7	290.1	356.6
6	374.3	359.2	327.2	287.7
7	371.3	358.2	323.7	292.1
8	391.0	384.7	352.6	242.6
9	393.5	387.2	346.0	234.2
10	403.2	389.9	351.3	216.6

E.5.1: Effect of water pH: Mixed metal solution (pH7)_REV1

Feed Volume Interval	Cd mg/L	Mn mg/L	Zn mg/L	Na mg/L
1	113.3	61.5	43.4	3793.9
2	225.6	158.4	129.7	1023.2
3	280.0	223.5	188.7	670.0
4	320.2	278.3	233.3	520.3
5	335.9	311.2	274.4	455.2
6	348.3	320.2	282.6	441.0
7	353.2	345.8	306.9	391.4
8	369.1	356.4	322.6	363.7
9	339.7	335.8	296.4	369.4
10	332.1	347.1	303.1	229.9

E.5.2: Effect of water pH: Mixed metal solution (pH7)_REV2

Feed Volume Interval	Cd mg/L	Mn mg/L	Zn mg/L	Na mg/L
1	108.7	59.0	41.7	3566.2
2	216.6	152.1	124.5	961.8
3	268.8	214.5	181.1	629.8
4	307.4	267.2	224.0	489.1
5	322.5	298.8	263.4	427.9
6	334.3	307.4	271.3	414.5
7	339.1	331.9	294.6	367.9
8	354.3	342.2	309.7	341.9
9	326.2	322.4	284.6	347.3
10	318.8	333.3	291.0	216.1

E.5.3: Effect of water pH: Mixed metal solution (pH7)_REV3

Feed Volume Interval	Cd mg/L	Mn mg/L	Zn mg/L	Na mg/L
1	122.3	66.5	46.9	3528.3
2	243.7	171.1	140.1	951.5
3	302.4	241.4	203.8	623.1
4	345.8	300.6	252.0	483.9
5	362.8	336.1	296.4	423.3
6	376.1	345.8	305.2	410.1
7	381.5	373.4	331.5	364.0
8	398.6	384.9	348.4	338.3
9	366.9	362.7	320.2	343.6
10	358.6	374.9	327.3	213.8

Appendix F

F.1.1: Effect of mineral characteristics: Alkaline mine drainage_REV1

	Clinoptilolite			Clinoptilolite & Quartz		
Feed Volume Interval	Ca mg/L	Mg mg/L	K mg/L	Ca mg/L	Mg mg/L	K mg/L
1	317.6	154.9	80.7	575.5	168.8	56.7
2	60.8	38.4	24.4	351.1	115.7	43.1
3	59.3	45.8	19.0	133.8	63.5	24.9
4	72.2	54.9	17.5	103.9	56.3	21.8
5	82.4	60.5	16.8	100.0	60.1	21.4
6	82.5	72.5	16.7	98.7	75.5	21.0
7	93.0	82.6	16.0	106.4	83.3	19.5
8	98.3	82.7	15.7	107.1	87.1	19.7
9	95.3	82.0	15.7	97.8	90.7	20.8
10	96.6	82.2	15.5	98.8	91.2	20.6

F.1.2: Effect of mineral characteristics: Alkaline mine drainage_REV2

	Clinoptilolite			Clinoptilolite & Quartz		
Feed Volume Interval	Ca mg/L	Mg mg/L	K mg/L	Ca mg/L	Mg mg/L	K mg/L
1	308.0	150.2	78.3	558.2	163.7	53.9
2	59.0	36.1	23.2	340.5	112.3	41.8
3	57.5	44.4	19.1	127.1	60.3	24.2
4	78.0	53.2	17.5	100.8	54.6	21.9
5	78.3	59.9	16.3	100.0	58.3	20.8
6	80.0	70.3	16.6	99.6	73.2	20.4
7	90.2	80.1	15.6	103.2	82.4	18.9

8	98.7	81.9	15.5	103.9	84.5	19.1
9	92.4	79.6	15.3	94.9	88.0	20.1
10	91.8	79.7	15.1	95.8	88.5	20.0

F.1.3: Effect of mineral characteristics: Alkaline mine drainage_REV3

	Clinoptilolite			Clinoptilolite & Quartz		
Feed Volume Interval	Ca mg/L	Mg mg/L	K mg/L	Ca mg/L	Mg mg/L	K mg/L
1	327.1	164.2	85.5	610.0	178.9	60.1
2	64.4	40.7	25.9	372.1	109.9	42.7
3	62.8	48.5	20.1	127.1	67.3	26.4
4	76.6	58.2	18.6	110.1	59.7	23.1
5	79.9	59.9	17.8	106.0	58.3	22.7
6	87.4	76.9	17.7	104.6	80.0	20.4
7	92.1	80.1	17.0	105.3	88.3	20.6
8	104.1	87.7	16.6	103.9	92.3	20.8
9	101.0	87.0	15.3	103.7	96.1	22.0
10	102.4	87.1	15.4	104.7	96.7	22.0

F.2.1: Effect of mineral characteristics: Acid mine drainage_REV1

	Clinoptilolite						Clinoptilolite & Quartz					
Feed Volume Interval	Ca mg/L	Mg mg/L	K mg/L	Al mg/L	Fe mg/l	Mn mg/L	Ca mg/L	Mg mg/L	K mg/L	Al mg/L	Fe mg/L	Mn mg/L
1	583.4	288.1	50.1	1.2	0.3	1.0	364.8	124.9	42.3	11.0	0.4	4.0
2	66.5	40.8	12.1	0.6	0.1	1.3	163.4	63.3	20.7	15.9	0.8	4.8
3	52.6	36.8	8.3	1.1	0.1	2.1	139.8	57.7	19.3	14.9	0.8	4.6
4	56.0	42.2	7.3	3.0	0.2	3.2	112.9	51.2	15.7	19.8	1.1	5.2
5	61.8	47.9	6.6	6.1	0.2	4.2	97.9	52.4	13.2	22.7	1.4	6.4

6	64.7	50.4	6.5	8.7	0.4	4.8	87.7	52.6	11.7	25.6	2.4	5.8
7	69.3	51.8	5.8	14.8	0.7	6.0	806	54.7	10.3	29.8	3.7	6.4
8	70.7	52.2	5.6	19.3	1.0	6.6	81.5	59.4	9.3	32.1	5.6	6.8
9	69.6	51.8	5.5	20.1	1.2	6.5	80.6	55.0	8.9	34.4	7.6	7.1
10	71.1	51.7	5.2	24.6	1.8	6.9	82.4	57.2	8.8	37.1	9.0	7.4

F.2.2: Effect of mineral characteristics: Acid mine drainage_REV2

	Clinoptilolite						Clinoptilolite & Quartz					
Feed Volume Interval	Ca mg/L	Mg mg/L	K mg/L	Al mg/L	Fe mg/l	Mn mg/L	Ca mg/L	Mg mg/L	K mg/L	Al mg/L	Fe mg/L	Mn mg/L
1	630.1	311.1	54.1	1.3	0.3	1.0	547.1	127.4	43.2	11.2	0.4	4.1
2	71.9	44.0	13.1	0.7	0.1	1.4	166.6	64.5	21.1	16.2	0.8	4.9
3	56.8	39.7	8.9	1.2	0.1	2.3	142.5	58.8	19.7	15.2	0.8	4.7
4	60.4	45.6	7.8	3.2	0.2	3.4	115.2	52.2	16.1	20.2	1.1	5.3
5	66.7	51.8	7.2	6.6	0.3	4.6	93.0	53.4	13.5	23.2	1.5	6.5
6	69.8	54.5	7.1	9.4	0.4	5.2	89.4	53.6	11.9	26.2	2.5	6.0
7	74.9	55.9	6.3	16.0	0.8	6.5	82.2	55.8	10.5	30.4	5.6	6.6
8	76.4	56.4	6.0	20.9	1.1	7.1	83.1	60.5	9.5	32.7	5.7	7.2
9	75.2	56.0	5.9	21.7	1.3	7.0	82.2	56.1	9.0	35.1	7.7	7.3
10	77.4	55.9	5.6	26.6	1.9	7.5	90.6	58.3	8.7	38.9	9.2	7.5

F.2.3: Effect of mineral characteristics: Acid mine drainage_REV3

	Clinoptilolite						Clinoptilolite & Quartz					
Feed Volume Interval	Ca mg/L	Mg mg/L	K mg/L	Al mg/L	Fe mg/l	Mn mg/L	Ca mg/L	Mg mg/L	K mg/L	Al mg/L	Fe mg/L	Mn mg/L
1	554.2	273.7	47.6	1.2	0.3	0.9	350.2	119.9	6.3	10.5	0.4	3.8
2	63.2	38.7	11.5	0.6	0.1	1.3	156.8	60.7	19.8	15.3	0.8	4.6
3	50.5	34.9	7.9	1.0	0.1	2.0	134.2	55.4	18.6	14.3	0.7	4.4

4	53.2	40.1	6.9	2.8	0.1	3.0	108.4	49.1	15.1	19.0	1.1	5.0
5	58.7	45.5	6.4	5.8	0.2	4.0	94.0	50.3	12.7	21.8	1.4	6.1
6	61.4	47.9	6.2	8.3	0.3	4.6	84.1	50.5	11.2	24.6	2.3	5.6
7	65.9	49.2	5.5	14.1	0.7	5.7	77.4	52.5	9.8	28.6	3.6	6.2
8	67.2	49.6	5.3	18.4	1.0	6.2	78.2	57.0	8.9	30.8	5.4	6.5
9	66.4	49.2	5.2	19.1	1.2	6.1	77.3	52.8	8.5	33.0	7.3	6.8
10	68.1	49.1	5.1	24.7	1.7	6.6	79.1	62.9	8.4	35.6	13.5	7.1

F.3.1: Effect of mineral characteristics: Mixed metal solution (Cadmium)

	Clinoptilolite			Clinoptilolite & Quartz		
Feed Volume Interval	Cd mg/L REV 1	Cd mg/L REV 2	Cd mg/L REV 3	Cd mg/L REV 1	Cd mg/L REV 2	Cd mg/L REV 3
1	94,6	97,4	89,8	225,7	226,2	207,7
2	242,9	250,2	230,8	335,5	336,2	308,7
3	299,3	308,3	284,3	352,4	353,1	324,2
4	346,3	356,7	329,0	373,9	374,6	344,0
5	368,5	379,5	350,0	410,7	411,6	377,9
6	380,8	392,2	361,7	431,1	432,0	396,6
7	375,8	387,0	357,0	437,9	438,7	402,8
8	395,0	406,8	375,2	436,4	437,3	401,5
9	392,1	403,9	372,5	443,0	443,9	407,6
10	400,4	412,4	380,4	451,5	452,4	415,3

F.3.2: Effect of mineral characteristics: Mixed metal solution (Manganese)

	Clinoptilolite			Clinoptilolite & Quartz		
Feed Volume Interval	Mn mg/L REV 1	Mn mg/L REV 2	Mn mg/L REV 3	Mn mg/L REV 1	Mn mg/L REV 2	Mn mg/L REV 3

1	53,17	54,8	51,0	175,8	179,3	170,6
2	177,36	182,7	170,3	252,6	257,7	245,1
3	247,54	255,0	237,6	268,0	273,3	259,9
4	295,56	304,4	283,7	296,5	302,5	287,6
5	332,82	342,8	319,5	340,8	347,6	330,6
6	359,47	370,2	345,1	368,2	375,6	357,2
7	359,70	370,5	345,3	381,7	389,4	370,3
8	381,79	393,2	366,5	387,0	394,7	375,4
9	382,87	394,4	367,6	395,3	403,2	383,5
10	389,30	401,0	373,7	407,3	415,4	395,0

F.3.3: Effect of mineral characteristics: Mixed metal solution (Zinc)

	Clinoptilolite			Clinoptilolite & Quartz		
Feed Volume Interval	Zn mg/L REV 1	Zn mg/L REV 2	Zn mg/L REV 3	Zn mg/L REV 1	Zn mg/L REV 2	Zn mg/L REV 3
1	23,1	24,8	22,5	145,4	152,7	142,5
2	133,7	143,1	129,7	207,8	218,2	203,6
3	198,4	212,3	192,5	217,8	228,7	213,5
4	243,1	260,2	235,9	256,5	269,3	251,3
5	282,5	302,2	274,0	295,4	310,2	289,5
6	309,2	330,9	300,0	323,8	340,0	317,3
7	309,3	331,0	300,0	324,9	341,1	318,4
8	332,4	355,6	322,4	349,3	366,8	342,3
9	330,4	353,6	320,5	358,7	376,7	351,6
10	337,3	360,9	327,2	378,7	397,6	371,1